ABSTRACT

BEREMAN, MICHAEL SETH. The Development of Desorption Electrospray Ionization and Nano Flow Liquid Chromatography Mass Spectrometric Methods for Glycan Analysis: Applications for Biomarker Discovery in Epithelial Ovarian Cancer. (Under the direction of Dr. David C. Muddiman.)

Ovarian cancer is often referred to as the “silent killer” due to the deadly nature of this malignancy and its asymptomatic nature. The disease will affect an estimated 24,000 women in the United States in 2009. If the disease is caught in its early stages over 90 % of patients survive longer than 5 years; however, 7 out of 10 patients are diagnosed in the late stages, after metastasis, where 1 in 5 people meet this 5-year survival mark. Advancements in early diagnosis are critical for both early intervention as well as a more in-depth understanding of this cancer such that therapeutic targets can be elucidated.

One of the major limitations for biomarker discovery research is the massive amount of time that must be allocated for preparation and analysis of large sample sets. The recent development of hybrid ionization techniques which combine ambient analysis with limited sample preparation and lead to higher sample throughput could help circumvent this current limitation. Herein, the development of a newly introduced ionization technique termed desorption electrospray ionization (DESI) is characterized for various biomarker discovery applications including proteomics and glycomics.

Glycomics is an emerging field for biomarker discovery research. Herein, a method for the analysis of *N*-linked glycans is provided. This method is then utilized to compare the *N*-linked glycan profile between 48 plasma samples derived from epithelial ovarian cancer patients, 48 controls samples

and 8 healthy samples. Three glycans were evaluated for their ability to differentiate between EOC and control and these results were compared to the gold standard in EOC detection, CA 125. Results indicated limited diagnostic value for three glycans in distinguishing control and EOC patients and moderate diagnostic value in differentiating EOC and healthy samples.

The Development of Desorption Electrospray Ionization and Nano Flow Liquid Chromatography Mass Spectrometric Methods for Glycan Analysis: Applications for Biomarker Discovery in Epithelial Ovarian Cancer

by
Michael Seth Bereman

A dissertation submitted to the Graduate Faculty of
North Carolina State University
In partial fulfillment of the
Requirements for the degree of
Doctor of Philosophy

Chemistry

Raleigh, North Carolina

September 21, 2009

APPROVED BY:

_____	_____
David C. Muddiman Professor, Chemistry Committee Chair	Edmond F. Bowden Professor, Chemistry
_____	_____
Christopher B. Gorman Professor, Chemistry	Lin He Assistant Professor, Chemistry

DEDICATION

This dissertation is dedicated to my parents Dr. Robert and Mrs. Barbara Bereman, my brother, Dr. Robert Matthew Bereman, and my fiancé, Meagan Myers. Without their love, support, guidance, friendship and encouragement this journey would not even have begun much less have finished. My ultimate gratitude extends to these four very special and important people.

BIOGRAPHY

Michael Seth Bereman was born at Rex Hospital in Raleigh, North Carolina on July 3, 1981 to Robert and Barbara Bereman. He began his education at North Carolina State University where he received his Bachelors of Science in chemistry and a minor in mathematics. He initially became interested in research and mass spectrometry while doing summer internships at Vector Research Ltd and BASF Corporation both in Durham, NC. After finishing his undergraduate degree, he worked in quality control at GlaxoSmithKline in Zebulon, NC. Although a nice experience, Michael knew he wanted to continue research specifically in the realm of biological mass spectrometry. In the fall of 2004, Michael was contemplating accepting a teaching assistant at either Florida State University or Purdue; both well known for their mass spectrometry programs. In early spring of 2005, Michael learned that Dr. David Muddiman recently accepted an analytical faculty position at North Carolina State University. After several phone conversations with Dr. Muddiman, Michael decided to stay home near his family and start his graduate career.

ACKNOWLEDGMENTS

I would like to acknowledge several people who have been instrumental in my journey throughout graduate school. My advisor, Dr. David Muddiman, provided me with leadership, reassurance, and encouragement. Observing his work ethic and his love and excitement for science will continue to motivate me throughout my career. I would like to thank Dr. Adam Hawkridge for his encouragement and numerous discussions we had pertaining to nanoLC. Dr. Taufika Williams was essential in getting me started and excited about the field of glycomics. In addition, I would like to thank the Muddiman group, specifically Brent Dixon and Keith Williams, for their support and friendships.

TABLE OF CONTENTS

LIST OF TABLES

LIST OF FIGURES

LIST OF PUBLICATIONS

Peer reviewed manuscripts:

1. Bereman M.S.; Muddiman DC; Development of a Robust and High Throughput Method for *N*-linked Glycan Profiling of Plasma Glycoproteins by nanoLC FTICR Mass Spectrometry *J. Proteome Res*, 2009 8, (7), 3764-3770.

2. Bereman M.S.; Williams,T.I.; Muddiman D.C.; Development of a nanoLC LTQ Orbitrap Mass Spectrometric Method for Profiling Glycans Derived from Plasma from Healthy, Benign Tumor Control, and Epithelial Ovarian Cancer Patients. *Anal Chem*. 2009, *81*, 1130–1136.

3. Bereman M.S.; Dixon, R.B.; Lyndon, M., Muddiman, D.C. Mass Measurement Accuracy Comparisons between a Double Focusing Magnetic Sector and a Time of Flight Mass Analyzer. *Rapid Commun. Mass Spectrom*. 2008, 22, 1563-1566.

4. Bereman M.S.; Williams T.I.; Muddiman D.C., Carbohydrate Analysis by Desorption Electrospray Ionization Fourier Transform Ion Cyclotron Resonance Mass Spectrometry. *Anal Chem*. 2007, 79, 8812-8815.

5. Dixon, R.B.; Bereman M.S.; Muddiman D.C; Hawkridge A.M , Remote Mass Spectrometric Sampling of Electrospray and Desorption Electrospray-Generated Ions Using an Air Ejector. *J. Am Soc. Mass Spectrom*. 2007, 1844-1847.

6. Bereman, M.S.; Muddiman, D.C.; Detection of Attomole Amounts of Analyte by Desorption Electrospray Ionization Mass Spectrometry (DESI-MS) Determined using Fluorescence Spectroscopy. *J. Am. Soc. Mass Spectrom*. 2007 1093-1096.

7. Bereman, M.S..; Fernandez, F.M; Nyadong, L.; Muddiman, D.C. Direct high resolution peptide and protein analysis by desorption electrospray ionization (DESI) Fourier transform ion cyclotron resonance mass spectrometry. *Rapid Commun. Mass Spectrom.* 2006, 22, 3409-3411.

Abstracts for presentation (Oral):

1. *Exploring the N-linked Glycome for Early Detection of Epithelial Ovarian Cancer by NanoLC FT-ICR Mass Spectrometry.* The 57th American Society for Mass Spectrometry Conference, Philadelphia, PA, June 2009. M.S. Bereman, William Cliby and David C. Muddiman.

2. *Profiling N-linked Glycans derived from Plasma Glycoproteins for Early Detection of Epithelial Ovarian Cancer by NanoLC FTICR Mass Spectrometry.* The 60th Pittsburgh Conference on Analytical Chemistry and Applied Spectroscopy, Chicago IL. March 2009. M.S. Bereman, T.I. Williams, W.A. Cliby, and D.C. Muddiman

3. *Glycan Analysis by Nano LC-MS: Applications for Biomarker Discovery in Epithelial Ovarian Cancer (EOC),* The Ninth Annual Atlanta-Athens Mass Spectrometry Discussion Group, Athens GA, October 2008. M.S Bereman, T. I. Williams, K. R. Kalli, W. A. Cliby and D.C. Muddiman.

4. *Characterization and Biological Applications of Desorption Electrospray Ionization coupled to hybrid FT-ICR Mass Spectrometry,* The Southeastern Regional Meeting of the American Chemical Society (SERMACS), Greenville, South Carolina. October 2007. M.S. Bereman, T.I. Williams, and D.C. Muddiman.

5. *The Development and Fundamental Studies of a Desorption Electrospray Ionization Source coupled to FT-ICR and Linear Ion Trap Mass Spectrometers*. NC Local American Chemical Society Conference Durham, NC. April, 2007. M.S. Bereman and D.C. Muddiman.

6. *Desorption Electrospray Ionization coupled to Fourier transform ion cyclotron resonance mass spectrometry (DESI-FT-ICR-MS) for the analysis of proteins and peptides,* The Southeastern Regional Meeting of the American Chemical Society Augusta, Georgia. November, 2006. M.S. Bereman, F.M. Fernandez, L. Nyadong, D.C. Muddiman.

Abstracts for presentation (Poster):

1. *Analysis of O-linked Glycans Derived from Control and Epithelial Ovarian Cancer Plasma by Nano LC LTQ Orbitrap Mass Spectrometry*, 56th American Society for Mass Spectrometry Conference, Denver, Colorado June 2008. M.S. Bereman, T.I. Williams and D.C. Muddiman.

2. *The Development of a Nano-LC Mass Spectrometric Method for Profiling Glycans in Epithelial Ovarian Cancer (EOC) and Control Plasma*, 25th Triangle Chromatography Symposium and Instrument Exhibit. Raleigh, North Carolina May 2008. M.S. Bereman, T.I. Williams, and D.C. Muddiman.

3. *Development and Characterization of a Desorption Electrospray Ionization Source Coupled to Hybrid Fourier Transform Ion Cyclotron Resonance Mass Spectrometry for Biological Analyses*, 55th American Society for Mass Spectrometry Conference, Indianapolis, Indiana June 2007. M.S. Bereman, T.I Williams, D.C. Muddiman.

Chapter 1

Introduction

1.1 Epithelial Ovarian Cancer

1.1.1 The Female Reproductive System – The Ovaries

The female reproductive system consists of several organs located within the pelvic region of the body. The ovaries are two almond shaped organs that reside on the upper right and left sides of the uterus and are responsible for the development and release of the female gamete through a process called ovulation. Once the egg is released, it travels down the fallopian tube where it can potentially become fertilized. In addition, the ovaries are the primary source of female hormones, estrogen and progesterone, which regulate the different stages of the menstrual cycle.

The ovaries are composed of three different types of cells; 1) the germ tissues which develop into the ovum or egg; 2) the stromal cells which are responsible for the production of female hormones; and 3) the epithelial cells which cover the surface of the ovary. Over 90% of ovarian tumors begin on the surface of the ovary (i.e., epithelial cells).[1]

1.1.2 Disease Statistics and Etiology

Epithelial ovarian cancer (EOC) is currently the most lethal of all gynecologic cancers.[2, 3] In the United States, an estimated 24,000 women will be diagnosed

annually with ovarian cancer and roughly 14,000 of those will ultimately succumb to the disease.[1] These numbers make ovarian cancer the 5th leading cause of cancer deaths in women in the United States. Despite improvements in care for ovarian cancer patients, the median survival length is approximately 40 months. This time period is characterized by struggles with recurrence, multiple surgical procedures and multiple treatment cycles with cytotoxic chemotherapeutic regimens, culminating in a protracted and painful death. The current human suffering and expense for these women is not measurable. The single most important factor in the management of ovarian cancer remains the clinical stage at diagnosis. For some cancers (*e.g.*, breast, cervix) the availability of a widely applied screening test has resulted in a shift in stage distribution from advanced stage to early stage. Other cancers (e.g., uterine) present symptoms early in their pathogenesis and lead to a prompt diagnosis. Similar to lung cancer, EOC most commonly presents in an advanced stage with grossly metastatic lesions distributed in the abdominal cavity or beyond, which represent stages III and IV, respectively. This is due to a combination of characteristics of EOC including the lack of: 1) specific early warning symptoms; 2) a reliable screening test for diagnosing early stage EOC; and 3) identifiable markers for a particularly high-risk subgroup of women. Five year survival rates are approximately 90% when detected early (stage I or II); however, 70% of cases are not diagnosed until late stages (stage III or IV) where only 1 in 5 patients survive longer than 5 years.[1]

1.1.3 Causes and Risk Factors for EOC

Despite ongoing research, little is known about the *pathogenesis* or *risk factors* for EOC. The most important *risk factors* for the disease continue to be family history and age. Genetics appear to play a role in the development of the disease for up to 10% of EOC cases.[4] A specific measure of risk is available for a subset of these patients through genetic analysis of two genes known to be important in both breast cancer and EOC: *BrCA1* and *BrCA2*. The exact genetic mediators of the disease for the remainder of the familial cases remain ambiguous. Age remains the single best risk factor with *incidences* ranging from 9.4 cases per 100,000 women under the age of 65 years old to a peak incidence of 54.8 cases per 100,000 women in patients over 65 years of age.[5] Minor modifiers of risks include *parity*, use of oral contraceptives, *lactation*, or *hysterectomy*.[5] These factors ultimately decrease the number of ovulatory events that a woman undergoes throughout her lifetime. The theory that relates the number of ovulatory events to a woman's risk of developing EOC is called the Incessant Ovulation Hypothesis and was first described by Fathalla[6] in 1971.

Obviously, the ability to effectively screen for EOC would be the most immediate and direct way to improve the current impact on human lives by shifting the stage at disease presentation and decreasing the overall number of deaths associated with this disease.

1.1.4 Disease Detection

The intense search for a highly sensitive and specific biomarker for EOC has been conducted over the last 30 years; however, the most widely used serum tumor marker for EOC, the carbohydrate (cancer) antigen 125 (CA-125)[7], was developed in the early 1980's primarily as a *prognostic* indicator for patients undergoing treatment for the disease.[8] Although this immunological assay remains a viable tool for physicians to track the progress of patients, it is not a viable screening tool for the general population[9] due to the lack of *sensitivity* and *specificity* of the marker. In fact, a multimodal approach is now being pursued whereby screening is done using a combination of non-invasive techniques such as CA-125 screening and transvaginal ultrasonography.[10]

1.2 Emerging Field of Glycomics

1.2.1 Introduction to Glycosylation

Currently, there are over 400 modifications that occur on proteins after translation.[11] *Glycosylation* is both one of the most important and prevalent as it has been estimated that 50% of all gene products are glycosylated.[12] Glycans mediate significant biological functions including cell-cell communication and signal transduction.[13, 14] The majority of glycans are either *O*-linked to a serine or a threonine or *N*-linked to an asparagine residue. Other glycans are used to attach proteins to cell membranes through a glycosylphosphatidylinositol anchor (GPI

anchor). In addition within a cell, several classes of glycolipids exist and play major roles in cellular recognition.

The *glycosylation* pathway is an enzyme directed process and commences within the endoplasmic reticulum of a eukaryotic cell. From there, nascent proteins are transferred to the Golgi apparatus where further processing of glycans occurs via various glycotransferases and glycosidases. From the Golgi apparatus, most glycoproteins are transported, via vesicles, either to the cellular membrane or secreted into the extracellular matrix. The exact mechanism of protein glycosylation, the factors that affect the processes, and the various biological functions of glycans are quite complex and still under significant investigation.[13]

Glycosylation is highly sensitive to its cellular environment[15] and aberrant protein glycosylation is known to occur in various diseases.[14, 16-19] Wu *et al.* first implicated the significance of glycosylation in cancer when it was demonstrated that healthy fibroblasts have smaller membrane glycoproteins than their diseased counterpart.[20] Later, Rostenberg *et. al.* reported altered glycosylation patterns in alpha-1-antitrypsin in various types of cancer.[21] In the 1980's, Gehrke and coworkers linked glycan abundance to ovarian and lung carcinomas by gas-liquid chromatography (GLC).[22] Recent research continues to emphasize the significance of glycosylation in cancer development.[18, 19, 23-28] For example, it has been reported that sialylation of glycoproteins is altered between normal and malignant conditions.[18, 29, 30] In addition, the increase in size and branching of *N*-

linked glycans characteristic of cancer cells is attributed to an increase in activity of various glycotransferases. [31, 32]

1.2.2 Ionization Methods for Glycan Analysis

Due to both its unparalleled molecular specificity and ability to offer structural information, mass spectrometry has become a prominent and powerful analytical tool for glycan characterization. *Matrix-assisted laser desorption ionization* (MALDI) has been the ionization technique of choice[33] for glycan analysis. Scientists often dope in salts (e.g., NaCl) for MALDI analysis of glycans to promote metal adduction in the positive ion mode which significantly enhances ionization.[34, 35] However, MALDI has its significant disadvantages including vacuum constraints, potential for fragmentation, and the need for an organic matrix which often adducts with glycans; therefore, complicating data interpretation.

The development of direct analysis methods, often referred to as hybrid ionization techniques, is arguably the fastest growing field in mass spectrometry.[36, 37] These ionization methods offer a propitious platform for glycan studies as they combine the rapid direct analysis, characteristic of MALDI, with the ability to create multiply charged ions, characteristic of ESI. Multiple charging of ions provides for higher MMA, improved fragmentation, and higher resolving power in FT-ICR mass spectrometry. In addition, these techniques are performed in the ambient environment (no vacuum constraints) and in the case of many (e.g., Desorption Electrospray Ionization) require no need for an exogenous matrix.

The low detectability of glycans by electrospray ionization (ESI) is contributed to the hydrophilic nature and lack of basic sites characteristic of glycan structure. The hydrophilicity limits the surface activity of the species inside the electrospray droplet and ultimately leads to low ionization efficiency. With the continued development in pump technology, highly precise split-less nano-flow rates can be achieved, creating much smaller ESI droplets than conventional micro-spray. Smaller droplets lead to increased surface to volume ratios which correspond to higher ionization efficiency and sensitivity for glycan analysis.[38-42] As a result, electrospray ionization is increasingly being utilized for glycan studies often coupling the technique with liquid chromatography.[42-44]

1.3 Electrospray Ionization

Electrospray Ionization (ESI) is referred to as a soft ionization technique due to its ability to prevent fragmentation as a result of the ionization process. Seminal work by Dole in the mid 1960's demonstrated the ability of electrospray to produce ions from macropolymers[45, 46]; however, it was John Fenn in the mid 1980's who coupled the technique to mass spectrometry for analysis of biological macromolecules.[47, 48] In 2002, Fenn was awarded the Nobel Prize for his development of electrospray ionization for the analysis of biological macromolecules by mass spectrometry. As a result, ESI has created a particular interest in the applications of mass spectrometry to the biological sciences due to it ability to effectively ionize high molecular weight biopolymers.

In ESI-MS, ions are created in the ambient environment by applying a high voltage (± 2 kV) to a conducting solution. The charged solution exits the end of a tapered silica capillary, often referred to as the ESI tip, where a *Taylor cone* is formed. Dispersion of charged droplets occurs when the forces due to Coulombic repulsion overcome the forces due to surface tension and thus a fine mist of charged droplets is created. Evaporation of solvent occurs, increasing the charge density of the *parent droplets*.

$$q_r = \sqrt{64\pi^2 \varepsilon_0 \gamma r^3} \qquad \textbf{1.1}$$

The *Rayleigh limit*[49] is eventually reached and Coulombic fission occurs creating *offspring droplets*. The Rayleigh limit, given in **Equation 1.1**, is proportional to the permittivity of free space (ε_0), surface tension (γ) and the radius of the droplet (**r**).

After the onset of electrospray there are two proposed mechanisms for ion production. The first mechanism, referred to as the Charge Residue Model, was described by Dole and states that charge droplets will undergo a series of several Coulombic explosions until an "ultimate" solvent droplet is created and contains only a single molecule.[45, 46] Upon further evaporation of residual solvent the ion enters the gas phase.

The other mechanism reported by Iribarne and Thomson is referred to as the Ion Evaporation Theory and is similar to the previous mechanism in that parent droplets undergo a series of coulombic explosions to create offspring droplets. However, this mechanism differs from Dole's theory in that an ultimate droplet containing 1 analyte never forms. Instead the charge density increases on the

offspring droplets and ions residing at the surface of the droplet are lifted or desorbed into the gas phase due to the electric field created on the droplet's surface.[50, 51] Currently, the Ion Evaporation Model is the more accepted explanation of the processes by which ions are created in electrospray ionization; however, it should be noted that these mechanisms are not clearly understood and are still under significant investigation.

1.4 Ambient Ionization Techniques

1.4.1 Introduction to Ionization in Mass Spectrometry

The advent of ESI and MALDI ionization techniques has created a particular interest in the applications of mass spectrometry to the biological sciences. The two techniques have effectively connected the high sensitivity and molecular specificity of mass spectrometry to biological samples given their ability to ionize macromolecules. When coupled to high *resolving power* mass spectrometry platforms such as Fourier transform ion cyclotron resonance (FT-ICR) and orbitrap (*vide infra*), ESI and MALDI are essential tools for investigating significant and complex biological problems. However as science advances and new problems emerged, the inherent limitations of MALDI and ESI (vacuum constraints and matrix effects in MALDI, and extensive sample preparation for ESI) have warranted the continued development of alternate "hybrid" ionization techniques.

1.4.2 History of Hybrid Ionization Techniques

The working definition of what constitutes a Hybrid Ionization Source is an ionization source which utilizes properties from two or more existing ionization techniques for which there exists a distinct benefit or attribute from using each source. In the 1980's, several groups introduced the concept of "hybrid ionization sources" where the events of desorption and ionization were separated into two discrete events. In 1980, R.J. Cotter demonstrated laser desorption (LD) to generate neutrals from the surface under vacuum; these neutrals were then ionized by CI.[52] In 1982, Kambara demonstrated that neutrals produced via nebulization at atmospheric pressure could be subsequently ionized via CI.[53] In 1986, Lubman and coworkers demonstrated that neutrals could be desorbed by an IR laser and post-ionized using multi-photon ionization with a UV laser.[54] Lubman also presented in this same year LDCI in which neutrals were desorbed at atmospheric pressure by using LD and subsequently ionized via CI; significant increases in ionization efficiencies were reported for high proton affinity molecules.[55] This initial work was carried out using a radioactive ^{63}Ni source using air as the reagent gas; however, in 2002, Harrison and coworkers demonstrated that the CI could readily be accomplished using reagent ions produced by corona discharge.[56] In 1994, Hill and coworkers introduced the concept of interacting neutrals with an ESI beam, where they observed an increase in ionization efficiency.[57] This was later termed

Secondary Electrospray Ionization (SESI) and was coupled to ion mobility spectrometry-mass spectrometry for the analysis of illicit drugs.[58] These were some of the first reports of integrating two different ionization sources (*e.g.*, LD and CI) for improved ionization. In these examples, the goal was to improve ionization efficiencies and/or reduce fragmentation and background ions. It is important to note that these hybrid ionization sources did not impart multiple-charges on the analytes of interest.

1.4.3 Contemporary Ion Sources

A host of new hybrid ionization sources that produce predominately singly-charged ions have been introduced in the recent years including Laser-Induced Acoustic Desorption (LIAD) with post-ionization using EI or CI by Kenttamaa and coworkers[59], *Direct Analysis in Real Time* (DART) by Cody *et al.*,[60] and *Atmospheric-Pressure Solids Analysis Probe* (ASAP) by McEwen *et al*.[61] In 2004, Cooks and coworkers demonstrated that they could generate multiply-charged ions from analytes that had been deposited onto a surface which they called *Desorption Electrospray Ionization* (DESI).[62] This was a very significant observation because until this paper, ESI was the only other reported ionization method that had been demonstrated to produce multiply-charged species. Arguably, DESI[62] essentially started the "gold rush" towards the development of ambient/hybrid ionization sources.

In 2005, Shiea *et al.* demonstrated that they could desorb neutrals using a laser and post-ionize using ESI, for which they observed multiply-charged ions for cytochrome c.[63] They called this *Electrospray-assisted Laser Desorption/Ionization* (ELDI).[63-66] ELDI was in part, likely based on their concept and observations of *Fused-Droplet Electrospray Ionization* (FD-ESI), where they interacted aerosols containing non-volatile analytes produced via ultrasonic nebulization with an ESI beam.[67, 68] In a similar technique, and based on their earlier work with *Electrosonic Spray Ionization* (ESSI)[69], Cooks and co-workers presented *Extractive Electrospray Ionization* (EESI) for the analysis of complex mixtures without sample preparation.[70] The Muddiman group developed *Matrix-Assisted Laser Desorption Electrospray Ionization* (MALDESI)[71-74] as a method to produce multiply-charged ions for subsequent interrogation by top-down mass spectrometric methods. Importantly, both ELDI and MALDESI made use of UV lasers[63-65, 71, 72, 75]. In 2007, Vertes reported the concept of ELDI/MALDESI but used an IR laser and named the ionization method *Laser Ablation Electrospray Ionization* (LAESI).[76] The use of an IR laser holds a particular benefit for tissue imaging in that an external matrix in not required. A recent report by Murray and co-workers also reported the use of an IR laser with post-ionization by ESI termed *IR Laser-Assisted Desorption Electrospray Ionization* (IR LADESI).[77]

In summary, there has always been an active interest in ionization methods for mass spectrometry; however, in the past few decades, the intensity of this pursuit has markedly increased as a result of the wide range of biological problems

that can be addressed using mass spectrometry. Aside from the ionization methods already discussed (*vide supra*), there has been several other ionization sources reported in the past decade.[78-84] The interest in the Muddiman group is centered around the development of these hybrid sources coupled to high performance mass spectrometry for biomarker discovery applications where rapid screening, limited sample preparation and high throughput are essential.

1.5 High Performance Mass Spectrometry

1.5.1 Fourier Transform Ion Cyclotron Resonance Mass Spectrometry

High resolving power (RP*)* (>500,000$_{fwhm}$) and *high mass measurement accuracy (*MMA*)* (< 3 ppm) are key advantages of Fourier transform ion cyclotron resonance mass spectrometry (FT-ICR-MS)[85] when compared to other MS platforms for biological analyses. Increased *peak capacity* (i.e. high resolving power) is essential when interrogating complex samples as it dramatically increases the ability to identify species. In addition, high MMA afforded by FT-ICR-MS reduces the number of false positives when conducting database searches, thus, further aiding in the positive identification.

Due to the degrading performance of FT-ICR-MS as a function of *m/z*[86], the propensity of *multiple charging* characteristic of ESI renders the technique well suited for FT-ICR-MS.[87] Ions are sampled by the mass spectrometer and are accumulated in a sub-atmospheric hexapole region.[88] After a certain time period, ions are then injected into the ICR cell via various voltage gradients.

Within the ICR cell the ions are trapped in the axial direction (horizontal) by applied electric fields and in the radial direction by the force of the magnetic field and assume a natural cyclotron motion.[86] This circular motion is a result of the *Lorentz force* acting on a charge particle residing in a magnetic field which deflects the particle in a direction perpendicular to its velocity. Subsequently ions are excited to a larger radius using an excite waveform which is applied to two opposite plates. This event is performed for two main reasons: 1) to achieve *phase coherence* of all ions with the same *m/z* value 2) and to force the ions closer to the detection plates in order to induce appreciable signal. An image current of the orbiting ion packets is then recorded by the detection plates.

$$f_c = \frac{qB_0}{2\pi m} \qquad \textbf{1.2}$$

The time domain is digitized, fast Fourier transformed (FFT) into the frequency domain, and a mass spectrum is obtained by converting to the *m/z* domain (**Equation 1.2**). **Figure 1.1** displays a schematic of the ICR cell along with

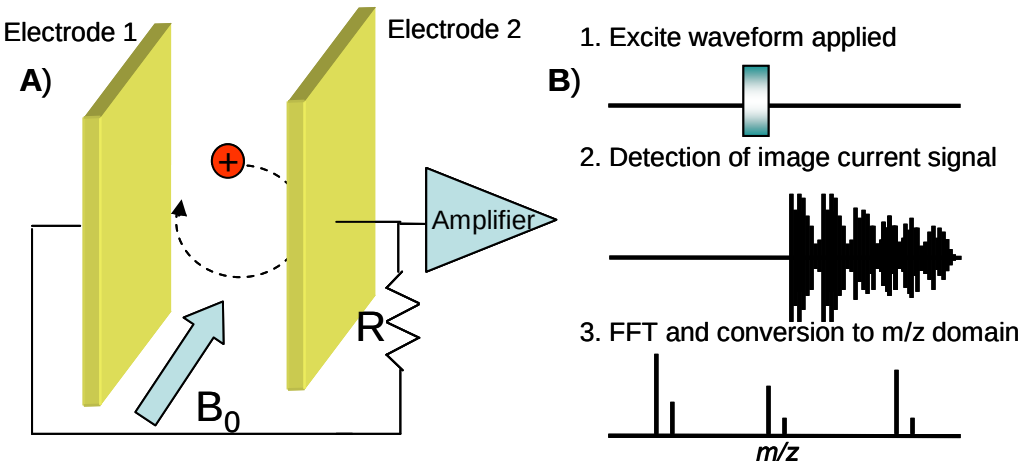

Figure 1.1 A) Schematic of an ICR cell **B**) Overview of excite, detect and FFT processes.

a flow chart of the overall process.

As mentioned previously the inverse relationship of *cyclotron frequency* to *m/z*[87] allows for ESI-FT-ICR-MS analysis of large biomolecules. However, multiple charging is advantageous for several other reasons including: 1) increased resolving power; 2) more efficient fragmentation; 3) high MMA; and 4) decreased limits of detection. The increased *peak capacity* afforded by the high RP is critical when identifying species in complex biological samples. *Cyclotron frequency* and *resolving power* in FT-ICR-MS are defined by **Equations 1.2 and 1.3,** respectively. *Resolving power* is proportional to detection time (**T**), amount of charge (**z**), the strength of the magnetic field ($\mathbf{B_0}$) and inversely proportional to mass (**m**).

$$RP_{fwhm} = \frac{(1.274 * 10^7) z B_0 T}{m} \qquad \textbf{1.3}$$

Additionally multiple charging of proteins is more conducive to tandem mass spectrometry. It is known that *collision induced dissociation* (CID) of singly charged molecules becomes much less efficient with increasing molecular weight.[89] This inefficient process is a result of the linear relationship between the number of internal energy modes and increasing molecular mass. High molecular weight species have more energy modes in which internal energy can be redistributed prior to bond cleavage (3N-6). Thus, the coulombic energy imparted into the molecule aids in destabilization of the large protein molecules leading to more efficient dissociation.[89-91]

Poor mass accuracy in FT-ICR-MS, described in **Equation 1.4**, is a result of mutual repulsion of charged ion packets within the ICR cell, commonly referred to as the "*space-charge-effect.*"[92, 93]

$$MMA = \frac{m_{exp} - m_{theo}}{m_{theo}} * 10^6 \qquad \textbf{1.4}$$

To the first approximation, all ions within the ICR cell experience the same space charge induced frequency shift.[94] Since *cyclotron frequency* is linearly related to charge in FT-ICR-MS, as stated in **Equation 1.1**, highly charged molecules have greater frequencies. With increasing cyclotron frequencies, the proportion of frequency shift due to space charge decreases, perturbing the experimental *m/z* value less and affording high *mass measurement accuracy*.

Multiple charging in FT-ICR-MS also allows for deeper analyte coverage of complex samples by decreasing limits of detection. The limit of detection in FT-ICR-MS, described in **Equation 1.5**, is defined as the minimum amount of induced current required to overcome the resistance of the FT-ICR circuit.

$$Q(t) = \frac{-Nrq\cos(\omega t)}{d} \qquad \textbf{1.5}$$

As **Equation 1.5** states the current Q(t) is directly proportional to the amount of charge on an ion (**q**). To produce an appreciable signal in FT-ICR-MS, approximately 200 charges are required for any one isotopic species.[95] Moreover,

producing an ion with 4 charges theoretically requires only 50 ions, decreasing the LOD by “q” times.

1.5.2 Orbitrap Mass Analyzer

Until recently, the resolving power and mass accuracy afforded by FT-ICR mass analyzers surpassed all other MS platforms. However, the development of the orbitrap by Makarov [96] in the last decade has provided for similar performance to ICR mass analyzers without the expensive up-front and maintenance costs associated with a high field superconducting magnet. The orbitrap is similar to an earlier ion storage device termed the Kindon trap[97] which utilized a purely electrostatic field for ion trapping and has been used to study molecular beams[98] and ion spectroscopy[99, 100]

The orbitrap consists of two electrodes, an inner spindle electrode surrounded by outer barrel electrode.[96, 101] A 2-dimensional cut away view of the obitrap is shown in **Figure 1.2**. The static electric field created by the specially designed electrodes trap ions in a 3 dimensional space. There are three different frequencies that can be measured and used for mass analysis; however, the frequency in the z direction is the only frequency that

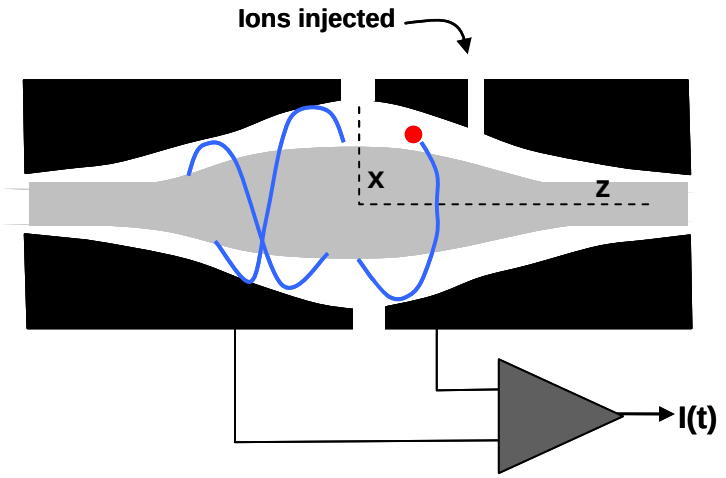

Figure 1.2 A cutaway 2 dimensional schematic of the Orbitrap

does not depend on kinetic energy and thus is used for mass analysis. The frequency measured in the orbitrap is inversely proportional to the square root of the *m/q (m/z)*. **Equation 1.6** describes the measured obitrap frequency where **k** is the field curvature.

$$\omega = \sqrt{(q/m)k} \qquad \textbf{1.6}$$

Detection in the orbitrap is analogous to that of the ICR instruments except that there is no excitation event. Oscillations along the z-axis are detected using an image current and are transformed into the frequency domain utilizing a fast Fourier transform. From the frequency domain, calibration laws are used to produce mass spectra. As mentioned the orbitrap rivals the ICR analyzer in terms of *resolving power* and routinely can attain < 2 ppm mass measurement accuracy utilizing the *lock mass* feature.[43, 102] Due to the inverse relationship of the square root of the *m/z* to frequency the resolving power of the obitrap exceeds a 7T ICR instrument after a certain *m/z*. A comparison between resolving power of the different instruments as a function of *m/z* is shown in **Figure 1.3**. This plot was constructed assuming a 1 second acquisition time for both instruments.

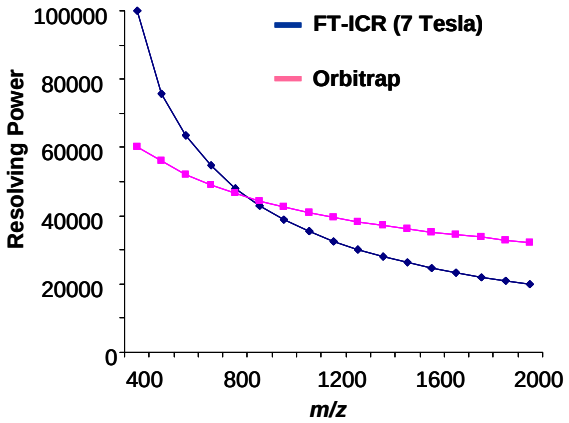

Figure 1.3 Resolving power as a function of *m/z* for two different FTMS based instruments.

1.6 Synopsis of Completed Research

The research presented in this dissertation describes the development and characterization of different methods for glycan analysis. **Chapter 2** describes the first implementation of a DESI source on an FTICR mass spectrometer for high resolution data of peptides and proteins. In addition, this chapter describes in detail the development of the three different DESI sources; each source improving on limitations realized by the previous.

Characterization of the various processes in DESI is the subject of **Chapter 3.** Fluorescence spectroscopy is utilized to investigate the effect of several experimental conditions on the size of the DESI spot and the amount of material removed from the surface. In an alternative approach, a quartz crystal microbalance is utilized to determine the material removed. The limitations in these techniques for evaluating the sensitivity of DESI-MS are discussed.

Chapter 4 discusses the potential of DESI for glycomic applications. Detection limits for several different standard glycans are provided as well as a comparison between DESI-FT-ICR and MALDI-FT-ICR MS analysis of *O*-linked glycans chemically cleaved from Mucin. The advantages of DESI-FT-ICR mass spectrometry are presented.

Due to the low abundance of glycans in plasma samples and the limitations of MALDI-FT-ICR mass spectrometry, it was necessary to develop a nanoLC-MS method for analysis of glycans chemically released from plasma glycoproteins. In

Chapter 5, two different stationary phases are compared and evaluated for their ability to separate glycans. Finally, the glycan profiles resulting from the nanoLC-MS analysis of a small set of glycan samples derived from healthy, benign control and EOC plasma are compared. Results are evaluated using ROC statistics and indicated up-regulation of two fucosylated glycans in healthy when compared to disease and control samples.

Previous work targeted *O*-linked glycans using chemical release; however, **Chapter 6** describes the development of a method to enzymatically release and purify *N*-linked glycans from plasma. Different incubation methods and incubation times are evaluated. Glycan abundances are normalized to internal standards (ISDs) and the reproducibility of the method is compared between when these ISDs are added to the mixture. A vast experimental space was explored in the development of this method and these parameters are summarized in **Chapter 6**.

Chemical tagging of species for improved response by mass spectrometry has had a long and productive history. Due to the bias in ESI towards more hydrophobic species, many groups have focused their efforts in increasing the hydrophobicity of molecules through chemical derivatization.[103-106] **Chapter 7** describes the synthesis of two hydrazides and use of these reagents to improve glycan detection by increasing the hydrophobicity of the analyte and imparting a permanent charge. The chemistry is performed in high yield and provides for much higher throughput than reductive amination, the more commonly used glycan derivatization procedure.

Chapter 8 describes the analysis of 104 plasma samples (48 EOC; 48 controls; 8 healthy samples) utilizing the procedure for glycan release, purification, and normalization discussed in **Chapter 6**. There are approximately 50 different glycan species that have been identified in plasma by exact mass and tandem MS/MS. Three glycan species were chosen and their abundances are tracked through the different stages of disease and compared to the control plasma and healthy samples.

1.7 References

1. Williams, T.I., et al., Epithelial ovarian cancer: Disease etiology, treatment, detection, and investigational gene, metabolite, and protein biomarkers. *J. Proteome Res.*, 2007. **6**. 2936-2962.

2. Jemal, A., et al., Cancer statistics, 2002. *CA - A Cancer J. Clin.*, 2002. **52**. 23-47.

3. Greenlee, R.T., et al., Cancer statistics, 2001. *CA - A Cancer J. Clin.*, 2001. **51**. 15-36.

4. Langston, A.A. and E.A. Ostrander, Hereditary ovarian cancer. *Curr. Opin. Obstet. Gynecol.*, 1997. **9**. 3-7.

5. La Vecchia, C., Epidemiology of ovarian cancer: a summary review. *European Journal of Cancer Prevention*, 2001. **10**. 125-129.

6. Fathalla, M.F., Incessant Ovulation - Factor in Ovarian Neoplasia. *Lancet*, 1971. **2**. 163-&.

7. Wong, N.K., et al., Characterization of the oligosaccharides associated with the human ovarian tumor marker CA125. *J. Biol. Chem.*, 2003. **278**. 28619-28634.

8. Mills, G.B., R.C. Bast, and S. Srivastava, Future for ovarian cancer screening: Novel markers from emerging technologies of transcriptional profiling and proteomics. *Journal of the National Cancer Institute*, 2001. **93**. 1437-1439.

9. Fritsche, H.A. and R.C. Bast, CA 125 in ovarian cancer: Advances and controversy. *Clin. Chem.*, 1998. **44**. 1379-1380.

10. Goff, B.A., et al., Ovarian carcinoma diagnosis - Results of a National Ovarian Cancer Survey. *Cancer*, 2000. **89**. 2068-2075.

11. Krueger, K.E. and S. Srivastava, Posttranslational protein modifications - Current implications for cancer detection, prevention, and therapeutics. *Molecular & Cellular Proteomics*, 2006. **5**. 1799-1810.

12. Apweiler, R., H. Hermjakob, and N. Sharon, On the frequency of protein glycosylation, as deduced from analysis of the SWISS-PROT database. *Biochimica Et Biophysica Acta-General Subjects*, 1999. **1473**. 4-8.

13. Varki, A., Biological Roles of Oligosaccharides - All of the Theories Are Correct. *Glycobiology*, 1993. **3**. 97-130.

14. Dwek, R.A., Glycobiology: Toward understanding the function of sugars. *Chemical Reviews*, 1996. **96**. 683-720.

15. Varki, A., Nothing in glycobiology makes sense, except in the light of evolution. *Cell*, 2006. **126**. 841-845.

16. Peracaula, R., et al., Glycosylation of human pancreatic ribonuclease: differences between normal and tumor states. *Glycobiology*, 2003. **13**. 227-244.

17. Dwek, M.V. and S.A. Brooks, Harnessing changes in cellular glycosylation in new cancer treatment strategies. *Current Cancer Drug Targets*, 2004. **4**. 425-442.

18. Varki, A., Sialic acids in human health and disease. *Trends in Molecular Medicine*, 2008. **14**. 351-360.

19. Zhao, Y.Y., et al., Functional roles of N-glycans in cell signaling and cell adhesion in cancer. *Cancer Science*, 2008. **99**. 1304-1310.

20. Wu, H.C., et al., Comparative Studies on Carbohydrate-Containing Membrane Components of Normal and Virus-Transformed Mouse Fibroblasts .I. Glucosamine-Labeling Patterns in 3t3 Spontaneously Transformed 3t3 and Sv-40-Transformed 3t3 Cells. *Biochemistry*, 1969. **8**. 2509-&.

21. Rostenberg, I., J. Guizarvazquez, and R. Penaloza, Altered Carbohydrate Content of Alpha-1-Antitrypsin in Patients with Cancer. *Journal of the National Cancer Institute*, 1978. **61**. 961-965.

22. Gehrke, C.W., et al., Quantitative Gas-Liquid-Chromatography of Neutral Sugars in Human-Serum Glycoproteins - Fucose, Mannose, and Galactose as Predictors in Ovarian and Small Cell Lung-Carcinoma. *J. Chromatogr.*, 1979. **162**. 507-528.

23. Casey, R.C., et al., Cell membrane glycosylation mediates the adhesion, migration, and invasion of ovarian carcinoma cells. *Clinical & Experimental Metastasis*, 2003. **20**. 143-152.

24. Dennis, J.W., M. Granovsky, and C.E. Warren, Protein glycosylation in development and disease. *BioEssays*, 1999. **21**. 412-421.

25. Lau, K.S. and J.W. Dennis, N-Glycans in cancer progression. *Glycobiology*, 2008. **18**. 750-760.

26. Hollingsworth, M.A. and B.J. Swanson, Mucins in cancer: Protection and control of the cell surface. *Nature Reviews Cancer*, 2004. **4**. 45-60.

27. Hakomori, S., Glycosylation defining cancer malignancy: New wine in an old bottle. *Proc. Natl. Acad. Sci. U. S. A.*, 2002. **99**. 10231-10233.

28. Gorelik, E., U. Galili, and A. Raz, On the role of cell surface carbohydrates and their binding proteins (lectins) in tumor metastasis. *Cancer and Metastasis Reviews*, 2001. **20**. 245-277.

29. Peracaula, R., et al., Altered glycosylation pattern allows the distinction between prostate-specific antigen (PSA) from normal and tumor origins. *Glycobiology*, 2003. **13**. 457-470.

30. Kim, Y.J. and A. Varki, Perspectives on the significance of altered glycosylation of glycoproteins in cancer. *Glycoconjugate Journal*, 1997. **14**. 569-576.

31. Dube, D.H. and C.R. Bertozzi, Glycans in cancer and inflammation. Potential for therapeutics and diagnostics. *Nature Reviews Drug Discovery*, 2005. **4**. 477-488.

32. Dennis, J.W., et al., Beta-1-6 Branching of Asn-Linked Oligosaccharides Is Directly Associated with Metastasis. *Science*, 1987. **236**. 582-585.

33. Harvey, D.J., Matrix-assisted laser desorption/ionization mass spectrometry of carbohydrates. *Mass Spectrom. Rev.*, 1999. **18**. 349-450.

34. Williams, T.I., et al., Investigations with O-linked protein Glycosylations by Matrix-Assisted Laser Desorption/Ionization Fourier Transform Ion Cyclotron Resonance Mass Spectrometry. *Journal of Mass Spectrometry*, 2008. **43**. 1215-1223.

35. Williams, T.I., D.A. Saggese, and D.C. Muddiman, Studying O-linked protein glycosylations in human plasma. *J. Proteome Res.*, 2008. **7**. 2562-2568.

36. Cooks, R.G., et al., Ambient mass spectrometry. *Science*, 2006. **311**. 1566-1570.

37. Harris, G.A., L. Nyadong, and F.M. Fernandez, Recent developments in ambient ionization techniques for analytical mass spectrometry. *Analyst*, 2008. **133**. 1297-1301.

38. Karlsson, N.G., et al., Negative ion graphitised carbon nano-liquid chromatography/mass spectrometry increases sensitivity for glycoprotein oligosaccharide analysis. *Rapid Commun. Mass Spectrom.*, 2004. **18**. 2282-2292.

39. Barroso, B., et al., On-line high-performance liquid chromatography/mass spectrometric characterization of native oligosaccharides from glycoproteins. *Rapid Commun. Mass Spectrom.*, 2002. **16**. 1320-1329.

40. Bahr, U., et al., High sensitivity analysis of neutral underivatized oligosaccharides by nanoelectrospray mass spectrometry. *Anal. Chem.*, 1997. **69**. 4530-4535.

41. Karas, M., U. Bahr, and T. Dulcks, Nano-electrospray ionization mass spectrometry: addressing analytical problems beyond routine. *Fresenius Journal of Analytical Chemistry*, 2000. **366**. 669-676.

42. Wuhrer, M., et al., Normal-phase nanoscale liquid chromatography - Mass spectrometry of underivatized oligosaccharides at low-femtomole sensitivity. *Anal. Chem.*, 2004. **76**. 833-838.

43. Bereman, M.S., T.I. Williams, and D.C. Muddiman, Development of a NanoLC LTQ Orbitrap Mass Spectrometric Method for Profiling Glycans Derived from Plasma from Healthy, Benign Tumor Control, and Epethelial Ovarian Cancer Patients. *Anal. Chem.*, 2009. **81**. 1130-1136.

44. Chu, C.S., et al., Profile of native N-linked glycan structures from human serum using high performance liquid chromatography on a microfluidic chip and time-of-flight mass spectrometry. *Proteomics*, 2009. **9**. 1939-1951.

45. Dole, M., L.L. Mack, and R.L. Hines, Molecular Beams of Macroions. *J. Chem. Phys.*, 1968. **49**. 2240-&.

46. Mack, L.L., et al., Molecular Beams of Macroions .2. *J. Chem. Phys.*, 1970. **52**. 4977-&.

47. Yamashita, M. and J.B. Fenn, Electrospray Ion-Source - Another Variation on the Free-Jet Theme. *J. Phys. Chem.*, 1984. **88**. 4451-4459.

48. Fenn, J.B., et al., Electrospray Ionization for Mass-Spectrometry of Large Biomolecules. *Science*, 1989. **246**. 64-71.

49. Rayleigh, L., *Philos. Mag. A*, 1882. **14**. 184.

50. Iribarne, J.V. and B.A. Thomson, Evaporation of Small Ions from Charged Droplets. *J. Chem. Phys.*, 1976. **64**. 2287-2294.

51. Thomson, B.A. and J.V. Iribarne, Field-Induced Ion Evaporation from Liquid Surfaces at Atmospheric-Pressure. *J. Chem. Phys.*, 1979. **71**. 4451-4463.

52. Cotter, R.J., Laser Desorption Chemical Ionization Mass-Spectrometry. *Anal. Chem.*, 1980. **52**. 1767-1770.

53. Kambara, H., Sample Introduction System for Atmospheric-Pressure Ionization Mass-Spectrometry of Non-Volatile Compounds. *Anal. Chem.*, 1982. **54**. 143-146.

54. Tembreull, R. and D.M. Lubman, Pulsed Laser Desorption with Resonant 2-Photon Ionization Detection in Supersonic Beam Mass-Spectrometry. *Anal. Chem.*, 1986. **58**. 1299-1303.

55. Kolaitis, L. and D.M. Lubman, Detection of Nonvolatile Species by Laser Desorption Atmospheric-Pressure Mass-Spectrometry. *Anal. Chem.*, 1986. **58**. 2137-2142.

56. Coon, J.J., K.J. McHale, and W.W. Harrison, Atmospheric pressure laser desorption/chemical ionization mass spectrometry: a new ionization method based on existing themes. *Rapid Commun. Mass Spectrom.*, 2002. **16**. 681-685.

57. Chen, Y.H., H.H. Hill, and D.P. Wittmer, Analytical Merit of Electrospray Ion Mobility Spectrometry as a Chromatographic Detector. *J. Micro. Sep.*, 1994. **6**. 515-524.

58. Wu, C., W.F. Siems, and H.H. Hill, Secondary Electrospray Ionization Ion Mobility Spectrometry/Mass Spectrometry of Illicit Drugs. *Anal. Chem.*, 2000. **72**. 396-403.

59. Crawford, K.E., et al., Laser-induced acoustic desorption/Fourier transform ion cyclotron resonance mass spectrometry for petroleum distillate analysis. *Anal. Chem.*, 2005. **77**. 7916-7923.

60. Cody, R.B., J.A. Laramee, and H.D. Durst, Versatile new ion source for the analysis of materials in open air under ambient conditions. *Anal. Chem.*, 2005. **77**. 2297-2302.

61. McEwen, C.N., R.G. McKay, and B.S. Larsen, Analysis of solids, liquids, and biological tissues using solids probe introduction at atmospheric pressure on commercial LC/MS instruments. *Anal. Chem.*, 2005. **77**. 7826-7831.

62. Takats, Z., et al., Mass Spectrometry Sampling under Ambient Conditions with Desorption Electrospray Ionization. *Science*, 2004. **306**. 471-473.

63. Shiea, J., et al., Electrospray-Assisted Laser Desorption/Ionization Mass Spectrometry for Direct Ambient Analysis of Solids. *Rapid Commun. Mass Spectrom.*, 2005. **19**. 3701-3704.

64. Peng, I.X., et al., Electrospray-assisted laser desorption/ionization and tandem mass spectrometry of peptides and proteins. *Rapid Commun. Mass Spectrom.*, 2007. **21**. 2541-2546.

65. Huang, M.Z., et al., Direct protein detection from biological media through electrospray-assisted laser desorption ionization/mass spectrometry. *J. Proteome Res.*, 2006. **5**. 1107-1116.

66. Shiea, J., et al., Detection of native protein ions in aqueous solution under ambient conditions by electrospray laser desorption/ionization mass spectrometry. *Anal. Chem.*, 2008. **80**. 4845-4852.

67. Chang, D.Y., C.C. Lee, and J. Shiea, Detecting Large Biomolecules from High-Salt Solutions by Fused-Droplet Electrospray Ionization Mass Spectrometry. *Anal. Chem.*, 2002. **74**. 2465-2469.

68. Lee, C.C., et al., Generating Multiply Charged Protein Ions via Two-Step Electrospray Ionization Mass Spectrometry. *J. Mass Spectrom.*, 2002. **37**. 115-117.

69. Takats, Z., et al., Electrosonic Spray Ionization. A Gentle Technique for Generating Folded Proteins and Protein Complexes in the Gas Phase and for Studying Ion - Molecule Reactions at Atmospheric Pressure. *Anal. Chem.*, 2004. **76**. 4050-4058.

70. Chen, H.W., A. Venter, and R.G. Cooks, Extractive Electrospray Ionization for Direct Analysis of Undiluted Urine, Milk and Other Complex Mixtures Without Sample Preparation. *Chem. Comm.*, 20062042-2044.

71. Sampson, J.S., A.M. Hawkridge, and D.C. Muddiman, Generation and Detection of Multiply-Charged Peptides and Proteins by Matrix-Assisted Laser Desorption Electrospray Ionization (MALDESI) Fourier Transform Ion Cyclotron Resonance Mass Spectrometry. *J. Am. Soc. Mass. Spectrom.*, 2006. **17**. 1712-1716.

72. Sampson, J.S., A.M. Hawkridge, and D.C. Muddiman, Direct characterization of intact polypeptides by matrix assisted laser desorption electrospray ionization (MALDESI) quadrupole fourier transfrom ion cyclotron resonance mass spectrometry. *Rapid Commun. Mass Spectrom.*, 2007. **21**. 1150-1154.

73. Sampson, J.S., A.M. Hawkridge, and D.C. Muddiman, Construction of a Versatile High Precision Ambient Ionization Source for Direct Analysis and Imaging. *J. Am. Soc. Mass. Spectrom.*, 2008.

74. Dixon, R.B., et al., Ambient aerodynamic ionization source for remote analyte sampling and mass spectrometric analysis. *Anal. Chem.*, 2008. **80**. 5266-5271.

75. Pan, Z.Z., et al., Principal component analysis of urine metabolites detected by NMR and DESI-MS in patients with inborn errors of metabolism. *Analytical and Bioanalytical Chemistry*, 2007. **387**. 539-549.

76. Nemes, P. and A. Vertes, Laser Ablation Electrospray Ionization for Atmospheric Pressure, In Vivo, and Imaging Mass Spectrometry. *Anal. Chem.*, 2007. **79**. 8098-8106.

77. Rezenom, Y.H., J. Dong, and K.K. Murray, Infrared Laser-Assisted Desorption Electrospray Ionization Mass Spectrometry. *Analyst*, 2008. **133**. 226-232.

78. Aderogba, S., et al., Nanoelectrospray ion generation for high-throughput mass spectrometry using a micromachined ultrasonic ejector array. *Appl. Phys. Lett.*, 2005. **86**. -.

79. Cristoni, S., et al., Surface-Activated No-Discharge Atmospheric Pressure Chemical Ionization. *Rapid Comm. Mass Spectrom.*, 2003. **17**. 1973-1981.

80. Haapala, M., et al., Desorption atmospheric pressure photoilonization. *Anal. Chem.*, 2007. **79**. 7867-7872.

81. Hiraoka, K., et al., Explosive Vaporization of a Liquid Water Beam by Irradiation with a 10.6 um Infrared Laser. *Rapid Commun. Mass Spectrom.* , 1997. **11**. 474-478.

82. Na, N., et al., Development of a Dielectric Barrier Discharge Ion Source for Ambient Mass Spectrometry. *J. Am. Soc. Mass Spectrom.*, 2007. **18**. 1859-1862.

83. Ratcliffe, L.V., et al., Surface analysis under ambient conditions using plasma-assisted desorption/ionization mass spectrometry. *Anal. Chem.*, 2007. **79**. 6094-6101.

84. Takats, Z., et al., Direct, Trace Level Detection of Explosives on Ambient Surfaces by Desorption Electrospray Ionization Mass Spectrometry. *Chem. Commun.* , 20051950-1952.

85. Comisaro.Mb and A.G. Marshall, Fourier-Transform Ion-Cyclotron Resonance Spectroscopy. *Chem. Phys. Lett.*, 1974. **25**. 282-283.

86. Marshall, A.G., C.L. Hendrickson, and G.S. Jackson, Fourier transform ion cyclotron resonance mass spectrometry: A primer. *Mass Spectrom. Rev.*, 1998. **17**. 1-35.

87. Henry, K.D., et al., Fourier-Transform Mass-Spectrometry of Large Molecules by Electrospray Ionization. *Proc. Natl. Acad. Sci. U. S. A.*, 1989. **86**. 9075-9078.

88. Senko, M.W., et al., External accumulation of ions for enhanced electrospray ionization Fourier transform ion cyclotron resonance mass spectrometry. *J. Am. Soc. Mass Spectrom.*, 1997. **8**. 970-976.

89. Loo, J.A., C.G. Edmonds, and R.D. Smith, Tandem Mass-Spectrometry of Very Large Molecules - Serum-Albumin Sequence Information from Multiply Charged Ions Formed by Electrospray Ionization. *Anal. Chem.*, 1991. **63**. 2488-2499.

90. Rockwood, A.L., M. Busman, and R.D. Smith, Coulombic Effects in the Dissociation of Large Highly Charged Ions. *International Journal of Mass Spectrometry*, 1991. **111**. 103-129.

91. Smith, R.D., et al., Collisional Activation and Collision-Activated Dissociation of Large Multiply Charged Polypeptides and Proteins Produced by Electrospray Ionization. *J. Am. Soc. Mass Spectrom.*, 1990. **1**. 53-65.

92. Francl, T.J., et al., Experimental-Determination of the Effects of Space-Charge on Ion-Cyclotron Resonance Frequencies. *Int. J. Mass Spectrom. Ion Processes*, 1983. **54**. 189-199.

93. Jeffries, J.B., S.E. Barlow, and G.H. Dunn, Theory of Space-Charge Shift of Ion-Cyclotron Resonance Frequencies. *Int. J. Mass Spectrom. Ion Processes*, 1983. **54**. 169-187.

94. Taylor, P.K. and I.J. Amster, Space charge effects on mass accuracy for multiply charged ions in ESI-FTICR. *International Journal of Mass Spectrometry*, 2003. **222**. 351-361.

95. Limbach, P.A., P.B. Grosshans, and A.G. Marshall, Experimental-Determination of the Number of Trapped Ions, Detection Limit, and Dynamic-Range in Fourier-Transform Ion-Cyclotron Resonance Mass-Spectrometry. *Anal. Chem.*, 1993. **65**. 135-140.

96. Makarov, A., Electrostatic axially harmonic orbital trapping: A high-performance technique of mass analysis. *Anal. Chem.*, 2000. **72**. 1156-1162.

97. Kingdon, K.H., A method for the neutralization of electron space charge by positive ionization at very low gas pressures. *Physical Review*, 1923. **21**. 408-418.

98. Brooks, P.R. and D.R. Herschbach, Kingdon Cage as Molecular Beam Detector. *Rev. Sci. Instrum.*, 1964. **35**. 1528-&.

99. Lewis, R.R., Motion of Ions in the Kingdon Trap. *J. Appl. Phys.*, 1982. **53**. 3975-3980.

100. Yang, L.S. and D.A. Church, Confinement of Injected Beam Ions in a Kingdon Trap. *Nuclear Instruments & Methods in Physics Research Section B-Beam Interactions with Materials and Atoms*, 1991. **56-7**. 1185-1187.

101. Hardman, M. and A.A. Makarov, Interfacing the orbitrap mass analyzer to an electrospray ion source. *Anal. Chem.*, 2003. **75**. 1699-1705.

102. Olsen, J.V., et al., Parts per million mass accuracy on an orbitrap mass spectrometer via lock mass injection into a C-trap. *Molecular & Cellular Proteomics*, 2005. **4**. 2010-2021.

103. Null, A.P., A.I. Nepomuceno, and D.C. Muddiman, Implications of hydrophobicity and free energy of solvation for characterization of nucleic acids by electrospray ionization mass spectrometry. *Anal. Chem.*, 2003. **75**. 1331-1339.

104. Williams, D.K., et al., Synthesis, characterization, and application of iodoacetamide derivatives utilized for the ALiPHAT strategy. *J. Am. Chem. Soc.*, 2008. **130**. 2122-+.

105. Frahm, J.L., et al., Achieving augmented limits of detection for peptides with hydrophobic alkyl tags. *Anal. Chem.*, 2007. **79**. 3989-3995.

106. Mirzaei, H. and F. Regnier, Enhancing electrospray ionization efficiency of peptides by derivatization. *Anal. Chem.*, 2006. **78**. 4175-4183.

CHAPTER 2

Design and Construction of a Desorption Electrospray Ionization Source Coupled to Fourier Transform Ion Cyclotron Resonance Mass Spectrometry

2.1 Introduction

The field of mass spectrometry has experienced significant growth over the past decade, which is largely attributed to new ionization techniques and to advances in mass analyzer technology. The advent of electrospray ionization[1] (ESI) and matrix-assisted laser desorption ionization[2] (MALDI) has generated a particular interest in the biological sciences due to their ability to ionize macromolecules. As with any ionization technique, MALDI and ESI have distinct disadvantages. Recently, new ambient ionization techniques have been introduced to overcome some of these inherent limitations, thereby increasing the number of applications that can be addressed using mass spectrometry. In concert with the development of new ionization methods, mass analyzers have also been improved in terms of duty cycle, mass measurement accuracy, resolving power, and limits of detection.

Novel ambient techniques that require minimal sample preparation include *atmospheric solid analysis probe* [3] developed by Larsen and coworkers[3] and *direct analysis in real time* (DART) introduced by Cody et al.[4] These two techniques have a large number of applications; however, they are not suited for proteomic studies due to their inability to ionize high molecular weight biomolecules.

Ambient ionization techniques that have illustrated a potential for use in proteomic studies include *desorption electrospray ionization* (DESI),[5] *electrospray-assisted laser desorption ionization* (ELDI)[6, 7] and *matrix-assisted laser desorption electrospray ionization* (MALDESI).[8] These techniques are similar in that they all produce multiply-charged proteins; however, they are significantly different from a desorption standpoint. *Multiple-charging* of proteins is advantageous in FT-ICR-MS due to the inverse relationship between *cyclotron frequency* and *m/z*.[9] The high mass *resolving power* offered by FT-ICR-MS is essential due to the complex nature of biological specimens (*i.e.* plasma, serum).

Figure 2.1A displays a schematic of the desorption electrospray ionization process. Desorption electrospray ionization (DESI)[5] utilizes high velocity charged solvent droplets directed towards an analyte bearing surface. A variety of materials can constitute the surface; however, when using metallic surfaces often a voltage is need to avoid loss of charge to the surface.[10] The mechanism of DESI is still under investigation but it seems that the formation of a thin liquid film on the surface aids in solubilizing analyte on the surface.[11-13] This thin film is then created into offspring droplets by subsequent bombardment of primary droplets. The secondary droplets are transferred to the atmospheric interface of the mass spectrometer by the dynamic drag of the mass spectrometer and likely the reflection of the nitrogen gas off the surface. More on the mechanism(s) of DESI will be discussed in Chapter 3.

The other ionization techniques ELDI[6, 7, 14, 15], MALDESI[8, 16, 17], IR-LADESI[18], and LAESI[19, 20] are all similar in that they use a laser to promote desorption of analyte either from a liquid[14, 15, 17] or solid state.[6, 7] Multiple charged ions are produced from the fusion of either gas phase molecules or small droplets with an electrospray plume of usually 1:1 acetonitrle/water with 0.1% formic acid. Once the neutral molecules or droplets fuse with the charged droplets it is believed that mechanisms similar to that of ESI of biomolecules[1, 21] occur and produced multiply charged ions. **Figure 2.1B** illustrates a typical setup for each of these techniques. ELDI and MALDESI were first introduced and use a UV laser to promote desorption and ionization. Later IR-LADESI and LAESI were both presented and

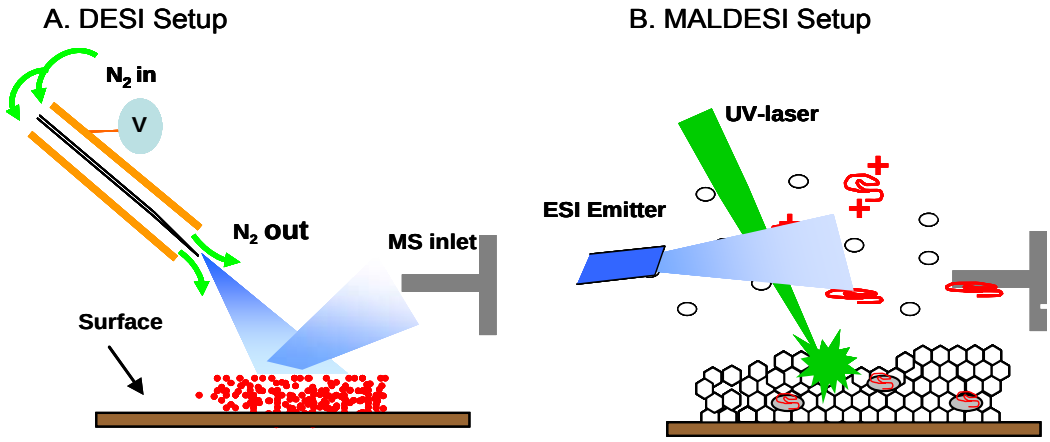

Figure 2.1 A schematic representation of both a typical (A) DESI and (B) MALDESI setup.

use an infrared wavelength laser for desorption. Since water absorbs in the IR wavelength region no organic matrix is required for the latter two methods. This

helps to speed up sample preparation and allows for clean spectra in the low *m/z* range where matrix ions typically provide complicated mass spectra.

These studies describe the first coupling of a DESI source to an FTICR mass spectrometer and subsequent improvements to the initial design. Furthermore, the multiple-charging observed, and the ability to analyze proteins deposited on a variety of surfaces will allow for numerous biological applications to be pursued. Although Bruce and coworkers[22] presented the DESI-FT-ICR mass spectrum of a low molecular weight peptide, focusing on the sensitivity improvement offered by a flared inlet capillary tube, this was the first presentation of DESI coupled to FTICR for protein analysis.

2.2. Experimental

2.2.1 Materials

All peptides and proteins used for these initial studies were from Sigma Aldrich (St Louis, MO). HPLC grade acetonitrile (ACN) and water were obtained from Burdick & Jackson (Muskegon, MI) and used as received. Pyrex glass slides were obtained in-house (NCSU Glass-blowing shop) and high purity nitrogen gas (99.98%) was obtained from MWSC High Purity Gases (Raleigh, NC).

2.2.2 Methods

All mass spectra were single acquisition and acquired in the positive ion mode using a highly modified Varian 9.4 Tesla ESI FT-ICR mass spectrometer

(Varian Corporation; Palo Alto, CA). The voltage on the DESI source was between +2800 and +3400 V while the entrance capillary was kept at a constant +40 V. Ions were accumulated for 3 seconds in RF-only hexapole[23] before being accelerated into the ICR cell. Spectra of bradykinin, melittin, glucagon, and insulin ranging in molecular weights from 1 kDa to 5 kDa were obtained by depositing 10 μL of 1 mg/mL (2-10 nmol) onto a Pyrex glass surface. The surface was then placed onto a XYZ stage for simple positional adjustment (Part Number 460A; Newport Corporation). The DESI spray plume consisted of water/acetonitrile (1:1) with 0.1% formic acid was directed at the sample spot. All other materials are discussed in the description of each source design (*vide infra*).

2.3. Construction of a Desorption Electrospray Ionization Source

2.3.1 Initial Design and Preliminary Data

Figure 2.2 illustrates the initial attempt at coupling a desorption electrospray ionization source to an FT-ICR mass spectrometer. The DESI source itself was a previously developed ESI source[24] and obtained in collaboration from Facundo Fernandez at Georgia Tech

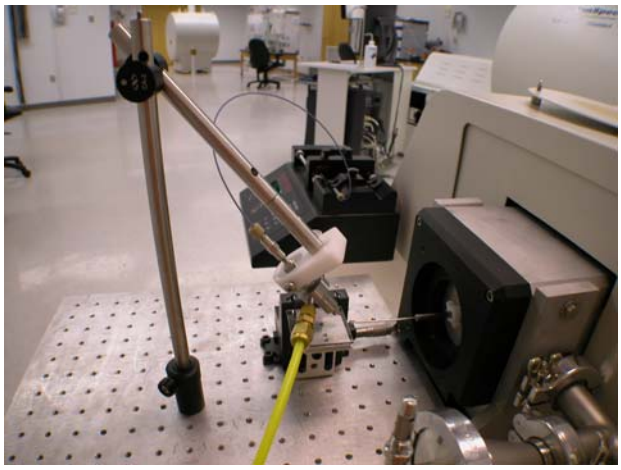

Figure 2.2 The "proof of principle" DESI-FTICR-MS experiment.

University. The converted DESI source consisted of two concentric silica capillaries. The spray emitter or liquid capillary (150 μm o.d. x 50 μm i.d; Part Number TSP050150; Polymicro Technologies), resided inside the gas capillary (350 μm o.d. x 250 μm i.d.; TSP250350; Polymicro Technologies) and protruded approximately 1 mm from the end of the gas capillary. The DESI source was mounted onto a six inch metal post (Newport Corporation; Part Number SP-6) using an in-house fabricated plastic holder, while the other end of this rod was affixed to an adjustable angle post clamp (Part Number Ca-2; Newport Corporation). Finally the 6 inch post was attached to a 16 inch post (Part Number SP-16; Newport Corporation) which was affixed to an in house breadboard. This clamp enabled both the incident angle of the electrospray plume (termed angle α) and the distance from the capillary to surface to be adjusted (termed d_1 distance). These angles and distances were found to be crucial in optimizing the DESI setup. Parameters introduced by Cooks and coworkers[5] to describe DESI analysis in this setup were as follows: d_1= 1-2

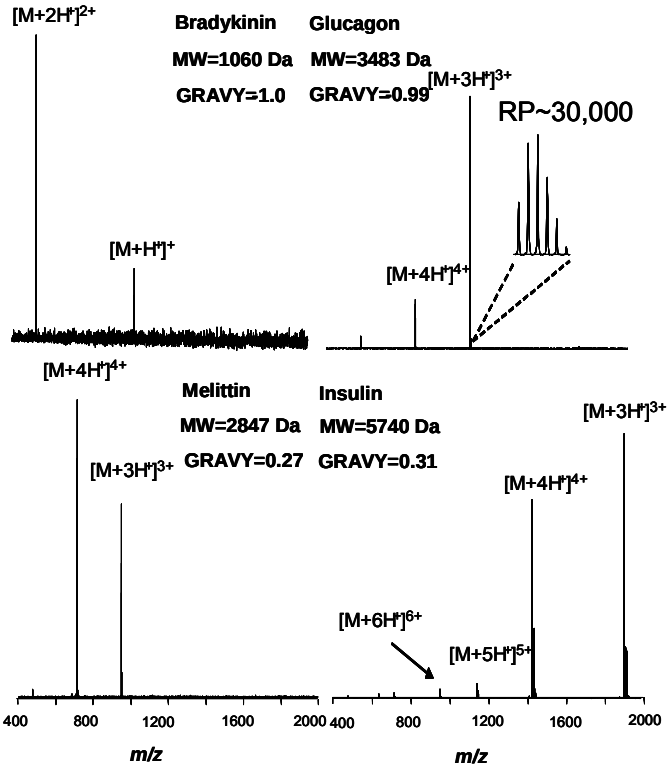

Figure 2.3 Preliminary DESI FT-ICR data of peptides and proteins deposited onto a glass surface. This data demonstrated the feasibility of DESI FT-ICR mass spectrometry.

mm (distance from surface to electrospray tip), d_2=<0.5 mm (distance from MS inlet to surface), α=60-70° (electrospray incident angle), and β=5-10° (collection angle). It is important to note that the ion abundance was the greatest when the distance from the glass surface to mass spectrometer inlet (d_2) was approximately zero.

Figure 2.3 illustrates the spectra obtained by the initial DESI-FT-ICR-MS[25] setup ranging in molecular weight from 1kDa to 5.7kDa and *GRAVY scores*[26] from -1.0 to 0.31. Multiply-charged species were observed, indicating charging mechanisms analogous to ESI of proteins. The inset in **Figure 2.3** illustrates the key advantage of coupling DESI with FT-ICR-MS, affording high resolving power. Importantly, the initial spectra were relatively free of any adducts. The inability to precisely adjust the parameters described above along with poor reproducibility warranted a new more robust DESI design.

2.3.2 A more Robust DESI Source

The new DESI design, developed in collaboration with Professor Graham Cooks (Purdue University) is illustrated in **Figure 2.4** and allows precise control over experimental parameters affording both improved reproducibility and greater ion abundance. The DESI source was housed in a PTFE holder (fabricated in house) which was affixed to a 360° rotational stage (Part Number 2525; Parker Motion) allowing the α angle to be precisely adjusted by 2° increments. The rotational stage was then attached to an XYZ stage (Part Number M4084M; Parker Motion), affording 25.4 mm of travel in all directions by 0.5 mm increments. Due to

the large physical size and awkwardness of manipulating the position of the original DESI source, a 1/16" Swagelok T union (Part Number SS-100-3; Raleigh Valve and Fitting, Raleigh NC), originally utilized in the development of electrosonic spray ionization,[27, 28] was used as the new DESI source. The Swagelok T union operated on the same basic principles as the previous DESI source, however, was much smaller and easier to maneuver. Finally a high magnification camera was mounted next to the sample to aid in the location of both the analyte spot and the DESI spray. The precise control of the geometric parameters afforded by the XYZ stage and rotational stages provided more reproducible DESI-MS data.

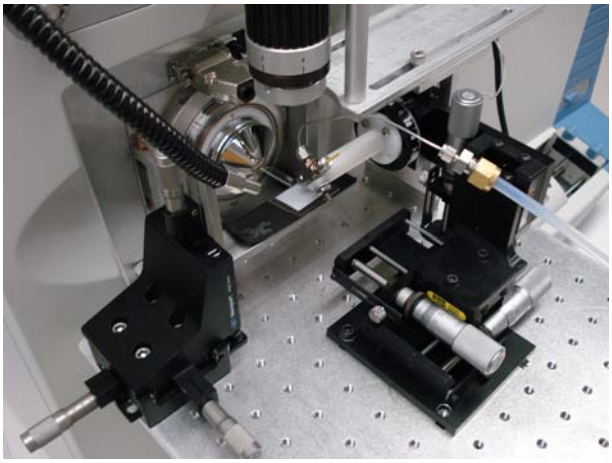

Figure 2.4 The 2nd generation DESI source

2.3.3 Final Source Design

The contemporary DESI source design is shown in **Figure 2.5** and is basically a further extension of the 2nd design. The DESI platform, from design 2, was mounted on an 8" x 8" adjustable height stage (Part Number 14-673-15; Fischer Scientific). This stage was then mounted onto a 24" x 30" breadboard table fabricated in house. Finally stainless steel casters (Part Number 1G196; Grainger Corporation) with brake kit (Part Number 4X698; Grainger Corporation)

provided portability and stability of the DESI source. In addition the final design allows for the facile implementation of DESI onto mass spectrometers with varying

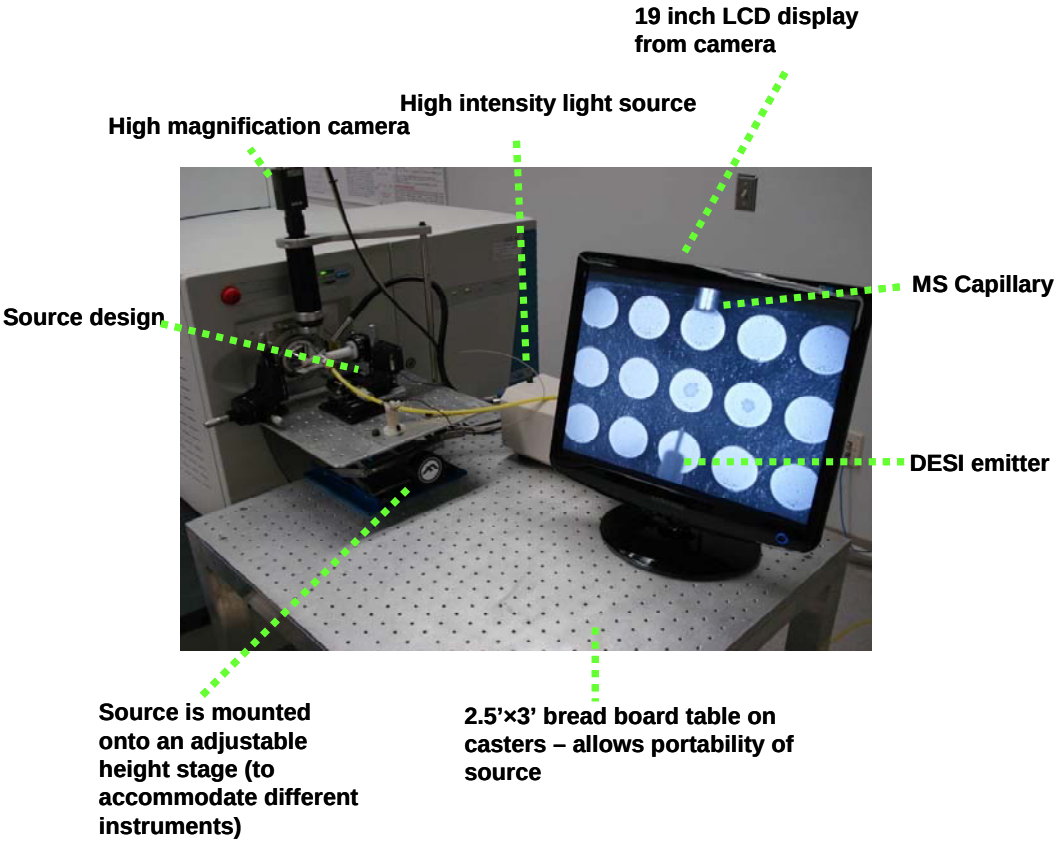

Figure 2.5 The contemporary DESI source design used in the Muddiman laboratory.

heights. The large area of the table top allows for permanent placement of the high magnification camera (Part Number KP-M1AN, Hitachi), light source (Part Number MI-150; Dolan Jenner), 19" LCD monitor (Staples Inc) and provides ample space for future modifications. The LCD monitor provides for visualization of both the position of the ESI emitter and sample spot, critical in obtaining optimal results.

2.4 Conclusions

There has been three different designs of a desorption electrospray ionization source with each subsequent design becoming more reproducible in terms of experimental geometry than the previous. The initial design demonstrated proof of principle; however, it was learned that the geometry of the source relative to the mass spectrometer played a major role in both signal stability and abundance. Therefore a XYZ stage and a precise angle rotator was incorporated into the 2nd design. The contemporary design further improved the reproducibility of these geometric parameters and provided permanent placement of several important components. In addition the source became portable and is currently able to be pulled up to any mass spectrometer with an atmospheric interface for direct analysis regardless instrument height. All further results discussed in this dissertation were obtained with either source design 2 or 3.

2.5 References

1. Fenn, J.B., et al., Electrospray Ionization for Mass-Spectrometry of Large Biomolecules. *Science*, 1989. **246**. 64-71.

2. Karas, M. and F. Hillenkamp, Laser Desorption Ionization of Proteins with Molecular Masses Exceeding 10000 Daltons. *Anal. Chem.*, 1988. **60**. 2299-2301.

3. McEwen, C.N., R.G. McKay, and B.S. Larsen, Analysis of solids, liquids, and biological tissues using solids probe introduction at atmospheric pressure on commercial LC/MS instruments. *Anal. Chem.*, 2005. **77**. 7826-7831.

4. Cody, R.B., J.A. Laramee, and H.D. Durst, Versatile new ion source for the analysis of materials in open air under ambient conditions. *Anal. Chem.*, 2005. **77**. 2297-2302.

5. Takats, Z., et al., Mass spectrometry sampling under ambient conditions with desorption electrospray ionization. *Science*, 2004. **306**. 471-473.

6. Shiea, J., et al., Electrospray-assisted laser desorption/ionization mass spectrometry for direct ambient analysis of solids. *Rapid Commun. Mass Spectrom.*, 2005. **19**. 3701-3704.

7. Huang, M.Z., et al., Direct protein detection from biological media through electrospray-assisted laser desorption ionization/mass spectrometry. *J. Proteome Res.*, 2006. **5**. 1107-1116.

8. Sampson, J.S., A.M. Hawkridge, and D.C. Muddiman, Generation and detection of multiply-charged peptides and proteins by matrix-assisted laser desorption electrospray ionization (MALDESI) Fourier transform ion cyclotron resonance mass spectrometry. *J. Am. Soc. Mass Spectrom.*, 2006. **17**. 1712-1716.

9. Henry, K.D., et al., Fourier-Transform Mass-Spectrometry of Large Molecules by Electrospray Ionization. *Proc. Natl. Acad. Sci. U. S. A.*, 1989. **86**. 9075-9078.

10. Takats, Z., J.M. Wiseman, and R.G. Cooks, Ambient mass spectrometry using desorption electrospray ionization (DESI): instrumentation, mechanisms and applications in forensics, chemistry, and biology. *J. Mass Spectrom.*, 2005. **40**. 1261-1275.

11. Bereman, M.S. and D.C. Muddiman, Detection of Attomole Amounts of Analyte by Desorption Electrospray Ionization Mass Spectrometry (DESI-MS) Determined Using Fluorescence Spectroscopy. *J. Am. Soc. Mass Spectrom.*, 2007. **18**. 1093-1096.

12. Costa, A.B. and R.G. Cooks, Simulation of atmospheric transport and droplet-thin film collisions in desorption electrospray ionization. *Chemical Communications*, 20073915-3917.

13. Costa, A.B. and R.G. Cooks, Simulated splashes: Elucidating the mechanism of desorption electrospray ionization mass spectrometry. *Chem. Phys. Lett.*, 2008. **464**. 1-8.

14. Peng, I.X., et al., Electrospray-assisted laser desorption/ionization and tandem mass spectrometry of peptides and proteins. *Rapid Commun. Mass Spectrom.*, 2007. **21**. 2541-2546.

15. Shiea, J., et al., Detection of native protein ions in aqueous solution under ambient conditions by electrospray laser desorption/ionization mass spectrometry. *Anal. Chem.*, 2008. **80**. 4845-4852.

16. Sampson, J.S., A.M. Hawkridge, and D.C. Muddiman, Direct characterization of intact polypeptides by matrix assisted laser desorption electrospray ionization (MALDESI) quadrupole fourier transfrom ion cyclotron resonance mass spectrometry. *Rapid Commun. Mass Spectrom.*, 2007. **21**. 1150-1154.

17. Sampson, J.S., A.M. Hawkridge, and D.C. Muddiman, Development and characterization of an ionization technique for analysis of biological macromolecules: Liquid matrix-assisted laser desorption electrospray ionization. *Anal. Chem.*, 2008. **80**. 6773-6778.

18. Rezenom, Y.H., J. Dong, and K.K. Murray, Infrared laser-assisted desorption electrospray ionization mass spectrometry. *Analyst*, 2008. **133**. 226-232.

19. Nemes, P. and A. Vertes, Laser ablation electrospray ionization for atmospheric pressure, in vivo, and imaging mass spectrometry. *Anal. Chem.*, 2007. **79**. 8098-8106.

20. Nemes, P., et al., Ambient molecular imaging and depth profiling of live tissue by infrared laser ablation electrospray ionization mass spectrometry. *Anal. Chem.*, 2008. **80**. 4575-4582.

21. Fenn, J.B., et al., Electrospray Ionization-Principles and Practice. *Mass Spectrom. Rev.*, 1990. **9**. 37-70.

22. Wu, S., et al., Incorporation of a flared inlet capillary tube on a Fourier transform ion cyclotron resonance mass spectrometer. *J. Am. Soc. Mass Spectrom.*, 2006. **17**. 772-779.

23. Senko, M.W., et al., External accumulation of ions for enhanced electrospray ionization Fourier transform ion cyclotron resonance mass spectrometry. *J. Am. Soc. Mass Spectrom.*, 1997. **8**. 970-976.

24. Hoang, T.T., S.W. May, and R.F. Browner, Developments with the oscillating capillary nebulizer--effects of spray chamber design, droplet size and turbulence on analytical signals and analyte transport efficiency of selected biochemically important organoselenium compounds. *J. Anal. At. Spectrom.*, 2002. **17**. 1575-1581.

25. Bereman, M.S., et al., Direct high-resolution peptide and protein analysis by desorption electrospray ionization Fourier transform ion cyclotron resonance mass spectrometry. *Rapid Commun. Mass Spectrom.*, 2006. **20**. 3409-3411.

26. Kyte, J. and R.F. Doolittle, A Simple Method for Displaying the Hydropathic Character of a Protein*. J. Mol. Biol.*, 1982. **157**. 105-132.

27. Takats, Z., et al., Amino acid clusters formed by sonic spray ionization*. Anal. Chem.*, 2003. **75**. 1514-1523.

28. Takats, Z., et al., Electrosonic spray ionization. A gentle technique for generating folded proteins and protein complexes in the gas phase and for studying ion - Molecule reactions at atmospheric pressure*. Anal. Chem.*, 2004. **76**. 4050-4058.

Chapter 3

Fundamentals of Desorption Electrospray Ionization coupled to Mass Spectrometry

3.1 Introduction

Recently several new ionization techniques, referred to in the literature as "direct analysis methods," have been introduced.[1] These techniques offer unique advantages because they allow for ambient analysis and require minimal sample preparation leading to higher throughput. *Atmospheric solid analysis probe* (ASAP) developed by Larsen and coworkers[2, 3] and *direct analysis in real time* (DART) introduced by Cody et al.[4-6] are both techniques with a potential for a range of applications for small molecule analysis; however, to date, there are few reports describing applications of these techniques. Introduced most recently are *electrospray laser desorption ionization*[7, 8] (ELDI), *matrix-assisted laser desorption electrospray ionization*[9, 10] *laser ablation electrospray ionization*[11, 12], and *infrared laser desorption electrospray ionization*.[13] These techniques have exhibited potential for proteomic analyses.

Presented by Cooks and coworkers in 2004, desorption electrospray ionization[14] (DESI) was one the first techniques introduced in this "family" of direct analysis methods. Presently the majority of the literature focuses on this technique and its applications ranging from small molecule to proteomic analyses.[15] This ionization method has been coupled to several different mass analyzer

technologies including: linear ion trap,[14] orbitrap,[16] Fourier transform ion cyclotron resonance,[17] and other hybrid MS platforms.[18-20]

DESI has proven its versatility in its ability to analyze a range of analytes[17, 19, 21-26]; however, certain fundamentals of the process remain unknown. In future biological applications of this ionization method, it is essential to explore and understand the several characteristics of this technique including: 1) the effects of solvent composition and surface type on spot size; 2) a method to optimize geometric parameters; 3) mechanism(s) of DESI; 4) and methods to determine amount of material initially required and the amount subsequently removed from the surface during DESI-MS analysis.

The size of the DESI solvent spray spot is dependent on a number of factors including surface properties, solvent composition, nitrogen pressure, flow rate, and the diameter of the DESI spray emitter.[27] The size of the DESI spot has been reported throughout the literature; however, a more comprehensive study of the effects of solvent composition and surface type has not been presented. Since the spot size will ultimately play a crucial role in the amount of material ablated and because high resolution (i.e. small spot size) is essential for potential applications in tissue imaging, a more detailed study of the experimental parameters affecting the DESI spot size was warranted. These studies presented show the dependence of surface type, flow rate, and solvent composition on spot size. Spot size, in the literature had been studied previously by fluorescence spectroscopy[18, 28]. Initially,

in these experiments, optical microscopy and fluorescence spectroscopy were utilized to estimate the spot size.

The geometric parameters in DESI have a significant impact on ion abundance.[27] Thus, in order to obtain optimal signal, it was necessary to explore certain experimental parameters including the α angle (angle between DESI emitter and surface), d_1 distance (distance between DESI emitter and surface), d_2 distance (distance between MS inlet and surface), and the d_3 distance (distance from the DESI emitter to the MS capillary). A method that allows for quick optimization of these parameters is described herein.

The mechanism of desorption and ionization in DESI is still not completely understood. However, in studies completed thus far, it seems that analyte is first dissolved on the surface (i.e. wetting of the surface) and secondly, analyte containing offspring droplets are sampled by the mass spectrometer.[29, 30] It is believed that the combination of Coulombic forces, reflection of nitrogen gas off the surface and the dynamic drag of the vacuum interface are responsible for both the creation and transfer of *offspring droplets* into the mass spectrometer.[27, 31] Once liberated from the surface, offspring droplets undergo ESI-like mechanisms for the generation of multiply-charged ions for peptide and protein analysis.

One of the more fundamental aspects of DESI-MS analysis, yet to be investigated, is quantifying the amount of material initially required and subsequently removed from the surface during analysis. Elementary in nature, these experiments present quite a formidable challenge. In future biological

applications of DESI, it is essential to explore and understand the detection limits of this technique. Cooks and coworkers have used a “down spotting technique” in which a decreasing amounts of material are spotted onto a surface until no signal is obtained to report limits of detection for a range of molecules.[27] Although this technique is quick and gives a rough estimate of the detection limits of the method, it is not quantitative since the majority of sample is often left unperturbed on the surface after DESI analysis. Described herein, is the development of methods utilizing fluorescence spectroscopy[32] and *quartz crystal microbalance* (QCM) to quantify the amount of material removed from the surface during DESI-MS analysis.

3.2 Experimental

3.2.1 Materials

Rhodamine 6G, formic acid, melittin, and quaternary amines were obtained from Sigma Aldrich (St. Louis, MI) and used without further purification. Methanol, acetonitrile, and water were purchased from Burdick & Jackson (Muskegon, MI). PTFE surfaces, utilized in these experiments, were acquired from McMaster Carr (Atlanta, GA).

3.2.2 Methods

The DESI spray solution was composed of acetonitrile and water (1:1 v/v) with 0.1% formic acid. For determining material removed by fluorescence

spectroscopy, rhodamine 6G stock standards were prepared in the same solvent composition and 10 μL of a 0.02 μM solution (200 fmol) were placed onto a PTFE surface and dried overnight in the ambient environment prior to fluorescent measurements and DESI-MS analysis. The fluorescent intensities of four samples were examined before and after DESI-MS analysis. Each sample was analyzed by DESI-MS for two minutes. In addition, three controls were used which underwent all processes (e.g., physical handling, length of light exposure) except DESI analysis and allowed for a correction in the final fluorescent intensities of the samples.

All mass spectra were acquired on an LTQ linear ion trap mass spectrometer (Thermo Finnegan, San Jose Ca) in the positive-ion mode. The maximum *injection time* was set at 200 ms and 3 microscans were obtained per mass spectrum. Automatic gain control (AGC) was set to 1×10^6 and never reached this target value, effectively allowing the ion trap to collect for 200 ms per mass spectrum. The source voltage and capillary voltage were kept constant through all experiments at 4 kV and 37 V, respectively. The capillary temperature was set at 200°C. Prior to interpretation, all EIC data were boxcar smoothed (n=7).

3.2.3 Fluorescence Measurements

A BioRad Pharos FX™ Plus Molecular Imager (Hercules, Ca) was used to obtain the total fluorescent intensity of rhodamine 6G before and after DESI-MS analysis. The decrease in total fluorescence was then used to quantitate the

amount of material removed from the surface. Excitation of the dye was achieved through an internal laser (532 nm). Data were acquired and analyzed via Quantity One software provided by BioRad.

3.2.4 Quartz Crystal Microbalance

Quartz crystal microbalances (10 MHz) were purchased from International Crystal Manufacturing (Oklahoma City, OK). The QCM system used in these studies has been previously described elsewhere.[33] The QCM measurements were performed outside the faraday cage and paralleled DESI-MS measurements. It was found that removing the QCM leads from the microbalance, even just for seconds, and then reattaching them led to inconsistencies in the resonant frequency. Thus, it was mandatory that the QCM leads be attached throughout the whole experiment. DESI mass spectrums were acquired for 1 minute.

3.3 Investigating parameters that affect Desorption Spot Size

Figure 3.1 illustrates an image of a protein deposited onto a glass surface before DESI and then the same glass surface after being exposed to the DESI spray (1:1 ACN:H20 0.1% FA) for approximately 8 seconds. From these two pictures an estimate of the spot size diameter of ~500 μm can be made. The area of removal in **Figure 3.1** is actually more of an oval shape than circular, an observation that can be attributed with the

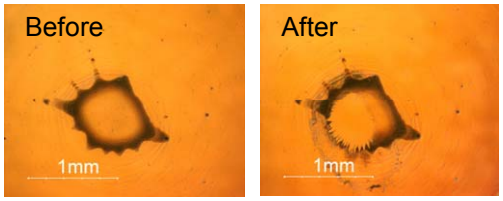

Figure 3.1 Optical Microscope images of before and after DESI analysis of a protein deposited on a glass surface

acute angle (α; emitter to surface) used in DESI-MS analysis. It is also important and interesting to note that in **Figure 3.1** (after DESI) some of the material was pushed outside the interaction area and not actually desorbed from the surface.

Further studies of the DESI spot size utilized a 20 μM solution of rhodamine 6G. The dye solution was used as the DESI solvent and sprayed onto a number of surfaces, using different flow rates and solvent compositions. After spraying for approximately 8-10 seconds the material was than imaged using a BioRad Pharos FX™ Plus Molecular Imager (Hercules, Ca). Displayed in **Figure 3.2** is a comparison between surfaces, solvent compositions, and flow rates and their effects on the DESI spot size. From the data in Figure 3.2, the PTFE surface allowed for the highest resolution obtained in the three difference solvent compositions used. Also shown is the direct correlation between percent aqueous and flow rate to the size of the DESI spot. The differences between PMMA and glass surfaces were not as significant.

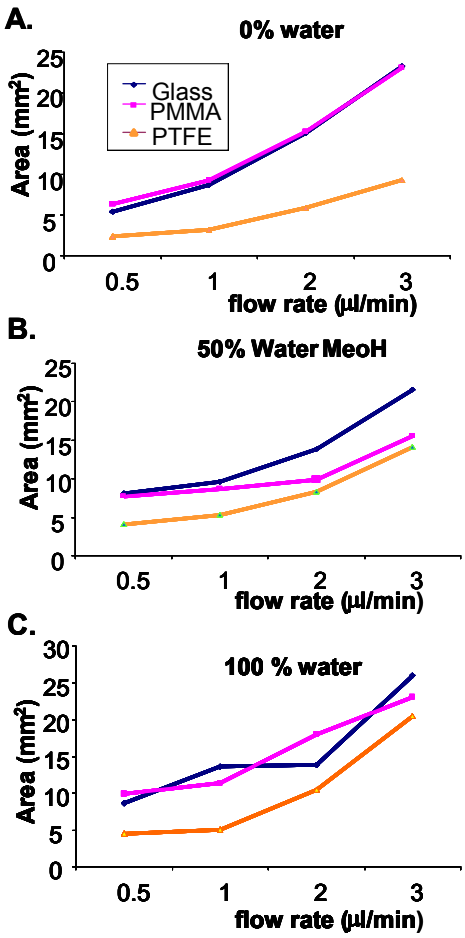

Figure 3.2 DESI spot size as a function of flow rate, solvent composition, and surface type.

3.4 Optimizing Geometric Parameters in DESI

The nature of DESI does not readily allow for efficient optimization where the population of ions must be constant over an extended period of time as characteristic of ESI. A decrease in signal may be related to a change in geometry or attributed to the depletion of analyte on the surface. Thus, it was necessary to have a constant ion flux. To accomplish this, a solution of melittin (3 μM) was used as the DESI solvent and sprayed onto a blank PTFE surface. This experiment allowed for constant ion generation.

Figure 3.3A illustrates the inverse relationship of the d_3 distance and ion abundance. From these experiments the optimal distance was between 3 and 4 mm. A smaller distance actually resulted in direct electrospray from

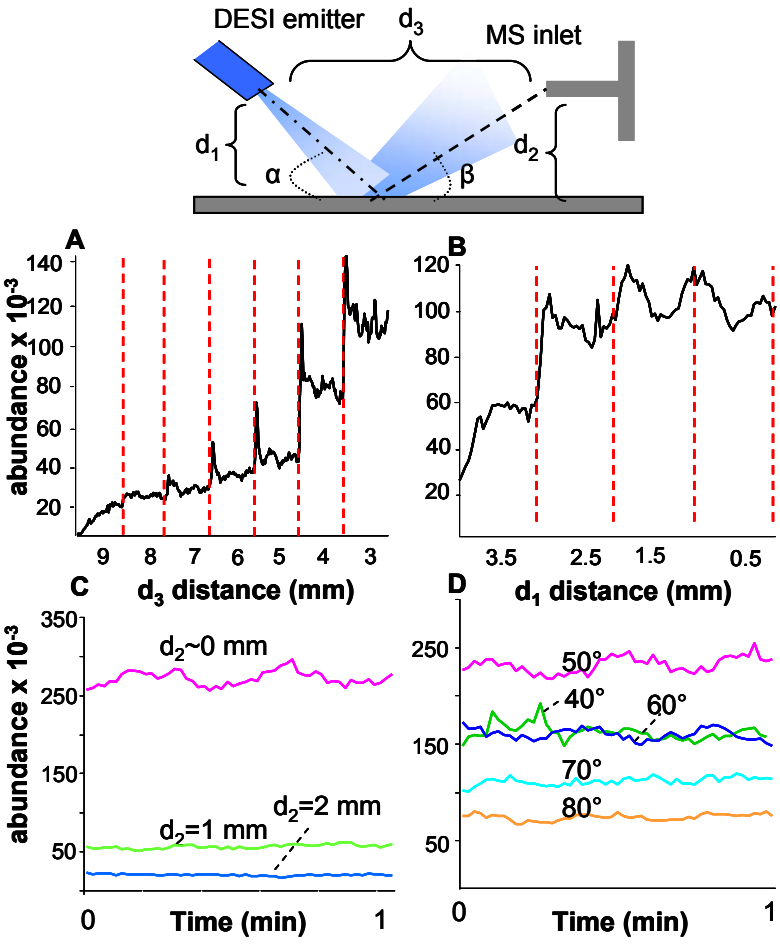

Figure 3.3 The dependence of ion abundance on several geometric parameters.

the emitter tip into the capillary, without first impacting the surface. **Figure 3.3B** displays a plot of the ion abundance as a function of d_1 distance. Signal increases with decreasing d_1 distance, with an optimal distance between 0.5-2 mm. However, when performing a "real" DESI experiment, it has been observed that a small d_1 distance (0.5-1) is associated with too much wetting of the surface, resulting in no signal or just a large spike in the total ion chromatogram (TIC). Shown in **Figure 3.3C** is the relationship between ion abundance and the d_2 distance. Again, as the distance decreases the ion abundance increases. The optimal ion abundance in this experiment was observed to be approximately 0.5 mm. Finally these optimized geometric parameters were used to investigate the dependence of the α angle on ion abundance. As displayed in **Figure 3.3D,** ion abundance reached a maximum between 50-60 degrees. Abundance dramatically declines with angles above 60°. For subsequent studies reported, these optimized parameters discussed here were used.

3.5 Mechanisms of Desorption and Ionization in DESI

During all comparison studies between ESI and DESI, experimental parameters were kept constant where possible (e.g., source voltage, capillary temperature, tube lens voltage, etc). Obviously certain parameters (e.g., geometric) were not constant due to the different nature of these two ionization methods.

The mechanism of desorption and ionization in DESI is still not completely understood. However, in studies completed thus far, it seems that analyte is first dissolved on the surface (i.e. wetting of the surface) and secondly, analyte containing offspring droplets are sampled by the mass spectrometer.[29, 30] **Figure 3.4A** displays the high correlation between the average charge state observed by DESI and ESI of peptides of increasing molecular weight. It is interesting to note that the slope of the line is greater than one, indicating increased charging of peptides analyzed by ESI. This is possibly due to the loss of charge to the insulating surface resulting in lower overall charging of the secondary droplets in DESI.

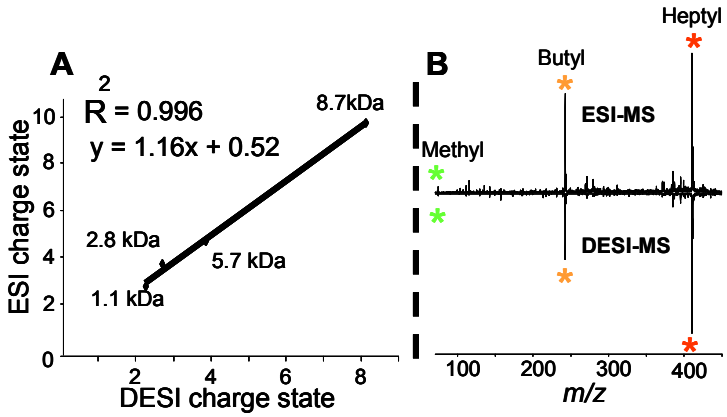

Figure 3.4 A) Charge state comparisons between ESI and DESI **B)** Response biases towards more hydrophobic molecules, characteristic of ESI, are also observed in DESI.

In ESI, the greater the hydrophobicity of a molecule, the greater the signal response.[34, 35] To further provide evidence for the similarities between the mechanism of ESI and DESI, studies were carried out by analyzing an equal molar mixture of quaternary halogenated amines of increasing hydrophobicity (methyl, butyl, heptyl) by DESI and ESI-MS. These molecules were strategically selected because of the permanent charge each possess and the only factor effecting ESI response would be the intrinsic properties

of each molecule (i.e hydrophobicity). For ESI-MS a 4 μM mixture (1.33 μM individual) was electrosprayed at a potential of 2.5 kV. For analysis by DESI-MS, 10 μL of a 100 μM (33 μM individual) mixture were placed onto a PTFE surface, dried and analyzed with a source voltage of 2.5 kV. The top mass spectrum in **Figure 3.4B**, displays the analysis of the quaternary amines by ESI-MS while the reflected axis shows the DESI-MS analysis. As exhibited by the figures, both DESI and ESI-MS analysis show increased ion abundance with increasing chain length (i.e. hydrophobicity), implicating the analyte location in DESI, is more towards the central area of the droplet instead of residing on the surface. These simple experiments provide further evidence for the droplet-pickup mechanism as both *multiple-charging* and the *hydrophobic effect*, characteristic of ESI, are also present in DESI.

3.6 Methods to Determine Amount of Material Removed

3.6.1 Fluorescence Spectroscopy

Displayed in **Figure 3.5** are representative selected ion chromatograms (*m/z* = 443±1 and 415±1) from the analysis of rhodamine 6G by DESI-MS. Confirmed by MS/MS experiments and possibly due to thermal degradation inside the

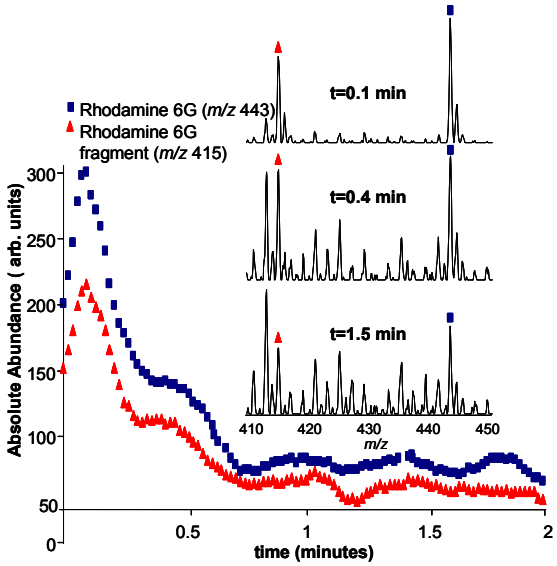

Figure 3.5 Selective ion chromatograms (SICs) of m/z 443 and 415 along with mass spectra

mass spectrometer inlet capillary, the ion at *m/z* 415 was determined to be a fragment of rhodamine 6G. As shown in **Figure 3.5,** the abundance of both ions track each other throughout the two minute analysis. The inset shows three representative mass spectra of decreasing S/N obtained at 0.1, 0.4 and 1.5 minutes.

	S1	S2	S3	S4
Material removed (fmol)	56	29	25	54
Amount/MS (amol)	96	49	42	90

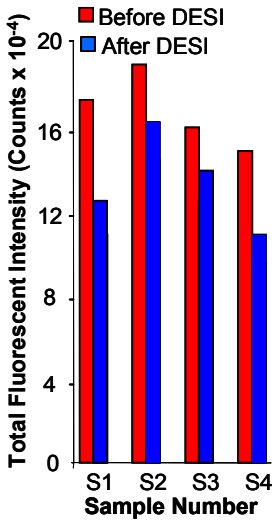

Figure 3.6 Fluorescence intensity of samples before and after DESI-MS analysis. Material removed from surface and amount per mass spectrum are displayed in table for each sample.

The fluorescence intensities of the 4 samples before and after DESI analysis are displayed in **Figure 3.6**. A decrease in intensity was observed not only in the samples (**S1, S2, S3, S4**), but also in the three controls. The controls underwent the same physical processes as the samples (e.g., handling, length of light exposure) except analysis by DESI-MS. The decrease in fluorescent intensity of the controls was not as significant as the decrease as a result of DESI-MS analysis. Thus, the fluorescence of each of the four samples after DESI-MS analysis was increased by 9.3% (average percentage decrease of the three controls) of the initial fluorescent intensity to account for this observation.

The total amount of material placed on the surface (200 fmol) along with the adjusted percentage decrease in fluorescence intensity allowed for a calculation of the total amount of material removed from the surface after two minutes of analysis

by DESI-MS. Furthermore, using the amount of material removed in conjunction with the length of the analysis (120 s) an average amount of material removed per second can be calculated. Finally, combined with the *injection time* (IT) in the ion trap (200 ms) and the previous calculation, an average amount of material per mass spectrum was determined. The average of all four samples indicates approximately 70 attomoles of rhodamine 6G were detected per mass spectrum. The table in **Figure 3.6** summarizes these data. The material per mass spectrum is a conservative calculation and in reality this number is much lower, simply due to the sampling efficiency of DESI-MS, which as in ESI, is very low.[36, 37] It is interesting to note that the amount of material removed from the surface in these studies varied by two-fold. This phenomenon is attributed to the non uniform distribution of the dye on the surface referred to as the sweet-spot effect.[27]

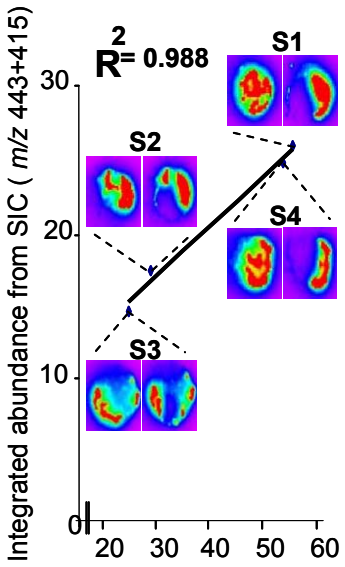

Figure 3.7 Plot of MS ion abundance as a function of material removed.

A strong correlation (R^2=0.988) exists between the integrated areas of the selected ion chromatograms (*m/z* 443+415) and the amount of material removed from the surface as shown in **Figure 3.7**. The plot in **Figure 3.7** emphasizes the ability of using fluorescence to monitor the amount of material removed, as a larger decrease in fluorescence (increase in material removed) directly corresponds to an

increase in signal abundance. Also displayed in **Figure 3.7** are representative before and after pictures illustrating both the area of analyte removal and the excess analyte left unperturbed on the surface.

3.6.2 Quartz Crystal Microbalance (QCM)

Alternative methods for determining the amount of material removed were explored due to the limitations discovered in using fluorescence spectroscopy (e.g., photobleaching). A *quartz crystal microbalance* (QCM) is an extremely sensitive mass detector capable of detecting changes in the nano-gram range. A QCM is a piezoelectric device fabricated from a thin quartz crystal with two metal electrodes attached to both sides. The crystal oscillates at its resonant frequency upon application of an rf voltage to the two electrodes. Changes in mass directly correlate to changes in the resonant frequency and can be calculated using Sauerbrey's equation (**Equation 3.1**). Change in mass density **(Δm_d)** is linear related to the change in frequency (**Δf**), density of the quartz crystal (**ρ_q**), speed of sound in quartz (**V_q**), and inversely related to the resonant frequency of the electrode (**f**).[38]

$$\Delta m_d = \frac{\Delta f \rho_q V_q}{2f^2} \qquad (3.1)$$

A gold QCM electrode (International Crystal Manufacturing, Oklahoma City, OK) was investigated as a potential method to determine the amount of rhodamine 6G removed from the surface. One hundred nanograms (1 μL of 0.1 mg/mL solution) of analyte were placed on the QCM electrode, actively dried and then

analyzed by DESI-MS for 1 minute. The analyte spot formed from depositing 1 μL of solution was analyzed 4 different times. Between each DESI-MS analysis the QCM electrode was slightly moved to expose fresh analyte to the DESI solvent plume. **Figure 3.8** displays a "real time" DESI-QCM experiment and also labels the different parts of the experiment. Calculations of material removed after each individual DESI experiment were made using Sauerbrey's equation and by calculating the difference in frequency before and after each experiment. Baseline frequencies were established by taking the average of 50 data points. A plot illustrating the strong correlation between the amount of material removed (calculated from the QCM response) and the MS ion abundance (m/z 443) is shown in **Figure 3.9**. A dual x-axis is provided showing the material removed in both nanograms and picomoles. Again using the

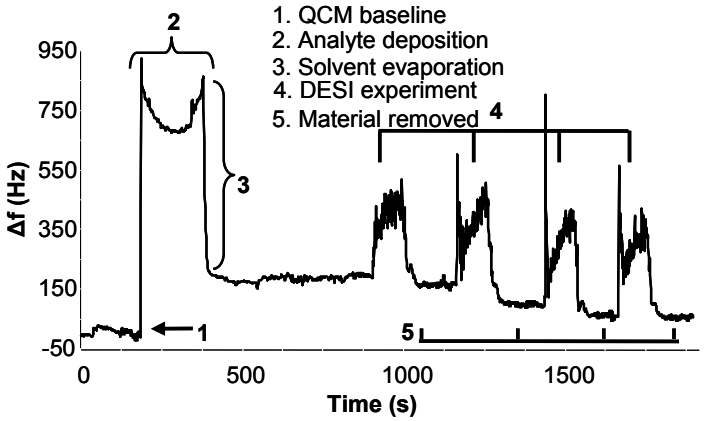

Figure 3.8 A real time plot relating QCM response to analyte deposition and DESI-MS analysis.

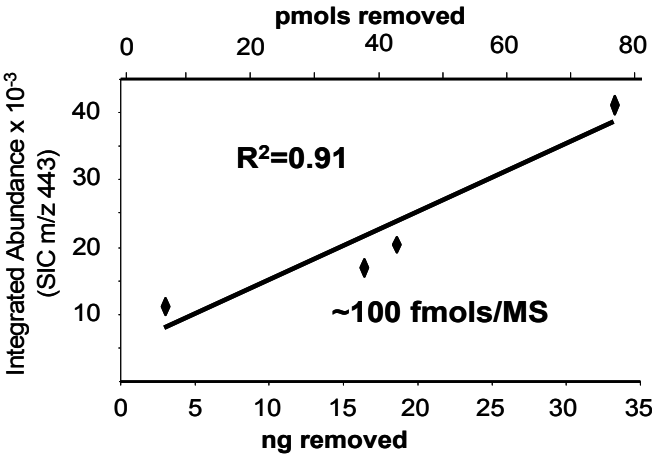

Figure 3.9 A plot of ion abundance as a function of material removed derived from Sauerbrey's equation

amount of material removed, length of analysis, and the IT fill time an average amount of material per mass spectrum can be determined (similar to fluorescent calculations). The average of the 4 spots analyzed indicates approximately 100 fmols per mass spectrum were consumed in these DESI/QCM experiments.

Similarities exist between the results obtained by the two methods used to quantitate the material removed. First the sweet-spot effect is present in both sets of data (QCM and fluorescence) as the amount of material removed varied significantly and depended on where the DESI plume impinged on the analyte bearing surface. In addition, a strong correlation exists between material removed and ion abundance in both methods. However, the material per mass spectrum, calculated using the fluorescence data, was a 1000-fold lower than using the data from the QCM experiment. In reality these results are difficult to compare given the different methods used, solutions, and days of analyses. A key contributing factor to this discrepancy may be the different surfaces used for analysis. For QCM the surface was metallic (i.e. gold) and for the fluorescence experiments an insulating surface was employed (i.e. PTFE). These results suggest that substrate properties play a significant role in determining the ion abundance in DESI-MS.

Both methods, fluorescence spectroscopy and quartz crystal microbalance, presented significant limitations. For fluorescence spectroscopy the main limitation was the requirement that molecule fluoresce and the problem of photobleaching which occurred during transport between DESI-MS analysis and the fluorescence scanner. The sensitivity of the quartz crystal microbalance presented the largest

problem during these experiments as the slightest vibrations within the lab would give large spikes in the baseline frequency. Also the residue of the DESI solvent was found to adversely effect the quartz oscillations.

3.7 Conclusions

Several parameters affect the DESI spot size, which subsequently determines the amount of material removed from the surface. The mechanism of DESI is analogous to ESI in that both *multiple-charging* and the *hydrophobic effect*, characteristic of ESI, are observed in DESI. Signal abundance depends significantly on the many geometric parameters in DESI. Efforts have been made to explore and optimize these parameters. Fluorescence spectroscopy and QCM have been both investigated as methods to determine amount of material removed from the surface by DESI-MS. Both methods give strong correlations between material ablated and ion abundance; however, calculations using the fluorescent data indicate 1000-fold higher sensitivity.

3.8 References

1. Harris, G.A., L. Nyadong, and F.M. Fernandez, Recent developments in ambient ionization techniques for analytical mass spectrometry*. Analyst*, 2008. **133**. 1297-1301.

2. McEwen, C.N., R.G. McKay, and B.S. Larsen, Analysis of solids, liquids, and biological tissues using solids probe introduction at atmospheric pressure on commercial LC/MS instruments*. Anal. Chem.*, 2005. **77**. 7826-7831.

3. McEwen, C. and S. Gutteridge, Analysis of the inhibition of the ergosterol pathway in fungi using the atmospheric solids analysis probe (ASAP) method*. J. Am. Soc. Mass Spectrom.*, 2007. **18**. 1274-1278.

4. Cody, R.B., J.A. Laramee, and H.D. Durst, Versatile new ion source for the analysis of materials in open air under ambient conditions*. Anal. Chem.*, 2005. **77**. 2297-2302.

5. Pierce, C.Y., et al., Ambient generation of fatty acid methyl ester ions from bacterial whole cells by direct analysis in real time (DART) mass spectrometry*. Chemical Communications*, 2007807-809.

6. Fernandez, F.M., et al., Characterization of solid counterfeit drug samples by desorption electrospray ionization and direct-analysis-in-real-time coupled to time-of-flight mass spectrometry*. Chemmedchem*, 2006. **1**. 702-+.

7. Shiea, J., et al., Electrospray-assisted laser desorption/ionization mass spectrometry for direct ambient analysis of solids*. Rapid Commun. Mass Spectrom.*, 2005. **19**. 3701-3704.

8. Huang, M.Z., et al., Direct protein detection from biological media through electrospray-assisted laser desorption ionization/mass spectrometry*. J. Proteome Res.*, 2006. **5**. 1107-1116.

9. Sampson, J.S., A.M. Hawkridge, and D.C. Muddiman, Generation and detection of multiply-charged peptides and proteins by matrix-assisted laser desorption electrospray ionization (MALDESI) Fourier transform ion cyclotron resonance mass spectrometry. *J. Am. Soc. Mass Spectrom.*, 2006. **17**. 1712-1716.

10. Sampson, J.S., A.M. Hawkridge, and D.C. Muddiman, Direct characterization of intact polypeptides by matrix assisted laser desorption electrospray ionization (MALDESI) quadrupole fourier transfrom ion cyclotron resonance mass spectrometry. *Rapid Commun. Mass Spectrom.*, 2007. **21**. 1150-1154.

11. Nemes, P. and A. Vertes, Laser ablation electrospray ionization for atmospheric pressure, in vivo, and imaging mass spectrometry. *Anal. Chem.*, 2007. **79**. 8098-8106.

12. Nemes, P., et al., Ambient molecular imaging and depth profiling of live tissue by infrared laser ablation electrospray ionization mass spectrometry. *Anal. Chem.*, 2008. **80**. 4575-4582.

13. Rezenom, Y.H., J. Dong, and K.K. Murray, Infrared laser-assisted desorption electrospray ionization mass spectrometry. *Analyst*, 2008. **133**. 226-232.

14. Takats, Z., et al., Mass spectrometry sampling under ambient conditions with desorption electrospray ionization. *Science*, 2004. **306**. 471-473.

15. Cooks, R.G., et al., Ambient mass spectrometry. *Science*, 2006. **311**. 1566-1570.

16. Hu, Q.Z., et al., Desorption electrospray ionization using an Orbitrap mass spectrometer: exact mass measurements on drugs and peptides. *Rapid Commun. Mass Spectrom.*, 2006. **20**. 3403-3408.

17. Bereman, M.S., et al., Direct high-resolution peptide and protein analysis by desorption electrospray ionization Fourier transform ion cyclotron resonance mass spectrometry. *Rapid Commun. Mass Spectrom.*, 2006. **20**. 3409-3411.

18. Van Berkel, G.J., M.J. Ford, and M.A. Deibel, Thin-layer chromatography and mass spectrometry coupled using desorption electrospray ionization. *Anal. Chem.*, 2005. **77**. 1207-1215.

19. Weston, D.J., et al., Direct analysis of pharmaceutical drug formulations using ion mobility spectrometry/quadrupole-time-of-flight mass spectrometry combined with desorption electrospray ionization. *Anal. Chem.*, 2005. **77**. 7572-7580.

20. Williams, J.P. and J.H. Scrivens, Rapid accurate mass desorption electrospray ionization tandem mass spectrometry of pharmaceutical samples. *Rapid Commun. Mass Spectrom.*, 2005. **19**. 3643-3650.

21. Kauppila, T.J., et al., Desorption electrospray ionization mass spectrometry for the analysis of pharmaceuticals and metabolites. *Rapid Commun. Mass Spectrom.*, 2006. **20**. 387-392.

22. Cotte-Rodriguez, I. and R.G. Cooks, Non-proximate detection of explosives and chemical warfare agent simulants by desorption electrospray ionization mass spectrometry. *Chemical Communications*, 20062968-2970.

23. Nyadong, L., et al., Reactive desorption electrospray ionization linear ion trap mass spectrometry of latest-generation counterfeit antimalarials via noncovalent complex formation. *Anal. Chem.*, 2007. **79**. 2150-2157.

24. Shin, Y.S., et al., Desorption electrospray ionization-mass spectrometry of proteins. *Anal. Chem.*, 2007. **79**. 3514-3518.

25. Talaty, N., Z. Takats, and R.G. Cooks, Rapid in situ detection of alkaloids in plant tissue under ambient conditions using desorption electrospray ionization. *Analyst*, 2005. **130**. 1624-1633.

26. Wiseman, J.M., et al., Tissue imaging at atmospheric pressure using desorption electrospray ionization (DESI) mass spectrometry. *Angewandte Chemie-International Edition*, 2006. **45**. 7188-7192.

27. Takats, Z., J.M. Wiseman, and R.G. Cooks, Ambient mass spectrometry using desorption electrospray ionization (DESI): instrumentation, mechanisms and applications in forensics, chemistry, and biology. *J. Mass Spectrom.*, 2005. **40**. 1261-1275.

28. Van Berkel, G.J. and V. Kertesz, Automated sampling and imaging of analytes separated on thin-layer chromatography plates using desorption electrospray ionization mass spectrometry. *Anal. Chem.*, 2006. **78**. 4938-4944.

29. Costa, A.B. and R.G. Cooks, Simulation of atmospheric transport and droplet-thin film collisions in desorption electrospray ionization. *Chemical Communications*, 20073915-3917.

30. Costa, A.B. and R.G. Cooks, Simulated splashes: Elucidating the mechanism of desorption electrospray ionization mass spectrometry. *Chem. Phys. Lett.*, 2008. **464**. 1-8.

31. Myung, S., et al., Coupling desorption electrospray ionization with ion mobility/mass spectrometry for analysis of protein structure: Evidence for desorption of folded and denatured states. *Journal of Physical Chemistry B*, 2006. **110**. 5045-5051.

32. Bereman, M.S. and D.C. Muddiman, Detection of Attomole Amounts of Analyte by Desorption Electrospray Ionization Mass Spectrometry (DESI-MS) Determined Using Fluorescence Spectroscopy. *J. Am. Soc. Mass Spectrom.*, 2007. **18**. 1093-1096.

33. Burgess, J.D. and F.M. Hawkridge, Octadecyl mercaptan sub-monolayers on silver electrodeposited on gold quartz crystal microbalance electrodes. *Langmuir*, 1997. **13**. 3781-3786.

34. Fenn, J.B., Ion Formation from Charged Droplets - Roles of Geometry, Energy, and Time. *J. Am. Soc. Mass Spectrom.*, 1993. **4**. 524-535.

35. Frahm, J.L., et al., Achieving Aumented Limits of Detection for Peptides with Hydrophobic Alkyl Tags. *Anal. Chem.*, 2007. **79**. 3989-3995.

36. Smith, R.D., et al., New Developments in Biochemical Mass-Spectrometry - Electrospray Ionization. *Anal. Chem.*, 1990. **62**. 882-899.

37. Zook, D.R. and A.P. Bruins, On cluster ions, ion transmission, and linear dynamic range limitations in electrospray (ionspray) mass spectrometry. *Int. J. Mass Spectrom. Ion Processes*, 1997. **162**. 129-147.

38. Sauerbrey, G., The use of quartz oscillators for weighing thin layers and for microweighing. *Z. Phys.*, 1959. **155**. 206-222.

CHAPTER 4

Glycan Analysis by DESI-FT-ICR Mass Spectrometry

4.1 Introduction

Facilitated by the advent of electrospray ionization[1, 2] (ESI) by Fenn and *matrix-assisted laser desorption ionization*[3, 4] (MALDI), the field of biological mass spectrometry has witnessed tremendous growth in the past decade. These advancements are partly due to the high sensitivity and the ability of these techniques to produce gas phase ions from biological macromolecules. In addition, mass analyzer technology has advanced in terms of *mass measurement accuracy* (MMA), *resolving power* (RP), and *limits of detection* (LODs) which have further aided this progression. However, the development of alternate ionization techniques continues in an effort to overcome the inherent limitations of ESI and MALDI and further increase the number of scientific problems that one can address using mass spectrometry.

In the last few years, research has focused on the development of ambient ionization methods.[5] These techniques benefit from atmospheric analysis combined with limited sample preparation, ultimately leading to faster analysis times. Introduced by Larsen and co-workers, *atmospheric-pressure solids analysis probe*[6] (ASAP) is easily implemented on existing ESI/APCI instrumentation. *Direct analysis in real time*[7] (DART) developed by Cody *et al*. has a potential for a wide

range of applications; however, both techniques are molecular weight limited. Most recently *electrospray-assisted laser desorption ionization*[8, 9] (ELDI) and *matrix-assisted laser desorption electrospray ionization*[10, 11] (MALDESI) have been introduced and both utilize a laser for desorption of molecules off a surface with subsequent charging using ESI. Presented by Cooks and co-workers in 2004, desorption electrospray ionization[12] was one of the first techniques introduced in this group of ambient methods. In DESI, charged solvent droplets are accelerated by high pressure nitrogen gas toward an analyte bearing surface. These droplets impact the surface and analyte containing secondary droplets are then sampled by the mass spectrometer. Currently, the majority of literature in this field has focused on this technique as it has a number of applications. However, as reported by Basile and co-workers[13] and observed in our laboratory, the analysis of high molecular weight species (> 20 kDa) can be challenging. This difficulty may be partly due to the inability of the DESI solvent stream to dissolve high molecular weight proteins on the surface; thus, creating a desorption problem and decreasing the overall sensitivity of DESI analysis for high molecular weight species. As a result of this problem and the high sensitivity of DESI for smaller molecules[14] we report herein a new biological application of DESI focusing on the study of oligosaccharides.

Glycoproteins are an extremely important informational group of molecules as they are known to regulate numerous crucial biological processes including adhesion, cellular recognition, and control of cell division. *Glycosylation* is the most

common form of post-translational modification (PTM) as it has been estimated that over 50% of proteins are glycosylated.[15] Differences exist between the glycosylation profiles of cancer cells when compared to normal cells[16] rendering carbohydrate studies as a possible area for biomarker research. Recent investigations using MALDI-FT-ICR-MS by Lebrilla and coworkers[17] have indicated significant differences in glycan profiles derived from glycoproteins in plasma between ovarian cancer (OVC) and normal patients.

DESI has been coupled to hybrid Fourier transform ion cyclotron resonance mass spectrometry (DESI-FT-ICR-MS)[18] for glycan studies. Preliminary data of neat carbohydrates are presented along with the *mass measurement accuracy* (MMA) obtained demonstrating the potential of DESI-FT-ICR-MS for carbohydrate analysis. In addition, a comparison is made between MALDI-FT-ICR-MS and DESI-FT-ICR-MS for the analysis of *O*-linked glycans selectively cleaved from mucin. Furthermore, we demonstrate the ability of high MMA afforded by DESI-FT-ICR-MS in addition to the MS/MS capabilities to accurately identify glycans from mucin. The high MMA afforded by automatic gain control (AGC) combined with fragmentation occurring outside the ICR cell (via CID in the linear ion trap) provide distinct advantages for the analysis of carbohydrates by DESI-FT-ICR-MS. It is important to mention that high MMA by DESI has been previously reported with an orbitrap[19] and time-of-flight[20, 21] (TOF) mass analyzers.

4.2 Experimental

4.2.1 Materials

2,5-dihydroxy-benzoic acid (DHB), sodium borohydride ($NaBH_4$), trifluoroacetic acid (TFA), sucrose, lacto-N-fucopentose (LNF), lacto-N-difucohexaose I (LND), lacto-N-tetraose (LNT), formic acid, sodium chloride (NaCl), hydrochloric acid (37% HCl), sodium hydroxide (NaOH) and mucin (porcine stomach; M1778) were purchased from Sigma Aldrich (St. Louis, MO). HPLC grade acetonitrile (ACN) and water were obtained from Burdick & Jackson (Muskegon, MI) and used as received. Glass microscope slides were purchased from Thermo Fischer Scientific (San Jose, CA) and high purity nitrogen gas (99.98%) was obtained from MWSC High Purity Gases (Raleigh, NC).

4.2.2 DESI-MS Conditions

The solvent used for the DESI studies consisted of acetonitrile:water (1:1 v/v) with 0.1% formic acid. For analyte deposition, glass substrates were rinsed with water, ethanol and finally acetone. The slides were then dried under a light stream of compressed air. As a result of this rinse procedure the glass substrates were cleaned and a residue, presumably from the acetone, was left on the surface. The authors observed that this residue increased the hydrophobicity of the glass surface and aided in concentrating the analyte on the surface thus increasing the sensitivity of the DESI experiments. For DESI-MS of neat carbohydrates, 0.1

mg/mL solutions were prepared in water. 3 μL of corresponding solutions were placed onto a glass surface and material was dried in the ambient environment.

The DESI source used in these studies was modeled after the Prosolia prototype[22] and has been previously described.[14] Solution was infused at 2 μL/min through a fused silica capillary (150 μm o.d., 50 μm i.d.; Polymicro Technologies, Phoenix, AZ). Measured at the regulator, the nitrogen pressure was 120 PSI and flowed through an outer fused silica capillary (250 μm i.d., 300 μm o.d.; Polymicro Technologies, Phoenix, AZ). The inner liquid capillary protruded slightly beyond the outer gas capillary (0.5 mm). The d_1 distance (distance from liquid capillary to surface) was approximately 2 mm and the d_2 distance (distance from MS capillary to surface) was <1 mm. The α and β angles (incidence angle and collection angle) were 54° and 5°, respectively. Distance from the DESI emitter tip to MS inlet was ~5 mm. The source and capillary voltages were 4 kV and 49 V, respectively and were kept constant throughout all experiments.

DESI mass spectra were acquired on a LTQ-FT-ICR mass spectrometer (Thermo Fisher, San Jose, CA) equipped with a 7 Tesla superconducting magnet. All experiments were performed in the positive-ion mode. Calibration of the instrument was achieved by following standard manufacturer protocol. Resolving power was set to 100,000 (@ *m/z* 400) for all studies and 1 microscan was acquired per mass spectrum. Automatic gain control (AGC) was 5×10^5 while the *injection time* (IT) was set to a maximum of 2 s. It is important to note that rarely during any of our studies did the mass spectrometer reach the maximum IT

allowed of 2 s. Normally the AGC limit reached its target value (5×10^5) in less than 500 ms. For tandem MS studies, analytes of interest were isolated, fragmented and analyzed in the linear ion trap. Injection times in the linear ion trap were 2 s and the AGC limit of 3×10^4 was never reached during these MS/MS studies.

Limits of detection for the neat carbohydrates analyzed by our DESI-FT-ICR-MS configuration were estimated by using the down spotting technique previously described by Cooks and coworkers[22] in which decreasing amounts of material are deposited onto the surface until no signal is obtained. For these experiments a 2-fold decrease in the amount of analyte deposited was made until there was no signal present. It is important to stress that these numbers are only estimates as sometimes all of the material was not consumed during analysis and the S/N ratio of the lowest amount of material deposited and analyzed was usually still greater than 3:1.

4.2.3 Cleavage of O-linked Glycans from Mucin

The procedure for cleavage of *O*-linked glycans from proteins using reductive β-elimination and purification has been previously described.[17] Briefly, 1 mg of mucin glycoprotein was dissolved in a basic borohydride solution (270 μL solution; 0.1M NaOH:1M $NaBH_4$). The mixture was heated at 42°C for 12-14 hours to promote the selective release of *O*-linked glycans. The reaction was terminated by slowly adding 1 M HCl in an ice bath until the pH was approximately 5. Preconditioned porous graphitized carbon (PGC) solid phase extraction (SPE)

columns (P/N 210101, Alltech, Deerfield, IL) were used to purify and enriched the cleaved glycans. Neutral and acidic glycans of increasing mass were eluted with aqueous 10% (elution 1) and 20% (elution 2) ACN solutions. Fractions were collected, dried using a Speed Vacuum (Thermo Fischer, San Jose, CA), and reconstituted in 40 μL of water. For DESI-MS analysis of *O*-linked glycans from mucin, 3 μL of each elutant were placed onto a glass surface and dried in the ambient environment. For MALDI-MS analysis, each elutant was mixed with a solution of 2,5-DHB (100 mg/mL in 1:1 ACN:50 mM NaCl) in a 1:1 (v/v) ratio and 0.8 μL of the resulting mixture was placed onto a MALDI target (P/N 433375, Applied Biosystems, Foster City, CA) and actively dried under a cold stream of air.[23] Sodium chloride was used as a cation dopant in these MALDI-MS experiments and promoted the formation of charged species by sodium adduction. All data were analyzed using the OSCAL program supplied by Lebrilla and co-workers (Personal Communication).

4.2.5 MALDI-FT-ICR Mass Spectrometry

Analysis by MALDI-FT-ICR-MS was performed on a ProMALDI ion source equipped with a 9.4 Tesla superconducting magnet (Varian Corporation, Palo Alto, CA). A Nd:YAG frequency-tripled laser (355 nm) promoted desorption and ionization of analyte (New Wave Research, Fremont, CA). The Varian Omega ZXP data station was used for all processing and signal generation. The standard broadband pulsed sequence was employed.

4.3 Glycan Analysis by DESI-FT-ICR Mass Spectrometry

Displayed in **Figure 4.1A-D** are FT-ICR mass spectra of neat carbohydrates ranging in molecular weights from ~350 to 1000 Da. As mentioned previously, 3 μL of 0.1 mg/mL stock carbohydrate solutions were placed onto a glass surface. It is important to note that multiple spectra could be acquired from a single spot. Although protonation and potassium adduction of carbohydrates did occur, sodium adduction was observed to be the dominant ionization pathway. During the analysis of sucrose (**Figure 4.1A**), an intense sodium adducted dimer was

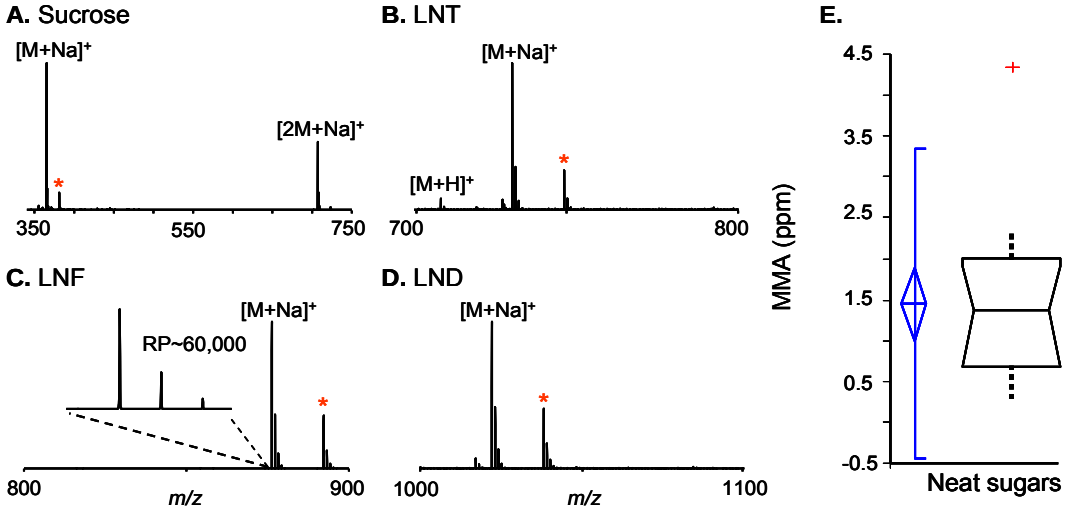

Figure 4.1 The DESI-FT-ICR mass spectra of **A)** sucrose, **B)** LNF, **C)** LNT, and **D)** LND. Sodium adduction of the monomers was observed to be the main ionization pathway, although protonation and sodiated-dimers were observed. Potassium adduction of carbohydrates also occurred (asterisk). The inset in **C** illustrates the high RP attainable by DESI-FT-ICR-MS. Five mass spectra of each carbohydrate (n=20) were used to generate the MMA data summarized by the box and whisker plot (**E**). Mass measurement accuracies correspond to the sodium adducted glycan.

observed, indicating the softness of ionization afforded by DESI. The inset in **Figure 4.1C** displays a key advantage of coupling DESI with a high resolving

power platform, such as FT-ICR-MS, for the analysis of complex samples (RP~60,000). Summarized by a box and whisker plot in **Figure 4.1E**, the average mass accuracy achieved for these studies was 1.45 ppm. Five mass spectra of each carbohydrate were used to generate the box and whisker plot data (n=20). Limits of detection (LOD) for these studies were determined to be sub-pmols for LNF (780 fmol), LNT (700 fmol), and LND (500 fmol). The LOD of sucrose was found to be 30 pmol. All LODs were determined by using the sodium adducted form of the carbohydrate. The high LOD observed for sucrose may be a result of two factors. First, the MS analysis of sucrose spanned multiple *m/z* channels, including sodium adduction, potassium adduction, and the sodium adducted dimer. Furthermore, there was a strong unknown interference at *m/z* 365.1357 which decreased the time allowed for collection before the AGC limit was reached. This effectively decreased the amount of sodium adducted sucrose (*m/z* 365.1059) that could be collected in the ICR cell for a given mass spectrum.

Displayed in **Figure 4.2** is a DESI-FT-ICR mass spectrum of *O*-linked glycans cleaved from mucin (elution 1). For comparative purposes, the MALDI-FT-ICR mass spectrum of the same sample is shown on a reflected axis. As exhibited in **Figure 4.2**, the mass spectra of the same sample analyzed by two different ionization methods are almost identical. This result is incredibly interesting considering the different mechanisms involved and that DESI is performed at ambient pressures whereas MALDI is performed under vacuum. More peaks were observed in the DESI mass spectrum due to both protonated and sodiated forms of

the glycans, whereas in MALDI only sodium adducted glycans were observed. The unique similarity between the two spectra demonstrates the potential of DESI-FT-ICR-MS for glycan studies of complex samples.

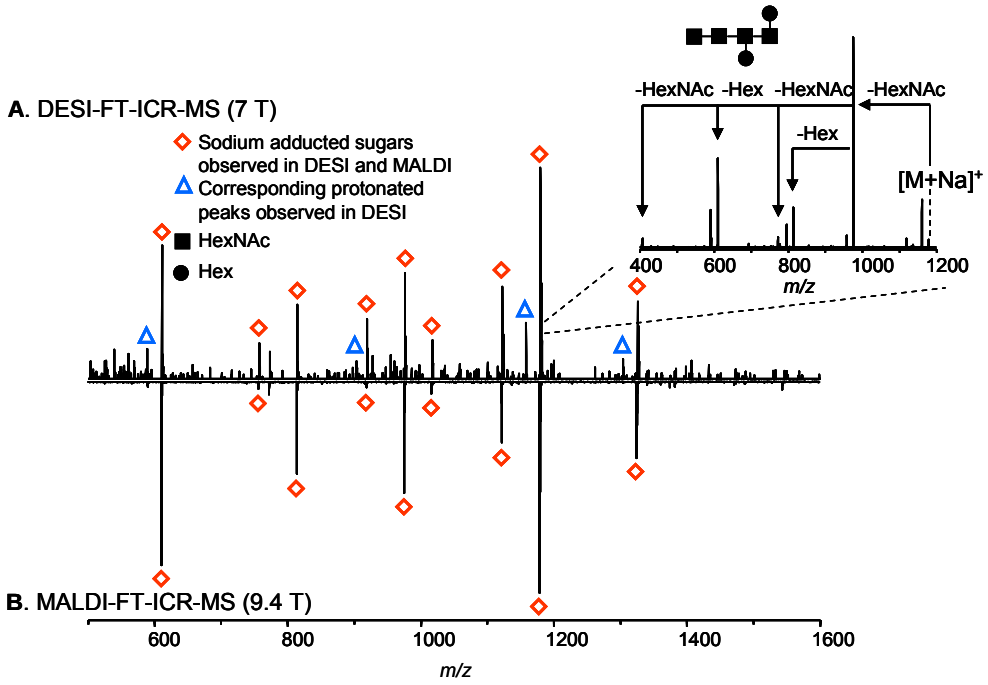

Figure 4.2 Compares the DESI and MALDI FTICR analysis of O-linked glycans cleaved from mucin

The inset in **Figure 4.2** shows one of the main advantages of DESI-FT-ICR-MS for glycan studies. In order to perform tandem MS studies by our MALDI-FT-ICR-MS, one could use *IRMPD*[17, 24] or *SORI*[25], both techniques are difficult to implement routinely. In DESI-FT-ICR-MS, fragmentation occurs via *collision induced dissociation* (CID) in the linear ion trap (outside the ICR cell). This method provides a fast and effective way to obtain information on the oligosaccharide composition, aiding in its confident identification. Combined with the high MMA, the MS/MS spectrum displayed in **Figure 4.2** confirms the composition of the

oligosaccharide at *m/z* 1179 to be 4HexNAc:2Hex. In addition, sequencing information can be derived as the proposed structure is consistent with the MS/MS data (**Figure 4.2**).

Displayed in **Table 4.1** is a summary of the glycans identified from mucin by DESI-FT-ICR-MS. The theoretical mass is listed along with the corresponding oligosaccharide composition from the OSCAL algorithm. Also given is the 95% confidence interval (CI) in the average absolute mass error (n=5) observed in these studies. All glycan compositions were confirmed by tandem MS. It is important to note that the majority of glycans observed in these studies came from elution 1 (10% ACN). Only two additional small carbohydrates (<1100 Da) were observed from DESI-FT-ICR mass spectral analysis of elution 2 (20% ACN). Normally analysis of the glycan fraction eluted with 20% ACN by MALDI-FT-ICR-MS yields carbohydrates with higher molecular weights (1000 to

Table 5.1. Summary of carbohydrates observed by DESI-FT-ICR-MS

Theoretical Mass	Oligosaccharide composition	95% CI Avg. MMA (ppm)
554.2056	1HexNAc:1Hex:1Fuc	0.3248±0.2921
611.2271	2HexNAc:1Hex	0.5889±0.5852
757.2850	2HexNAc:1Fuc:1Hex	1.03±0.7982
814.3065	3HexNAc:1Hex	0.9333±0.8040
919.3379	2HexNAc:1Fuc:2Hex	0.8049±0.9435
976.3593	3HexNAc:2Hex	0.6965±0.7545
1065.3960	2HexNAc:2Fuc:2Hex	0.4693±0.2733
1122.4170	3HexNAc:2Hex:1Fuc	0.8731±1.0878
1179.4390	4HexNAc:2Hex	0.8648±0.7078
1325.4970	4HexNAc:2Hex:1Fuc	0.9959±1.0892

Table 4.1 All masses correspond to the sodium adducted glycan. The majority of the species were observed by the analysis of elution 1. Analysis of the fraction eluted with 20% ACN yielded the identification of two sugars (*m/z* 554 and *m/z* 1065) that were not present in the previous fraction.

2000 Da). Several experimental parameters and conditions exist that may be related to this finding either due to DESI (i.e. geometric parameters, solvent compositions, desorption, surfaces) or to the experimental conditions of the mass spectrometer (i.e. source high voltage, tube lens voltage). Nevertheless, DESI-FT-ICR-MS has demonstrated the capability for carbohydrate applications both in terms of sensitivity and the ability to accurately identify glycans.

4.4 Conclusions

In regards to DESI, we report another application of this rapidly evolving ionization technique. The sensitivity, high MMA, and tandem MS capabilities provide an encouraging platform for carbohydrate analysis by DESI-FT-ICR-MS. Although similar glycan spectra were obtained between DESI and MALDI FTICR MS analysis of glycans cleaved from mucin, DESI-FTICR proved not sensitive enough for analysis of glycans derived from plasma samples. Efforts to implement an *air amplifier*[26-28] and an *air ejector*[29] did not significantly increase ion abundances. As a result, it was necessary to explore other options for analysis of glycans derived from plasma glycoproteins.

4.5 References

1. Fenn, J.B., et al., Electrospray Ionization for Mass-Spectrometry of Large Biomolecules. *Science*, 1989. **246**. 64-71.

2. Fenn, J.B., et al., Electrospray Ionization-Principles and Practice. *Mass Spectrom. Rev.*, 1990. **9**. 37-70.

3. Karas, M. and F. Hillenkamp, Laser Desorption Ionization of Proteins with Molecular Masses Exceeding 10000 Daltons. *Anal. Chem.*, 1988. **60**. 2299-2301.

4. Tanaka, K., et al., Protein and Polymer Analysis up to m/z 100,000 by Laser Ionization Time-of-Flight Mass Spectrometry. *Rapid Commun. Mass Spectrom.*, 1988. **2**. 151-153.

5. Cooks, R.G., et al., Ambient mass spectrometry. *Science*, 2006. **311**. 1566-1570.

6. McEwen, C.N., R.G. McKay, and B.S. Larsen, Analysis of solids, liquids, and biological tissues using solids probe introduction at atmospheric pressure on commercial LC/MS instruments. *Anal. Chem.*, 2005. **77**. 7826-7831.

7. Cody, R.B., J.A. Laramee, and H.D. Durst, Versatile new ion source for the analysis of materials in open air under ambient conditions. *Anal. Chem.*, 2005. **77**. 2297-2302.

8. Shiea, J., et al., Electrospray-assisted laser desorption/ionization mass spectrometry for direct ambient analysis of solids. *Rapid Commun. Mass Spectrom.*, 2005. **19**. 3701-3704.

9. Huang, M.Z., et al., Direct protein detection from biological media through electrospray-assisted laser desorption ionization/mass spectrometry. *J. Proteome Res.*, 2006. **5**. 1107-1116.

10. Sampson, J.S., A.M. Hawkridge, and D.C. Muddiman, Generation and detection of multiply-charged peptides and proteins by matrix-assisted laser desorption electrospray ionization (MALDESI) Fourier transform ion cyclotron resonance mass spectrometry. *J. Am. Soc. Mass Spectrom.*, 2006. **17**. 1712-1716.

11. Sampson, J.S., A.M. Hawkridge, and D.C. Muddiman, Direct characterization of intact polypeptides by matrix assisted laser desorption electrospray ionization (MALDESI) quadrupole fourier transfrom ion cyclotron resonance mass spectrometry. *Rapid Commun. Mass Spectrom.*, 2007. **21**. 1150-1154.

12. Takats, Z., et al., Mass spectrometry sampling under ambient conditions with desorption electrospray ionization. *Science*, 2004. **306**. 471-473.

13. Shin, Y.S., et al., Desorption electrospray ionization-mass spectrometry of proteins. *Anal. Chem.*, 2007. **79**. 3514-3518.

14. Bereman, M.S. and D.C. Muddiman, Detection of Attomole Amounts of Analyte by Desorption Electrospray Ionization Mass Spectrometry (DESI-MS) Determined Using Fluorescence Spectroscopy. *J. Am. Soc. Mass Spectrom.*, 2007. **18**. 1093-1096.

15. Apweiler, R., H. Hermjakob, and N. Sharon, On the frequency of protein glycosylation, as deduced from analysis of the SWISS-PROT database. *Biochimica Et Biophysica Acta-General Subjects*, 1999. **1473**. 4-8.

16. Hollingsworth, M.A. and B.J. Swanson, Mucins in cancer: Protection and control of the cell surface. *Nature Reviews Cancer*, 2004. **4**. 45-60.

17. An, H.J., et al., Profiling of glycans in serum for the discovery of potential biomarkers for ovarian cancer. *J. Proteome Res.*, 2006. **5**. 1626-1635.

18. Bereman, M.S., et al., Direct high-resolution peptide and protein analysis by desorption electrospray ionization Fourier transform ion cyclotron resonance mass spectrometry. *Rapid Commun. Mass Spectrom.*, 2006. **20**. 3409-3411.

19. Hu, Q.Z., et al., Desorption electrospray ionization using an Orbitrap mass spectrometer: exact mass measurements on drugs and peptides. *Rapid Commun. Mass Spectrom.*, 2006. **20**. 3403-3408.

20. Williams, J.P. and J.H. Scrivens, Rapid accurate mass desorption electrospray ionization tandem mass spectrometry of pharmaceutical samples. *Rapid Commun. Mass Spectrom.*, 2005. **19**. 3643-3650.

21. Williams, J.P., et al., Polarity switching accurate mass measurement of pharmaceutical samples using desorption electrospray ionization and a dual ion source interfaced to an orthogonal acceleration time-of-flight mass spectrometer. *Anal. Chem.*, 2006. **78**. 7440-7445.

22. Takats, Z., J.M. Wiseman, and R.G. Cooks, Ambient mass spectrometry using desorption electrospray ionization (DESI): instrumentation, mechanisms and applications in forensics, chemistry, and biology. *J. Mass Spectrom.*, 2005. **40**. 1261-1275.

23. Williams, T.I., et al., Effect of matrix crystal structure on ion abundance of carbohydrates by matrix-assisted laser desorption/ionization Fourier transform ion cyclotron resonance mass spectrometry. *Rapid Commun. Mass Spectrom.*, 2007. **21**. 807-811.

24. Woodin, R.L., D.S. Bomse, and J.L. Beauchamp, Multi-Photon Dissociation of Molecules with Low-Power Continuous Wave Infrared-Laser Radiation. *J. Am. Chem. Soc.*, 1978. **100**. 3248-3250.

25. Gauthier, J.W., T.R. Trautman, and D.B. Jacobson, Sustained Off-Resonance Irradiation for Collision-Activated Dissociation Involving Fourier-Transform Mass-Spectrometry - Collision-Activated Dissociation Technique That Emulates Infrared Multiphoton Dissociation. *Anal. Chim. Acta*, 1991. **246**. 211-225.

26. Zhou, L., et al., Incorporation of a venturi device in electrospray ionization. *Anal. Chem.*, 2003. **75**. 5978-5983.

27. Hawkridge, A.M., et al., Analytical performance of a venturi device integrated into an electrospray ionization Fourier transform ion cyclotron resonance mass spectrometer for analysis of nucleic acids. *Anal. Chem.*, 2004. **76**. 4118-4122.

28. Dixon, R.B., et al., Probing the Mechanism of an Air Amplifier using a LTQ-FT-ICR-MS and Fluorescence Spectroscopy. *J. Am. Soc. Mass Spectrom.*, 2007In press.

29. Dixon, R.B., et al., Remote mass spectrometric sampling of electrospray- and desorption electrospra-generated ions using an air ejector. *J. Am. Soc. Mass Spectrom.*, 2007. **18**. 1844-1847.

CHAPTER 5

Development of NanoLC Orbitrap Mass Spectrometric Methods for Profiling Glycans Chemically Released from Plasma Glycoproteins taken from Diseased and Control Patients

5.1 Introduction

In disease research, the need for more sensitive and specific clinical markers and the modest success of proteomic and metabolomic studies to identify such markers has lead to the development of other more targeted avenues such as glycomics. *Glycosylation*, occurring in an estimated 50% of all translational products[1], is one of the most critical post-translational modifications as glycosylation is known to regulate numerous biological processes including: adhesion, cellular recognition, and control of cell division, among others. In the late 1970's Rostenberg *et al*.[2] were the first to link aberrant protein glycosylation patterns to cancer. Later Gehrke and coworkers[3] implicated changes in glycan abundance in epithelial ovarian cancer (EOC) by gas-liquid chromatography (GLC). More recently, other reports have further linked the critical role of glycosylation to cancer.[4-8]

Due to the asymptomatic nature of early-stage EOC (stage I and stage II), the disease is often diagnosed in the late stages (stage III and stage IV) where only 1 in 5 patients survive longer than 5 years. Although 80% of cases are diagnosed in the later stages, if detected early the disease is rendered more treatable and 5

year survival rates increase to ~90%.[9, 10] The highly glycosylated CA-125 protein[11] is a FDA approved blood test for the diagnosis of EOC; however, this marker lacks the *sensitivity* and *specificity* to be used either as an early warning marker or for population screening. Advancements in diagnosis are both critical for early intervention as well as a more in-depth understanding of this gynecologic malignancy such that therapeutic targets can be elucidated.

Recently investigations have taken a global glycan approach for biomarker discovery in which glycans from glycoproteins in serum were chemically or enzymatically released and purified. These samples were then analyzed by *matrix-assisted laser desorption ionization* (MALDI) mass spectrometry and studies have shown differences in the glycan patterns when comparing data from healthy and epithelial ovarian cancer,[12] breast cancer,[13, 14] as well as liver cancer serum.[15] Preliminary studies by our research group, have also shown aberrant glycosylation in ovarian cancer plasma by matrix-assisted laser desorption ionization Fourier transform ion cyclotron resonance mass spectrometry (MALDI-FT-ICR-MS). However, the potential for post or in-source fragmentation of labile monomers by MALDI mass spectrometry is well known in the literature.[16, 17] While this fragmentation aids in structural elucidation of a single component, it is detrimental to glycan profiling and discovery research where a multitude of species in complex biological matrixes already can complicate data interpretation. Concerned by observations of only neutral glycans comprised of hexoses (Hex) and N-acetylhexosamines (HexNAc) with no detection of glycans containing labile

monomers by MALDI-FT-ICR-MS (e.g., sialic acids, fucose residues),[13, 18] we directed our efforts towards the development of a nanoLC mass spectrometric method for profiling glycans in plasma. Variation in fucosylated and sialylated glycans have been thought to have direct implications on biological activity.[19] Therefore, it is critical that the ability exists to detect, identify, and structurally characterize these species in biomarker discovery research. NanoLC coupled to orbitrap mass spectrometry provides a promising platform to accomplish such goals.

It is important to emphasize the necessity of nano-flow rates in glycan biomarker discovery. MALDI has long been the ionization source of choice for glycan analysis and has several advantages including higher throughput, more tolerance for contaminants, and, until recently, much more sensitive when compared to ESI. The lack of detectability in ESI is contributed to the hydrophilic nature and lack of basic sites characteristic of glycan structure. The hydrophilicity limits the surface activity of the species inside the electrospray droplet and ultimately leads to low ionization efficiency. This problem is mitigated by glycan derivatization by *permethylation*[20, 21] or *peracetylation*.[21, 22] Although these procedures increase ion abundance, they limit throughput and often lead to sample loss or contamination. With the continued development in pump technology, highly precise split-less nano-flow rates can be achieved, creating much smaller ESI droplets than conventional micro-spray. Smaller droplets lead to increased surface to volume ratios which corresponds to higher ionization efficiency and sensitivity for

glycan analysis.[23-27] Therefore, in glycan biomarker discovery research, where biologically relevant species may be at significantly low concentrations, low limits of detection are a necessity.

Although on-line liquid chromatography of glycans coupled to mass spectrometry is much less robust than the separation and analysis of peptides, the majority of literature reports the use porous graphitized carbon (PGC) for glycan separation.[23, 24, 28-35] In addition, *hydrophilic interaction chromatography* (HILIC)[36] a variant of normal phase chromatography and anion exchange chromatography have both shown potential for separation of glycans.[36, 37] HILIC, an increasing popular separation technique, recently has been used for numerous glycan applications including: solid phase sample preparation of *N*-linked glycans[38] and glycopeptides[39], site specific glycosylation[40], analysis of glycosaminoglycans[41, 42] and glycosphingolipids.[43]

Herein, we report the development of a split-less nanoLC LTQ orbitrap mass spectrometric method for profiling underivatized glycans chemically cleaved from glycoproteins in plasma. Porous graphitized carbon operating under reverse phase conditions and an amide stationary phase operating under hydrophilic interaction conditions are quantitatively compared for the separation of glycans in plasma. High mass measurement accuracy along with MS/MS spectra afforded by the LTQ orbitrap provides confident identification and structural information. Glycan profiles of plasma proteins from 10 epithelial ovarian cancer patients, 10 controls with

benign gynecologic tumors, and 10 completely normal individuals are compared using *receiver operator characteristic* (ROC) curves.

5.2 Experimental

5.2.1 Materials

Sodium borohydride ($NaBH_4$), trifluoroacetic acid (TFA), 2,5-dihydroxybenzoic acid (2,5-DHB), formic acid, sodium chloride (NaCl), hydrochloric acid (37% HCl), sodium hydroxide (NaOH), mucin (porcine stomach; M1778), ammonium bicarbonate (NH_4HCO_3) and pronase E (6 U/mg) were purchased from Sigma Aldrich (St. Louis, MO). HPLC grade acetonitrile (ACN) and water were obtained from Burdick & Jackson (Muskegon, MI) and used as received. The *N*-linked glycan standard was purchased from Sigma Aldrich (St. Louis, MO). All plasma samples were provided by the Mayo Clinic (Rochester, MN).

5.2.2 Glycan Release and Purification

The procedure for glycan cleavage from glycoproteins using reductive β-elimination[44] and purification of glycans has been described in detail elsewhere.[18, 45] Briefly, 100 μL of plasma were injected into a dialysis cassette (Pierce, Rockford, IL) and dialyzed against 300 mL of nanopure water for 24 hours to remove salt and low molecular weight contaminants. The sample was then lyophilized at 35° C and 4 mg of dried plasma was transferred to a Falcon tube.

The sample was subjected to reductive β-elimination (1 M $NaBH_4$: 0.1 M NaOH) for 16 hours at 42° C. The reaction was quenched by adding 1 M HCl (pH~5).

Glycans were enriched using solid-phase extraction (SPE) with graphitized carbon cartridges (Alltech, Deerfield, IL). The plasma sample was loaded onto the SPE column and washed with water and glycans were then eluted with a 10% aqueous acetonitrile solution. Glycan elutions were dried and reconstituted in 40 μL of water. Finally to remove further peptide contamination, 5 μL of sample were subjected to pronase digestion for 4 hours at 37° C. Samples were then drop dialyzed (Millipore, Burlington, MA) against nanopure water for 2 hours. Resulting purified samples were stored at -20° C until analysis. This procedure is targeted towards *O*-linked glycans; however, as observed in our laboratory and reported in the literature, *N*-linked glycans are also released.[13, 46-48]

5.2.3 MALDI-FT-ICR Mass Spectrometry

Mass spectrometric analyses by MALDI were achieved using a ProMALDI ion source equipped with a 9.4 Tesla superconducting magnet (Varian Corporation, Palo Alto, CA). An Nd-YAG frequency tripled laser promoted desorption and ionization of analyte. All data processing and signal generation were performed by the Varian ZXP data station. The standard broadband sequence was utilized. Analyte was mixed with a solution of 2,5-DHB (100 mg/mL in 1:1: ACN/50 mM NaCl) in a 1:1 (v/v) ratio and 0.8 μL of the resulting mixture was placed onto a MALDI target (Applied Biosystems, Foster City, CA) and dried under a cold stream

of air.[49] The addition of NaCl to the MALDI matrix promoted sodium adducted glycan species which effectively enhances ionization efficiency.

5.2.4 NanoLC Mass Spectrometry

Nano-flow liquid chromatography was performed using an Eksigent nanoLC-2D system (Dublin, CA). Sample was injected into a 10 μL loop using the autosampler. To desalt the sample, material was flushed out of the loop and washed onto a trap at 2 μL/min. After approximately 10 trap washes the 10-port valve (VICI, Houston, TX) switched inline with the gradient. Concurrent to the 10-port valve switching, both the gradient (500 nL/min) and data collection commenced.

For separation using reverse-phase porous graphitized carbon (RP-PGC), glycans were washed and subsequently eluted from a Hypercarb 30 mm × 180 μM I.D. trap column (catalog # 35005-030215, Thermo Fischer Scientific, San Jose, CA) onto a 10 cm × 100 μm I.D. analytical Hypercarb column (catalog # 35005-100165, Thermo Fischer Scientific, San Jose, CA). Solvents A and B were 98/2 water/ACN and 2/98 water/ACN respectively; both contained 0.2 % formic acid. Solvent B was held at 2% for 3 minutes, ramped to 20% at 8 minutes, and held constant at 20 % for 32 minutes. At 45 minutes, solvent B increased to 80%, held constant for 5 minutes and ramped back down to re-equilibrate the column. The increase to 80% solvent B was performed to remove species that had a high affinity towards PGC.

For separation under *hydrophilic interaction liquid chromatography* (HILIC) conditions, glycans were eluted from a 75 μM ID PicoFrit capillary column (New Objective, Woburn, MA) with a 15 μM tip packed in-house (~10 cm) with 5 micron TSKgel Amide-80 material (Tosoh Biosciences, San Francisco, CA). For trapping, a ~4.5 cm self-packed, 15 cm total length, IntegraFrit (New Objective, Woburn, MA) was placed into the 10-port valve. Solvents A and B consisted of a 50 mM ammonium acetate buffer (pH 4.5) and 100% acetonitrile, respectively. The LC gradient was held at initial conditions (20/80 aqueous buffer/acetonitrile) for 3 minutes and ramped to 50% solvent A over 40 minutes where it was held constant for 5 minutes and brought down to initial conditions for equilibration for an additional 5 minutes. The total gradient time was 55 minutes.

Mass spectrometric analyses were performed using a hybrid LTQ orbitrap mass spectrometer (Thermo Fischer Scientific, Brehmen, Germany). Electrospray ionization was initiated by applying 1.8 kV to a liquid junction pre-column. The capillary voltage and temperature were 42 V and 250°C respectively. Tube lens voltage was set to 150 V. External calibration was performed using the manufacture's calibration mix. Lock mass calibration was implemented using *m/z* 610.1841, corresponding to the ammonium adducted polysiloxane $[Si(CH_3)_2O]_8$ found in ambient air.[50] For full scans, performed in the orbitrap, the AGC was set to 1×10^6 with a maximum *injection time* of 1 s and a resolving power @ *m/z* 400 of 60,000. For MS/MS settings, five scans were performed in the ion trap per full scan at a normalized collisional energy of 24 with an AGC setting of 1×10^4 and a

maximum *injection time* of 400 ms. Dynamic exclusion time of 120 seconds was used to avoid repeated interrogation of abundant peaks.

5.2.5 Experimental Design and Data Interpretation

The 10 healthy, 10 benign tumor control and 10 cancer samples (3 stage I, 3 Stage II, 2 Stage III, 2 Stage IV) were distributed throughout the run in order to minimize any measurement biases. The different stages were run in random order and were chosen for this experiment based on the ultimate goal of finding an accurate diagnostic marker regardless of disease progression. After every 4th sample, a standard mixture of glycans was run to evaluate both trapping efficiency and peak shape. A blank (mobile phase A) was run between each standard and sample to ensure no sample carry-over

Glycan identifications were performed using OSCAL software provided by Lebrilla and co-workers (Personal Communication) and GlycoWorkbench.[51] SimGlycan 2 version 2.5.5 from Premier Biosoft International was used to aid in structural elucidation. Tandem MS spectra in conjunction with the intact masses were searched against all possible *N*- and *O*-linked glycans from glycoproteins in human plasma. Xcalibur software version 2.0.5 was used for data analysis and peak integration. In addition box plots were constructed using Analyze-It®, which is an add-in for Microsoft Excel®. ROC curves were generated using JMP® software version 7.0 from SAS Inc.

5.3 Results and Discussion

As, mentioned, the analysis of glycans containing labile monomers (e.g., sialic acid and fucose residues) by MALDI, often results in fragmentation whether it be in-source or post-source decay. In FT-ICR mass analyzers, this event is more severe due to the long detection times associated with analysis relative to other mass analyzers. Reports have attempted to mitigate this problem in MALDI-FT-ICR-MS using high pressure nitrogen to collisionally cool the ions during the ionization event[52, 53] or post-ionization in a high pressure hexapole region. However, Figure 5.1A demonstrates that fragmentation of glycans still remains a significant problem in MALDI-FT-ICR-MS as the analysis of a glycan standard yields no detectable intact species. Instead several losses of monomers from the intact molecule are

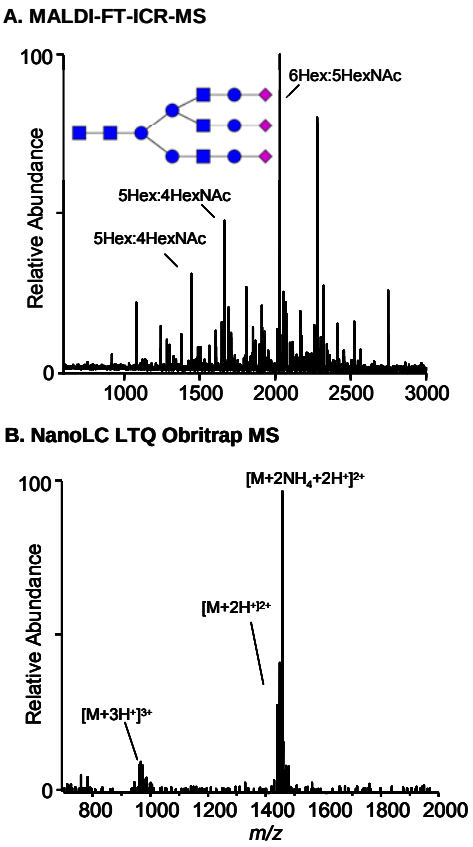

Figure 5.1: The analysis of a standard tri-sialyated glycan is compared between (A) MALDI-FT-ICR mass spectrometry and (B) nanoLC mass spectrometry. Even with hexapole cooling external to the ICR cell, no intact species is observed by MALDI-FT-ICR MS. The base peak corresponds to the loss of the three sialic acid residues. The fragmentation of the intact ion affords a complicated mass spectrum. Under LC conditions the intact species is present with no observed fragmentation.

observed and thus, yield a complicated mass spectrum. Several of these glycan fragments (**Figure 5.1A**) are also observed in the MALDI-FT-ICR mass spectrometric analysis of plasma[12, 13, 18] indicating that these species in plasma are potentially fragments from higher molecular weight glycans. In addition, the plasma glycans identified by MALDI-FT-ICR mass spectrometry correspond to $[M-H_20+Na]^+$ species.[12, 13, 18] The loss of water also suggest that these glycans correspond to B or Z fragment ions[54] from a larger species. Under the same experimental conditions and across a similar molecular weight range, the analysis of glycans cleaved from Mucin, correspond to the intact sodiated species with no loss of water.[45] It is important to note that laser power and voltages corresponding to detection were optimized for the MALDI mass spectrum shown in **Figure 5.1A**. It should be stated that matrices other than 2,5-DHB have been reported for more efficient desorption and ionization of intact acidic glycans by MALDI.[55, 56]

The nanoLC orbitrap mass spectrum displays a signal corresponding to the 2^+ and 3^+ charge states of the intact species, with no observed fragmentation (**Figure 5.1B**). There were several ammonium adducts observed due to the ammonium acetate buffer used for analysis. This analysis was conducted under HILIC conditions using the amide stationary phase. Interestingly, this glycan was not observed under RP-PGC possibly due to the high affinity of anionic species with PGC as previously reported.[30]

Considering the fragmentation observed by MALDI and the softness of ESI it was essential that nano-flow liquid chromatographic methods be developed for

glycan biomarker discovery. The importance of nano-flow rates cannot be overstated as reports indicate dramatic increase in glycan sensitivities by nano-flow ESI as opposed to higher flow rates.[23-26] **Figure 5.2** displays a comparison between *hydrophilic interaction liquid chromatography* (HILIC) (**Figure 5.2A**) and reverse-phase porous graphitized carbon (RP-PGC) (**Figure 5.2B**) for the analysis of glycans from plasma proteins. Even after the extensive sample preparation procedure, there were numerous peptide peaks in the glycan samples as shown by

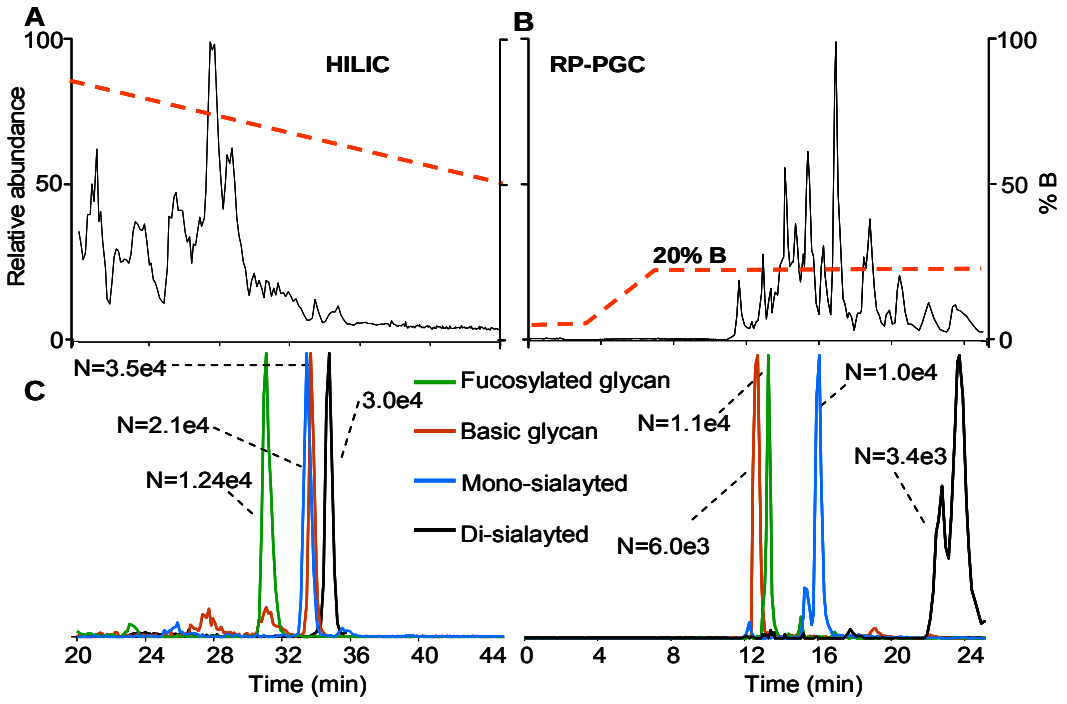

Figure 5.2 A comparison between (A) an amide-based stationary phase operating under HILIC conditions with (B) PGC operating under RP conditions for the analysis of glycans derived from late stage EOC plasma. The complexity of the sample is demonstrated by the base ion chromatograms. The axis on the far left represents the relative abundance while the one on the right represents the gradient. Glycans eluted later under HILIC conditions than RP PGC. Extracted ion chromatograms for various glycans are also displayed along with the number of theoretical plates calculated using the Foley-Dorsey equation for each stationary phase.

the base ion chromatograms for both stationary phases. We attribute the peaks to both the complex nature of plasma and to the possibility of pronase enzymatically digesting itself in the final stage of the sample preparation protocol. However, as shown by the extracted ion chromatograms (EIC), glycans were detected well above the limit of detection of the instrument. Also displayed are the numbers of theoretical plates, calculated using the Foley-Dorsey equation[57] accounting for peak asymmetry, for each glycan peak between the different stationary phases. The column efficiencies were similar among the different glycans present. This is attributed to the increased retention and wider peak widths observed under HILIC conditions which offset each other in the theoretical calculation. Peak widths, at 10% height, eluted under reverse-phase conditions were between 0.5-0.75 minutes; while the same peaks had widths of between 0.75-1.25 minutes under HILIC conditions. Sialic acid containing glycans tended to give split peaks under RP-PGC conditions, as shown in **Figure 5.2C**. In addition, the glycan containing two sialic acids eluted over a much broader time window when compared to other glycan peaks under RP-PGC. This problem potentially could be rectified by further gradient and solvent optimization; however, Pabst *et al*. has recently reported issues with elution of sialyted glycans using RP-PGC.[30]

Figure 5.3 compares the retention time reproducibility of two glycans in plasma between the different stationary phases. The data (n=20) used for construction of the box plots for comparison between the stationary phases were collected over a 5 day period. Overall, both stationary phases exhibited

exceptional RT reproducibility given the complexity of the sample (**Figure 5.2**). The diamond represents the mean and the 95% confidence interval of the mean. The median of the data is represented by the line crossing the box while the notches in the box show the 95% confidence interval of the median. The box also displays the upper and lower quartiles. The solid lines connect the nearest data points within 1.5 interquartile ranges (IQRs) of the lower and upper quartiles. The crosses (+) display the near outliers (between 1.5 and 3.0 IQRs away).

For direct comparisons amongst the data in **Figure 5.3**, each x-axis spans a time of 0.5 minutes. The 95% confidence interval of the average retention times for peaks with *m/z* 813 and 966, under HILIC conditions, were 30.75 min ± 2.2 sec and 33.51 min ± 1.8 sec, respectively. These species (*m/z* 996 and 813) under RP-

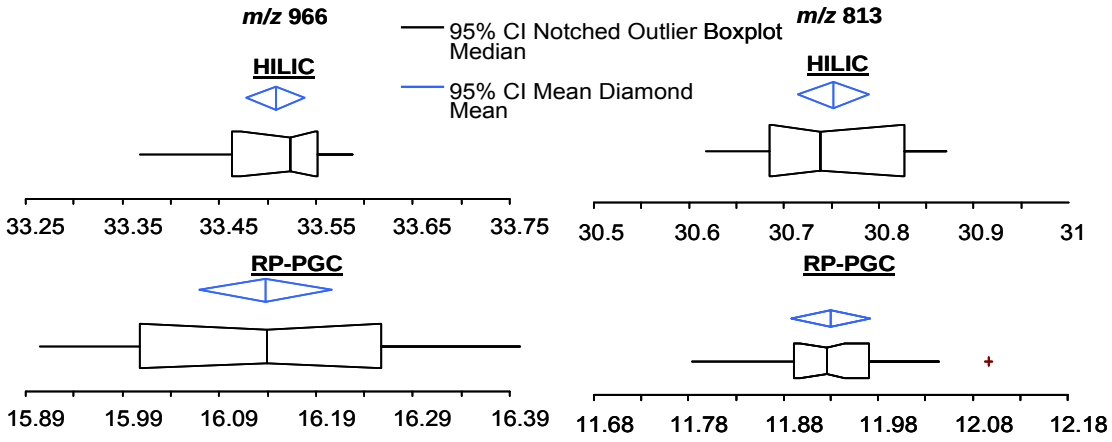

Figure 5.1 Box plots comparing the retention time reproducibility of two different glycans in plasma. Overall both stationary phases exhibited excellent RT reproducibility given the complexity of the sample. For relative comparisons, each x-axis spans 0.5 minutes. Under HILIC conditions, the 95% confidence interval of the average retention times for peaks with *m/z* 813 and 966 were 30.75 min ± 2.2 sec and 33.51 min ± 1.8 sec, respectively. These species (*m/z* 813 and 966) under RP-PGC conditions, had averages and intervals of 11.93 min ± 2.5 sec and 16.14 min ± 4.1 sec respectively. Twenty points were used to construct each box plot and data were collected over a 5 day period. See text for further description of the box plots.

PGC conditions, had averages and intervals of 11.93 min ± 2.5 sec and 16.14 min ± 4.1 sec, respectively. It is worth noting the importance of retention time reproducibility in glycan biomarker discovery research as it can be used for qualitative identifications and aid in structural elucidation.[29] For example, glycans eluting later ~16 minutes under RP-PGC conditions usually indicated that the species contained at least 1 sialic acid. Due to the well known response biases in ESI of analytes in various solvent compositions, it is critical, for semi-quantitation studies that analytes elute in the same solvent composition across an experimental sample set.

Prior to discussing further results, it is worth commenting on my experience with the different stationary phases. As previously discussed, the majority of the literature reports the use of RP-PGC for glycan separation. However, I found two major problems with RP-PGC. In more than a few different situations and after several successful LC-runs, the subsequent run revealed an introduction of air bubbles into the system. These air bubbles had detrimental effects on the analyses as signal was lost for at least tens of seconds and often the ESI tip had to be cleared of solvent accumulation using compressed air. The only dynamic part of the system was the 10-port valve and autosampler and after ruling these parts out as the potential cause of air, we believe that the air may be a result of solvent out-gassing. This out-gassing may be a result of the porous nature of the stationary phase which created a significantly lower back pressure compared to a

typical silica-based column. Efforts to thoroughly de-gas the solvents did not alleviate this problem.

The second problem discovered was the limited life-time of the PGC column, which leads to significant peak tailing and poor peak shape in our analyses. This limited life-time may be a result of the strong affinity of PGC towards various species. Attempts to clean and re-equilibrate the column using the manufacture's organic wash were moderately successful. Interestingly, others have recently reported a similar finding.[30] Due to these observations and to the comparable performance of the TSKgel AMIDE-80 stationary phase, all further results were collected under HILIC separation conditions.

Table 5.1. Summary of glycans Identified in plasma
[a]Aldehyde form. [b]Alditol form. Masses correspond to 2^+ charge state
*1^+ charge state

Measured *m/z*	Composition	MMA (ppm) 95 % CI N = 20
*1235.4435[a]	5Hex:2HexNAc	2.12 ± 0.19
732.2802[a]	3Hex:4HexNAc:1Fuc	0.88 ± 0.16
782.312[b]	2Hex:6HexNAc	0.76 ± 0.17
813.3069[a]	4Hex:4HexNAc:1Fuc	1.01 ± 0.17
833.8203[a]	3Hex:5HexNAc:1Fuc	1.17 ± 0.14
863.3386[b]	3Hex:6HexNAc	1.01 ± 0.20
883.8521[b]	2Hex:7HexNAc	1.20 ± 0.22
914.847[a]	4Hex:5HexNAc:1Fuc	1.50 ± 0.16
964.8789[b]	3Hex:7HexNAc	1.26 ± 0.10
966.8528[a]	5Hex:4HexNAc:1NeuAc	1.50 ± 0.16
1045.9058[b]	4Hex:7HexNAc	1.59 ± 0.21
1112.4006[a]	5Hex:4HexNAc:2NeuAc	1.52 ± 0.13

Table 5.1 displays the compositions and mass measurement accuracies (MMA) of glycans identified in plasma. As shown several glycans were identified containing the labile fucose and sialic acid residues. Confident identifications were provided by both MS/MS spectra and by high MMA. For the majority, utilization of the *lock mass feature*[50] provided MMAs of averages less than 1.6 ppm with upper confidence limits less

than 1.8 ppm. It is important to note that all mass errors were positive, indicating some type of systematic error. Without the utilization of lock mass the MMA of standard glycans (n=60) were found to be significantly lower with an average and 95% confidence interval of 6.19 ± 0.23 ppm (data not shown). Similar glycan peaks were observed in healthy controls, benign tumor controls and EOC samples.

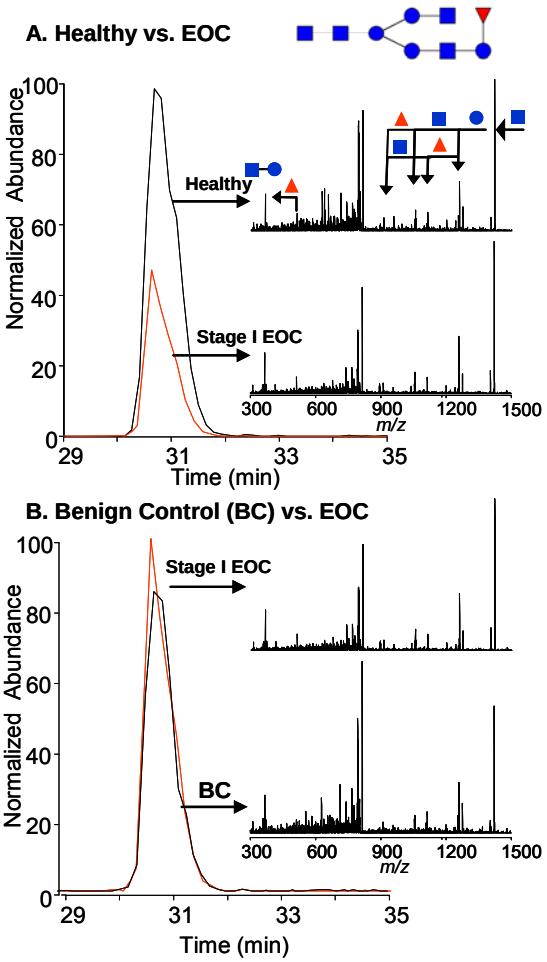

Figure 5.4 An example comparing the extractedion chromatograms (m/z 813.3 ± 0.5) between healthy, benign tumor control and EOC plasma. The fucosylated glycan seems to be down-regulated in EOC and benign tumor control samples when compared to healthy. The MS/MS spectra provide structural information and ensure that the same species is measured across all samples. The structure is consistent with the MS/MS spectra. Fucose (triangle), Hexose (circle), N-acetylhexosamine (square).

Displayed in **Figure 5.4A** is an extracted ion chromatogram (EIC) corresponding *m/z* 813 (4Hex:4HexNAc:1Fuc) from a healthy control sample. Overlaid on this spectrum is the EIC of *m/z* 813 from an EOC sample. Likewise, **Figure 5.4B** displays the same EOC sample overlaid with a benign tumor control. These spectra display the possibility that this fucosylated glycan is down-regulated in disease and benign tumor controls when compared to completely healthy controls.

In addition, the MS/MS spectra displayed aid in the identification, provide structural information and due to their high similarity, ensure that the same species is being measured across all samples. The proposed structure of the glycan is also displayed and is consistent with the MS/MS spectra. Often times the core structure is fucosylated; however, due to the presence of a fragment at *m/z* 512 which corresponds to 1HexNAc:1Hex:1Fuc, we believe the fucose is attached to the non-reducing end of the glycan. The data was searched using SimGlycan 2 version 2.5.5 from Premier Biosoft International. This search program helped confirm the initial structural assignment as the proprietary search algorithms listed the structure shown in **Figure 5.4** as the most likely match to the data.

Receiver operator characteristic (ROC) *curves* for two fucosylated glycans, both up-regulated in healthy samples, were constructed and are displayed in **Figure 5.5A**. Between healthy and EOC patients, *m/z* 813 (4HexNAc:4Hex:1Fuc) and *m/z* 914 (4Hex:5HexNAc:1Fuc) provided a moderately accurate diagnosis with areas under the curve (AUC) of 0.74 and 0.80 respectively. If both glycans are used to construct the ROC curve then the AUC increases to 0.87 and provides a sensitivity and specificity of 80% and 90%, respectively. This finding is significant as it suggests that utilizing multiple glycan markers increases diagnostic value. In addition, similar diagnostic accuracies were achieved when healthy was compared to benign tumor controls (**Figure 5.5B**). Interestingly, the fucose content of

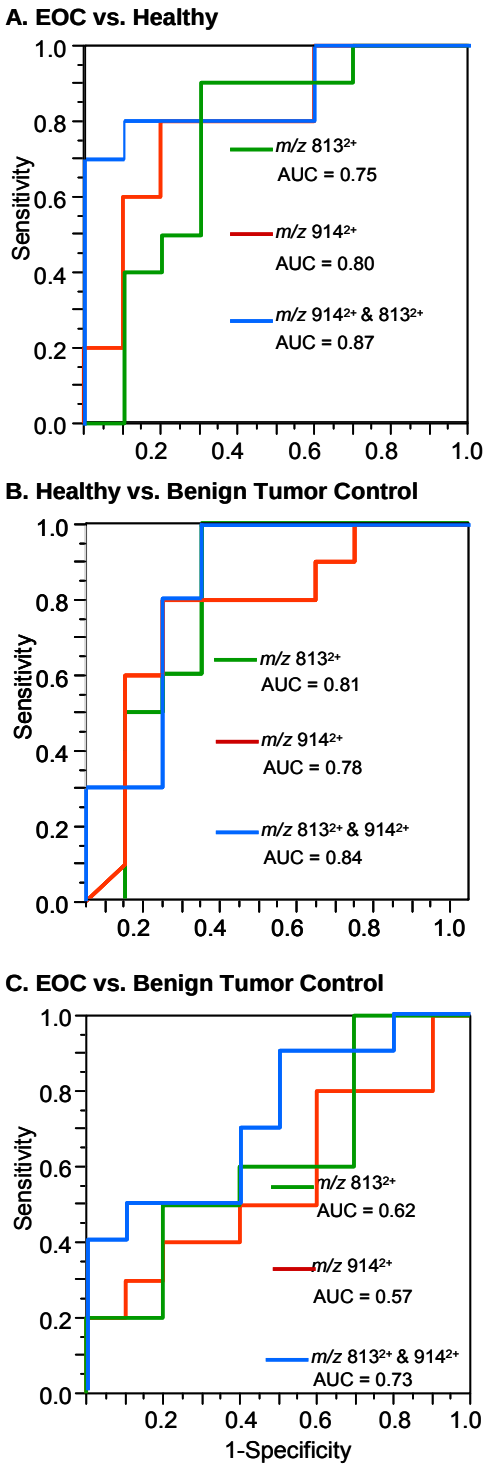

Figure 2.5 ROC analysis of (A) healthy vs. EOC, (B) healthy vs. benign tumor control, (C) benign tumor control vs. EOC samples for m/z 813 and m/z 914.

prostate specific antigen (PSA) has recently been reported to be higher in healthy plasma when compared to prostate cancer patients.[58]

However, these glycans demonstrated poor diagnostic values when used to compare the data between benign tumor controls and EOC samples as shown in **Figure 5.5C**. Glycans of *m/z* 813 and 914 gave AUCs of 0.62 and 0.57, respectively. Given these data, the glycans provide little accuracy in distinguishing EOC from benign tumor control. These results suggest that the markers may not be indicative of cancer but to some type of abnormal physiological process occurring within the body. The authors believe this finding is critical as it suggests that diagnostic markers discovered between healthy and disease states may not have the same value when used to diagnose cancer versus benign tumor controls, potentially leading to a false positive diagnosis. Nonetheless, if a tumor is present it would likely be removed regardless of whether it is benign or malignant.

5.4 Conclusions

This work emphasizes the importance of ESI-FTMS over MALDI-FTICR mass spectrometry for the analysis of labile sialyated glycans. Two stationary phases, TSKgel Amide-80 and porous graphitized carbon (PGC), have been compared for the separation of glycans derived from plasma glycoproteins. Both RP-PGC and HILIC demonstrated excellent retention time reproducibility and similar column efficiencies. However, the amide stationary phase was found to be more robust. The high MMA afforded by the lock mass feature in addition to the

MS/MS data provided confident identifications. Glycan patterns were similar across all disease, benign tumor control and healthy control samples. However, it was found that two fucosylated glycans were likely up-regulated in healthy samples when compared to cancerous and benign tumor control samples. These same glycans showed no diagnostic value when used to distinguish EOC from benign samples. Future work will entail a broader study and the analysis of glycans enzymatically released from plasma glycoproteins.

5.5 References

1. Apweiler, R., H. Hermjakob, and N. Sharon, On the frequency of protein glycosylation, as deduced from analysis of the SWISS-PROT database. *BBA-Gen. Subjects*, 1999. **1473**. 4-8.

2. Rostenberg, I., J. Guizarvazquez, and R. Penaloza, Altered Carbohydrate Content of Alpha-1-Antitrypsin in Patients with Cancer. *Journal of the National Cancer Institute*, 1978. **61**. 961-965.

3. Gehrke, C.W., et al., Quantitative Gas-Liquid-Chromatography of Neutral Sugars in Human-Serum Glycoproteins - Fucose, Mannose, and Galactose as Predictors in Ovarian and Small Cell Lung-Carcinoma. *J. Chromatogr.*, 1979. **162**. 507-528.

4. Casey, R.C., et al., Cell membrane glycosylation mediates the adhesion, migration, and invasion of ovarian carcinoma cells. *Clinical & Experimental Metastasis*, 2003. **20**. 143-152.

5. Dennis, J.W., M. Granovsky, and C.E. Warren, Protein glycosylation in development and disease. *BioEssays*, 1999. **21**. 412-421.

6. Hollingsworth, M.A. and B.J. Swanson, Mucins in cancer: Protection and control of the cell surface. *Nat. Rev. Cancer*, 2004. **4**. 45-60.

7. Hakomori, S., Glycosylation defining cancer malignancy: New wine in an old bottle. *Proc. Natl. Acad. Sci. U. S. A.*, 2002. **99**. 10231-10233.

8. Gorelik, E., U. Galili, and A. Raz, On the role of cell surface carbohydrates and their binding proteins (lectins) in tumor metastasis. *Cancer Metast. Rev.*, 2001. **20**. 245-277.

9. http://www.seer.cancer.gov/statfacts/html/ovary.html. *Accessed October 2, 2008* [cited.

10. Williams, T.I., et al., Epithelial ovarian cancer: Disease etiology, treatment, detection, and investigational gene, metabolite, and protein biomarkers. *J. Proteome Res.*, 2007. **6**. 2936-2962.

11. Wong, N.K., et al., Characterization of the oligosaccharides associated with the human ovarian tumor marker CA125. *J. Biol. Chem.*, 2003. **278**. 28619-28634.

12. An, H.J., et al., Profiling of glycans in serum for the discovery of potential biomarkers for ovarian cancer. *J. Proteome Res.*, 2006. **5**. 1626-1635.

13. Kirmiz, C., et al., A serum glycomics approach to breast cancer biomarkers. *Mol. Cell. Proteomics*, 2007. **6**. 43-55.

14. Kyselova, Z., et al., Breast cancer diagnosis and prognosis through quantitative measurements of serum glycan profiles. *Clin. Chem.*, 2008. **54**. 1166-1175.

15. Isailovic, D., et al., Profiling of human serum glycans associated with liver cancer and cirrhosis by IMS-MS. *J. Proteome Res.*, 2008. **7**. 1109-1117.

16. Zaia, J., Mass spectrometry of oligosaccharides. *Mass Spectrom. Rev.*, 2004. **23**. 161-227.

17. Harvey, D.J., Matrix-assisted laser desorption/ionization mass spectrometry of carbohydrates. *Mass Spectrom. Rev.*, 1999. **18**. 349-450.

18. Williams, T.I., D.A. Saggese, and D.C. Muddiman, Studying O-linked protein glycosylations in human plasma. *J. Proteome Res.*, 2008. **7**. 2562-2568.

19. Viseux, N., E. de Hoffmann, and B. Domon, Structural assignment of permethylated oligosaccharide subunits using sequential tandem mass spectrometry. *Anal. Chem.*, 1998. **70**. 4951-4959.

20. Ciucanu, I. and F. Kerek, A Simple and Rapid Method for the Permethylation of Carbohydrates. *Carbohydr. Res.*, 1984. **131**. 209-217.

21. Dell, A., Preparation and Desorption Mass-Spectrometry of Permethyl and Peracetyl Derivatives of Oligosaccharides. *Methods Enzymol.*, 1990. **193**. 647-660.

22. Bourne, E.J., et al., Studies on Trifluoroacetic Acid .1. Trifluoroacetic Anhydride as a Promoter of Ester Formation between Hydroxy-Compounds and Carboxylic Acids. *Journal of the Chemical Society*, 19492976-2979.

23. Karlsson, N.G., et al., Negative ion graphitised carbon nano-liquid chromatography/mass spectrometry increases sensitivity for glycoprotein oligosaccharide analysis. *Rapid Commun. Mass Spectrom.*, 2004. **18**. 2282-2292.

24. Barroso, B., et al., On-line high-performance liquid chromatography/mass spectrometric characterization of native oligosaccharides from glycoproteins. *Rapid Commun. Mass Spectrom.*, 2002. **16**. 1320-1329.

25. Bahr, U., et al., High sensitivity analysis of neutral underivatized oligosaccharides by nanoelectrospray mass spectrometry. *Anal. Chem.*, 1997. **69**. 4530-4535.

26. Karas, M., U. Bahr, and T. Dulcks, Nano-electrospray ionization mass spectrometry: addressing analytical problems beyond routine. *Fresenius Journal of Analytical Chemistry*, 2000. **366**. 669-676.

27. Wuhrer, M., et al., Normal-phase nanoscale liquid chromatography - Mass spectrometry of underivatized oligosaccharides at low-femtomole sensitivity. *Anal. Chem.*, 2004. **76**. 833-838.

28. Koizumi, K., Y. Okada, and M. Fukuda, High-Performance Liquid-Chromatography of Monosaccharides and Oligosaccharides on a Graphitized Carbon Column. *Carbohydr. Res.*, 1991. **215**. 67-80.

29. Pabst, M., et al., Mass plus retention time = structure: A strategy for the analysis of N-glycans by carbon LC-ESI-MS and its application to fibrin N-glycans. *Anal. Chem.*, 2007. **79**. 5051-5057.

30. Pabst, M. and F. Altmann, Influence of elctrosorption, solvent, temperature, and ion polarity on the performance of LC-ESI-MS using graphitic carbon for acidic oligosaccharides*. Anal. Chem.*, 2008. **80**. 7534-7542.

31. Davies, M.J., et al., Use of a Porous Graphitized Carbon Column for the High-Performance Liquid-Chromatography of Oligosaccharides, Alditols and Glycopeptides with Subsequent Mass-Spectrometry Analysis*. J. Chromatogr.*, 1993. **646**. 317-326.

32. Itoh, S., et al., N-linked oligosaccharide analysis of rat brain Thy-1 by liquid chromatography with graphitized carbon column/ion trap-Fourier transform ion cyclotron resonance mass spectrometry in positive and negative ion modes*. Journal of Chromatography A*, 2006. **1103**. 296-306.

33. Itoh, S., et al., Simultaneous microanalysis of N-linked oligosaccharides in a glycoprotein using microbore graphitized carbon column liquid chromatography-mass spectrometry*. Journal of Chromatography A*, 2002. **968**. 89-100.

34. Kawasaki, N., et al., Microanalysis of N-linked oligosaccharides in a glycoprotein by capillary liquid chromatography/mass spectrometry and liquid chromatography/tandem mass spectrometry*. Anal. Biochem.*, 2003. **316**. 15-22.

35. Hashii, N., et al., Glycomic/glycoproteomic analysis by liquid chromatography/mass spectrometry: Analysis of glycan structure alternation in cells*. Proteomics*, 2005. **5**. 4665-4672.

36. Alpert, A.J., Hydrophilic-Interaction Chromatography for the Separation of Peptides, Nucleic-Acids and Other Polar Compounds*. J. Chromatogr.*, 1990. **499**. 177-196.

37. Simpson, R.C., et al., Adaptation of a Thermospray Liquid-Chromatography Mass-Spectrometry Interface for Use with Alkaline Anion-Exchange Liquid-Chromatography of Carbohydrates*. Anal. Chem.*, 1990. **62**. 248-252.

38. Ruhaak, L.R., et al., Hydrophilic interaction chromatography-based high-throughput sample preparation method for N-glycan analysis from total human plasma glycoproteins. *Anal. Chem.*, 2008. **80**. 6119-6126.

39. Tajiri, M., S. Yoshida, and Y. Wada, Differential analysis of site-specific glycans on plasma and cellular fibronectins: application of a hydrophilic affinity method for glycopeptide enrichment. *Glycobiology*, 2005. **15**. 1332-1340.

40. Wuhrer, M., et al., Protein glycosylation analyzed by normal-phase nano-liquid chromatography-mass spectrometry of glycopeptides. *Anal. Chem.*, 2005. **77**. 886-894.

41. Hitchcock, A.M., et al., Comparative glycomics of connective tissue glycosaminoglycans. *Proteomics*, 2008. **8**. 1384-1397.

42. Naimy, H., et al., Characterization of heparin oligosaccharides binding specifically to antithrombin III using mass spectrometry. *Biochemistry*, 2008. **47**. 3155-3161.

43. Zarei, M., et al., Automated normal phase nano high performance liquid chromatography/matrix assisted laser desorption/ionization mass spectrometry for analysis of neutral and acidic glycosphingolipids. *Analytical and Bioanalytical Chemistry*, 2008. **391**. 289-297.

44. Schiffman, G., E.A. Kabat, and W. Thompson, Immunochemical Studies on Blood Groups 30 - Cleavage of a B + H Blood-Group Substances by Alkali. *Biochemistry*, 1964. **3**. 113-&.

45. Williams, T.I., et al., Investigations with O-linked protein Glycosylations by Matrix-Assisted Laser Desorption/Ionization Fourier Transform Ion Cyclotron Resonance Mass Spectrometry. *J. Mass Spectrom.*, 2008. **43**. 1215-1223.

46. Li, B., et al., Glycoproteomic analyses of ovarian cancer cell lines and sera from ovarian cancer patients show distinct glycosylation changes in individual proteins. *J. Proteome Res.*, 2008. **7**. 3776-3788.

47. Guerardel, Y., et al., The nematode Caenorhabditis elegans synthesizes unusual O-linked glycans: identification of glucose-substituted mucin-type O-glycans and short chondroitin-like oligosaccharides. *Biochem. J.*, 2001. **357**. 167-182.

48. Ogata, S. and K.O. Lloyd, Mild Alkaline Borohydride Treatment of Glycoproteins - a Method for Liberating Both N-Linked and O-Linked Carbohydrate Chains. *Anal. Biochem.*, 1982. **119**. 351-359.

49. Williams, T.I., et al., Effect of matrix crystal structure on ion abundance of carbohydrates by matrix-assisted laser desorption/ionization Fourier transform ion cyclotron resonance mass spectrometry. *Rapid Commun. Mass Spectrom.*, 2007. **21**. 807-811.

50. Olsen, J.V., et al., Parts per million mass accuracy on an orbitrap mass spectrometer via lock mass injection into a C-trap. *Mol. Cell. Proteomics*, 2005. **4**. 2010-2021.

51. Ceroni, A., et al., GlycoWorkbench: A tool for the computer-assisted annotation of mass spectra of Glycans. *J. Proteome Res.*, 2008. **7**. 1650-1659.

52. O'Connor, P.B., E. Mirgorodskaya, and C.E. Costello, High pressure matrix-assisted laser desorption/ionization Fourier transform mass spectrometry for minimization of ganglioside fragmentation. *J. Am. Soc. Mass Spectrom.*, 2002. **13**. 402-407.

53. O'Connor, P.B. and C.E. Costello, A high pressure matrix-assisted laser desorption/ionization Fourier transform mass spectrometry ion source for thermal stabilization of labile biomolecules. *Rapid Commun. Mass Spectrom.*, 2001. **15**. 1862-1868.

54. Domon, B. and C.E. Costello, A Systematic Nomenclature for Carbohydrate Fragmentations in Fab-Ms Ms Spectra of Glycoconjugates. *Glycoconjugate Journal*, 1988. **5**. 397-409.

55. Papac, D.I., A. Wong, and A.J.S. Jones, Analysis of acidic oligosaccharides and glycopeptides by matrix assisted laser desorption ionization time-of-flight mass spectrometry*. Anal. Chem.*, 1996. **68**. 3215-3223.

56. Snovida, S.I., J.M. Rak-Banville, and H. Perreault, On the use of DHB/aniline and DHB/N,N-dimethylaniline matrices for improved detection of carbohydrates: Automated identification of oligosaccharides and quantitative analysis of sialylated glycans by MALDI-TOF mass spectrometry*. J. Am. Soc. Mass Spectrom.*, 2008. **19**. 1138-1146.

57. Foley, J.P. and J.G. Dorsey, Equations for Calculation of Chromatographic Figures of Merit for Ideal and Skewed Peaks*. Anal. Chem.*, 1983. **55**. 730-737.

58. Tabares, G., et al., Different glycan structures in prostate-specific antigen from prostate cancer sera in relation to seminal plasma PSA*. Glycobiology*, 2006. **16**. 132-145.

CHAPTER 6

Development of a Robust and High Throughput Method for Profiling *N*-linked Glycans Derived from Plasma Glycoproteins by Nano LC FT-ICR Mass Spectrometry

6.1 Introduction

The study of glycans derived from glycoproteins, commonly referred to as glycomics, is an emerging research area. Most glycans are either *O*-linked to a serine or threonine or *N*-linked to an asparagine residue and occur on an estimated 50% of all translational products.[1] Glycosylation is known to play significant roles in numerous biological processes including: protein folding, stability, cellular adhesion, signaling and disease. For biomarker investigations, glycomics offers a more targeted approach as opposed to searching for a relevant disease marker in the proteome. However, the study of an entire glycome is no simple task as the complex biological processing of glycans within the Golgi apparatus of a cell leads to a range of diverse structures. In addition, both the lack of chromophores and the hydrophilic nature, inherent of the glycan structure, make glycan analysis difficult. Due to its unparalleled molecular specificity, mass spectrometry offers the most comprehensive approach for glycan analysis allowing for both determination of glycan composition and structural elucidation which are more difficult to determine by other analytical techniques.

Wu *et al.* first implicated the significance of glycosylation in cancer when it was demonstrated that healthy fibroblasts have smaller membrane glycoproteins

than their diseased counterpart.[2] In the late 1970's, Rostenburg *et. al.* reported altered glycosylation patterns in alpha-1-antitrypsin in various types of cancer.[3] Around the same time, Gehrke and coworkers linked glycan abundance to ovarian and lung carcinomas by gas-liquid chromatography (GLC).[4] Recently, glycosylation has been further implicated in cancer development.[5-11] Current investigations have taken a global glycan approach for *biomarker* discovery in which glycans are cleaved from glycoproteins in complex biological matrices (e.g., serum). These studies have shown promise for identifications of potential physiologically important species in several types of cancer including breast[12, 13], ovarian[14], liver[15], and prostate malignacies.[16]

Although there are several factors that must be considered when conducting a large scale discovery experiment (e.g., sample collection, sample type, statistical analyses, analytical variability) of two different physiological states (e.g., disease vs. control), one of the most important and initial steps is the development of a robust and reproducible method while maximizing throughput. We have recently detailed a method utilizing β-elimination chemistry[17] for the analysis of *O*-linked glycans derived from glycoproteins in plasma by both MALDI-FT-ICR mass spectrometry[18] and nanoLC Orbitrap mass spectrometry.[19] The analysis of the same sample by both techniques revealed that the low molecular weight glycans observed by MALDI-FT-ICR mass spectrometry were potential fragments of larger species detected intact by nanoLC mass spectrometry.[19] This fragmentation can be contributed to both the harsh ionization conditions of MALDI, relative to ESI, and

the long detection times associated with FT-ICR mass spectrometry. Although β-elimination targets the release of *O*-linked glycans, the majority of species identified in these studies by nanoLC MS are believed to be *N*-linked (based on exact mass and tandem MS spectra). This observation may be due to two reasons: **1**) β-elimination chemistry is known to release portions of *N*-linked glycans[20, 21] and **2**) glycosylation occurring on asparagine residues may be considerably more abundant than its *O*-linked counterpart as it has been estimated that 75% of all glycoproteins contain only *N*-linked glycans.[1] Therefore, it was decided that it would be beneficial for future discovery investigations to develop an optimized procedure that specifically targets these species.

Michalski and coworkers have described in great detail a method for *N*-linked glycan cleavage and purification derived from protein quantities greater than 50 μg.[22] In summary, this step by step procedure is time consuming as it involves reduction (4 hours), alkylation (12 hours), proteolytic digestion (24 hours), PNGase F digestion (18 hours), solid phase extraction (SPE), permethylation, followed by purification of permethylated glycans using another SPE step.[22] In addition, four 12-hour dialysis steps are recommended to purify the sample during preparation. Other similar procedures utilizing reduction and alkylation[15, 16] or a combination of reduction, alkylation, and proteolytic digestion[13, 23, 24] prior to *N*-glycan release, sample cleanup, derivatization and mass spectral analysis, have been briefly described throughout the literature. Wuhrer and coworkers recently reported a method utilizing SDS and heat for plasma protein denaturation followed by N-

glycan release and derivatization; however, the method utilized two SPE steps for sample purification and both MALDI-MS and CE-ESI-MS for glycan analysis.[25]

In this work, we describe a method for profiling of underivatized *N*-linked glycans from plasma by nanoLC FT-ICR mass spectrometry. Data can be collected from a plasma sample in less than one day using microwave irradiation or shorter incubation times during PNGase F digestion. The procedure involves plasma denaturation with SDS and β-mercaptoethanol, digestion by PNGase F and one SPE step. The effect of NP40 detergent and different PNGase F incubation methods on ion abundance are reported. In addition, three internal standards were spiked into the samples and allow for normalization of glycan abundance amongst samples across different experimental conditions. Finally, several glycan species were identified using the high *mass measurement accuracy* afforded by FT-ICR mass spectrometry.

6.2 Experimental

6.2.1 Materials

Peptide-N-Glycosidase F (2.5 mU/μL), the denaturing mixture consisting of 1 M β-mercaptoethanol and 2% (w/w) sodium dodecyl sulfate, and the detergent solution consisting of 15% nonidet P40 (NP40) in water were all purchased from Prozyme (San Leandro, CA). Formic acid, trifluoroacetic acid (TFA), ammonium acetate, lacto-*N*-difucohexaose I (LND), lacto-*N*-fucopentose (LNF), maltoheptoase, pronase E (6 U/mL) were purchased from Sigma Aldrich (St Louis,

MO). HPLC grade acetonitrile and water were obtained from Burdick & Jackson (Muskegon, MI). Pooled human plasma was purchased from Innovative Research (Novi, MI). Graphitized solid phase extraction cartridges (Part Number 210101) were from Alltech (Deerfield, IL) and drop dialysis membranes were from Millipore (Burlington, MA). Slide-A-Lyzer dialysis cassettes, molecular weight cut-off of 7 kDa, were obtained from Pierce (Rockford, IL).

6.2.2 Release and Purification of N-linked Glycans from Plasma

A large experimental space was initially explored in order to optimize this procedure and these parameters are summarized in **Table 6.1**. Herein, the final optimized protocol is described. Certain parameters from **Table 6.1** are further discussed (*vide infra*). A conservative estimate of the total time for each step is given and is based on a sample size of 15-20. This estimate is broken up into "personnel hours" and hours that require no attention (e.g., incubation).

Denaturing Plasma Proteins (0.5 Hours + 1 Hour of Lyophilization). 50 μL of pooled human plasma was lyophilized to dryness at 35° C. 250 μL of 50 mM tris-HCl buffer (pH=7.5) was added to the dried proteins and samples were vortexed vigorously for 5 minutes. 28 μL of stock denaturing solution (2% SDS/1 molar β-mercaptoethanol) was added to the sample, vortexed (30 s), centrifuged and heated in a 95°C water bath for 5 minutes.[26] NP40 detergent was *not* used in the final protocol; however, in the developmental stages 30 μL of stock detergent

solution was added after protein denaturation. It is important to note that higher

Table 6.1: The experimental conditions explored throughout the stages of method development.

Experiment	Hypothesis	Conclusion
Dialysis of plasma against 500 mL of nanopure H_20 for 24 h. MWCO 7 kDa. This was done prior to drying down and reconstituting in 50 mM Tris-HCl buffer.	Removal of low molecular weight contaminants (e.g., metabolites, salts, small peptides) would increase glycan spectra quality.	No real advantage was observed. Step significantly increased sample preparation time.
Varying the number of elutions from the SPE cartridge from 4 to 8.	Possible that elution of glycans from the SPE cartridge was incomplete using only 4 elutions.	The second set of 4 elutions showed no detectable glycans. 4 elutions is sufficient.
The use of a microwave during enzymatic digestion. Different conditions were explored. 1. 60 mins @ 37° C ~10 Watts 2. 5 mins @ 55° C ~100 Watts 3. 20 mins @ 25° C ~250 Watts	Reduce incubation times by increasing enzymatic activity through the use of a microwave.	Condition number 3 worked the best in terms of overall glycan abundance.
Comparing glycan abundance by normalizing glycans to internal standards between the microwave and conventional incubation methods with and without NP-40.	Is the microwave comparable with 18 hour digestion? What is the effect of NP-40 detergent.	See **Figure 6.2** and text.
Optimizing enzymatic incubation times for total glycan abundance using internal standards.	Can decreased incubations times still yield similar results?	See **Figure 6.3** and text.
After SPE, pronase digestion for 4 hours followed by drop dialysis for 2 hours.	Help purify the sample by removing interfering peptide peaks that eluted during SPE.	Proved detrimental as glycan abundance decreased and peptide contamination increased.

concentrations of plasma protein, higher temperatures, and/or longer incubation times resulted in an aggregate formation. This formation led to extremely viscous samples and both was irreversible and detrimental to analysis in the studies. If desirable, the volume of plasma starting material could be decreased; however, 50 μL of plasma resulted in 840 μL of sample yielding approximately 200 LC/MS runs.

Enzymatic Digestion (0.5 Hours Sample Preparation + 18 Hours Incubation). After allowing the mixture to cool to room temperature (20 mins), 5 μL of enzyme solution (12.5 mU) was added to the sample. The sample was vortexed (10 s), centrifuged, and incubated at 37°C for 18 hours. After 18 hours the enzyme was quenched by adding 500 μL of aqueous 0.1% TFA to lower the pH (~3.5). It is important to note shorter enzyme incubation times or the use of a microwave reactor could be used to decrease the length of this step and still resulted in acceptable data (*vide infra*).

Solid Phase Extraction (SPE) using Nonporous Graphitized Carbon (3 Hours for SPE + 4 Hours for Lyophilization)

Graphitized carbon is well suited for these applications as the material binds strongly to molecules with a range of hydrophobicities. Small molecules and salts were removed in **step A** and peptides and proteins were separated from glycans in **step B** (elution step) by strong interactions with the stationary phase.

Three solutions were used for SPE.

1) Wash solution (100% 18 MΩ nanopure H_2O containing 0.1% TFA)
2) Conditioning solution (80% ACN with 0.05% TFA)
3) Elution solution (25% ACN in 0.1% TFA)

A. Conditioning the Extraction Cartridges. The extraction cartridges were conditioned with two column volumes of solution 1, one column volume of solution 2, and two more column volumes of solution 1. External pressure

could be applied during the conditioning phase to achieve a flow rate of approximately 1 mL/min.

B. **Loading and Wash Phases**. The sample was loaded onto the SPE cartridge and allowed to pass through the cartridge with no external pressure. The ependorf tube containing the sample was rinsed twice with 500 μL of aqueous 0.1% TFA and both rinses were added to the column. The sample was then washed with 50 mL of solution 1. This step removed salts and other small molecules from the sample. If necessary, external pressure could be applied during the wash phase to achieve a flow rate of ~0.5 mL/min.

C. **Elution.** 1 mL of the elution solution (solution 3) was added to the column and the contents were collected in a 1.5 mL ependorf tube. This step was repeated 3 additional times for a total of four 1 mL aliquots. A greater number of elution aliquots was explored with no additional benefits in glycan abundance (**Table 6.1**). External pressure could be applied in the elution step to achieve a flow rate of 0.5-1 mL/min. However, it should be noted that too much external pressure could result in protein eluting from the SPE cartridge. In addition, at higher flow rates an unidentified black material was observed in the elution, presumably carbon from the SPE packing material. It also should be noted that higher concentrations of organic modifier (>25%) in the elution solution could result in peptide contamination. The four elutions were then lyophilized to dryness at 35° C for 4 hours.

D. Reconstitution Each aliquot was reconstituted in 10 μL of HPLC grade water and fractions were combined for a total of 40 μL of sample. It was occasionally observed that in the first elution aliquot, after lyophilization and reconstitution, there was insoluble protein material. In these cases the aliquot was centrifuged for 30 seconds and only the supernatant was used for analysis. This was not found to be detrimental to glycan analysis by LC/MS. All samples were stored at –20° C prior to analysis.

6.2.3 LC/MS Sample Preparation

LND, LNF and maltoheptoase were chosen for internal standards because these carbohydrates are not found attached to plasma glycoproteins, have different LC retention times and are commercially available. A 10 μM mixture of each internal standard was prepared. For experiments with ISDs added prior to sample processing, 40 μL of this mixture (400 pmols) were added directly to raw plasma. For other experiments the 10 μM mixture was diluted 25-fold in ACN/H20 (80:20) and mixed with 5 μL sample, resulting from reconstitution of the SPE elutions, prior to analysis. The sample was then placed in a low volume LC vial (part number CTV-0910P, Chromtech, Apple Valley, MN) for subsequent analysis by nanoLC mass spectrometry. The glycan ratio factor was calculated by summing the integrated areas of the extracted ion chromatograms of 6 plasma glycans and dividing this number by the areas of the internal standards. Due to significant ammonium exchange with hydroxyl hydrogens, which produced satellite peaks

17.03 Da apart, both the integrated areas from these species and the protonated species were used in the calculation.

6.2.4 Microwave Experiments

Plasma samples (~50 µL), that were prepared and denatured according to the described procedure, were placed in a microwave reaction vial and subjected to digestion with 5 µL of enzyme solution (12.5 mU) under the follwing microwave conditions using a CEM Discover system: **1**) standard mode (37^{o} C, 1 hour, ~10 W), **2**) power mode (~55^{o} C, 5 mins, 100 W), or **3**) under simultaneous cooling using a jacketed reaction vessel (CEM Coolmate) that enabled temperature control via continuous flow of coolant (–40^{o} C), allowing a maximal power input at a lower temperature in standard mode (25^{o} C, 20 mins, ~250 W). Temperatures were measured using a fiber optics probe. Condition 3 was found to be optimal and was further investigated with and without detergent. Irradiated samples were subsequently subjected to the described solid phase extraction (*vide supra*).

6.2.5 Time Course Experiments

We investigated the effect of different incubation times on glycan abundance using the described non-microwave protocol. Five different incubation periods (37° C) were explored in triplicate:1) T=0, 2) T=20 mins, 3) T=6 hours, 4) T=12 hours, 5) T=18 hours. Immediately after adding the enzyme to the denatured plasma sample and vortexing for 10 seconds, the reaction was quenched and this set of samples

(n=3) corresponded to T=0. After each incubation period the set of corresponding samples (n=3) was quenched by adding 500 μL aqueous 0.1% TFA solution and stored at –20°C. After 18 hours, solid phase extraction was performed on all samples following the described protocol. These samples were analyzed by nanoLC mass spectrometry in random order to avoid any measurement biases.

6.2.6 NanoLC FT-ICR Mass Spectrometry

Liquid chromatography was performed using an Eksigent nanoLC-2D system (Dublin, CA) operating under *hydrophilic interaction chromatography* (HILIC) conditions.[27] Solvents A and B were 50 mM ammonium acetate (pH=4.5) and acetonitrile, respectively. A vented column configuration was used in these studies and was recently found in our laboratory to provide superior chromatography of peptides when compared to the discontinuous configuration.[28] Four μL of sample were injected onto a 10 μL loop and flushed out of the loop onto a ~5 cm self packed IntegraFrit (New Objective, Woburn, MA) trap at 2 μL/min (80% ACN). During the wash phase the nano-flow pumps were running over a 15 cm self-packed IntegraFrit "dummy" column to provide sufficient backpressure prior to the valve switching. After approximately 10 trap washes, the 10-port valve (VICI, Houston, TX) switched in-line with the gradient and data collection commenced. Glycans were eluted at 500 nL/min from a 75 μm I.D. PicoFrit capillary column with a 15 μm I.D. tip (New Objective, Woburn, MA) packed in-house (10 cm) with TSK-Gel Amide80 stationary phase (Tosoh Biosciences, San Francisco, CA). After 3

minutes, the gradient ramped to 60% solvent A over 37 minutes, held constant for 5 minutes and was then brought back to initial conditions (80% B) to re-equilibrate the column for an additional 10 minutes. The total run time was 60 minutes.

Mass spectrometric analyses were performed using a hybrid linear ion trap Fourier transform ion cyclotron resonance mass spectrometer (Thermo Fischer Scientific, San Jose, CA) equipped with a 7 Tesla superconducting magnet. The instrument was calibrated by following the manufacturer's standard procedure. Electrospray ionization was achieved by applying a potential of 2 kV to a liquid junction pre-column. The capillary and tube lens voltage were set to 42 V and 120 V, respectively. The capillary temperature was 225° C. Full scans were performed in the ICR cell at a resolving power of $100{,}000_{FWHM}$ @ *m/z* 400, AGC of 1×10^6, and a maximum *injection time* (IT) of 1 second. Five MS/MS scans were performed in the ion trap per full scan at a normalized collisional energy of 22. For MS/MS spectra the AGC was set to 1×10^4 with a maximum IT of 400 ms. A dynamic exclusion of 120 s was used to avoid repeated interrogation of abundant peaks. Glycans were identified by using the OSCAL software provided by the Lebrilla laboratory (Personal Communication) and Glycoworkbench.[29] Xcalibur software version 2.0.5 was used for data analysis and peak integration.

6.3 Results and Discussion

Figure 1 displays a typical base-peak ion chromatogram of glycans derived from plasma using the described protocol. Glycans eluted between 20 and 35

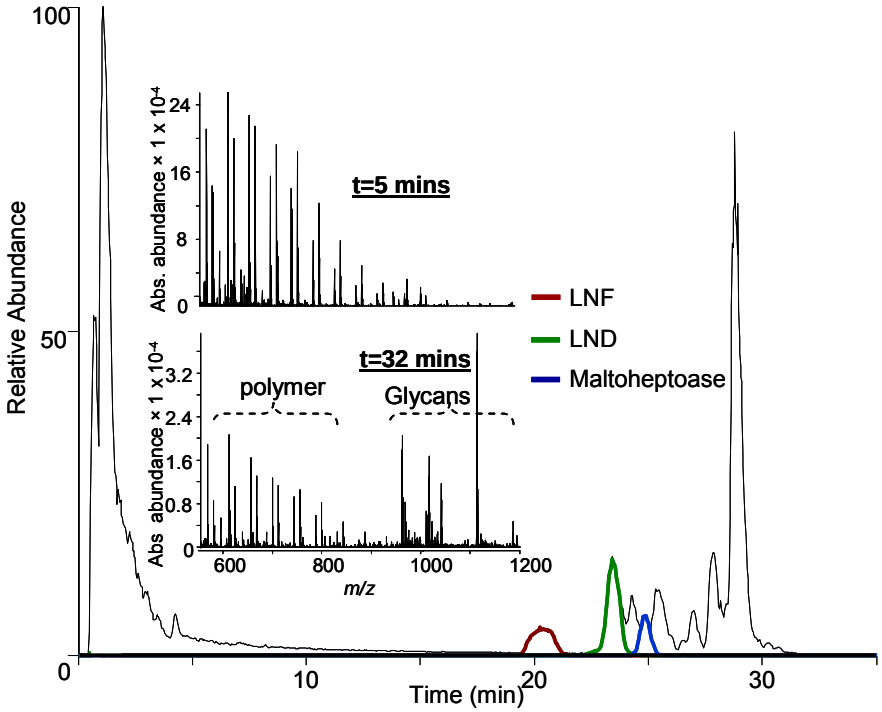

Figure 6.1 A base peak ion chromatogram of glycans resulting from the cleavage and purification of 50 μL of plasma. Glycans eluted between 20 and 35 minutes. One of the major problems discovered in the early stages of the method development was a strong polymer signal, resulting from the NP40 detergent used in the initial stages, which slowly bled off the column. After LC-MS analysis of a few samples the polymer signal began to suppress glycan intensity. The extracted ion chromatograms for three internal standards, used to normalize glycan abundance, are overlaid on the base peak ion chromatogram.

minutes and any interfering peptides eluted prior to 20 minutes. It is worth noting that peptide contamination observed in these studies was minimal, in contrast to our previously published procedure using β-elimination for *O*-linked glycan analysis.[19, 30] In order to compare the abundances of glycans under various experimental conditions, and for future studies across different physiological states, 3 standard glycans LND, LNF and maltoheptaose were spiked into the sample. **Figure 6.1** shows the elution order and relative abundances of these internal standards. The internal standards were chosen based on availability and the fact

they are not found linked to glycoproteins. This gave samples a point of reference at which plasma glycan abundances could be quantitatively compared across different experimental conditions. As described in the method sections, a ratio of abundances between the plasma glycans and the three internal standards was used to evaluate the various experimental conditions discussed herein.

One of the major problems discovered in the early stages of method development was the strong polymer signal that was present throughout the LC-MS analysis as shown in **Figure 6.1.** This polymer signal was determined experimentally to be the result of NP40, the detergent used in the early stages of method development. It has been reported that non-ionic detergents such as NP40 are used to maximize PNGase F activity in the presence of SDS[22] and thus, increase the effienciency of glycan cleavage.[25] In these studies the addition of NP40 was found to be detrimental as polymer was observed in these samples and slowly bled off the nanoLC column as shown in **Figure 6.1**. After running a few samples, even with blanks in between, the polymer signal began to significantly suppress glycan intensity.

Two main options existed in order to remedy the polymer contamination: **1**) Eliminate the use NP40 detergent during the sample preparation process or **2**) To investigate another method of sample cleanup (e.g., dialysis, organic solvent precipitation, or a second solid phase extraction). Due to the fact that adding another sample preparation step would add a significant amount of time to the sample preparation process and increase both the possibility for sample loss and

contamination, it was decided to explore the first option. Initially there was concern about the enzymatic activity of PNGase F in the presence of SDS without the NP40 detergent. As a result, microwave radiation was utilized in an effort to increase enzymatic activity, thus both counteracting the inhibitory effects of SDS and decreasing the overall time needed for incubation allowing for higher sample throughput. Microwave technology has been utilized previously to increase the enzymatic activity of PNGase F; however, those studies focused on model proteins.[31, 32] Microwaving the sample for 20 minutes @ 20°C and 250 watts was found to provide the most favorable results in terms of absolute glycan abundance (data not shown) for the three conditions investigated (**Table 6.1**).

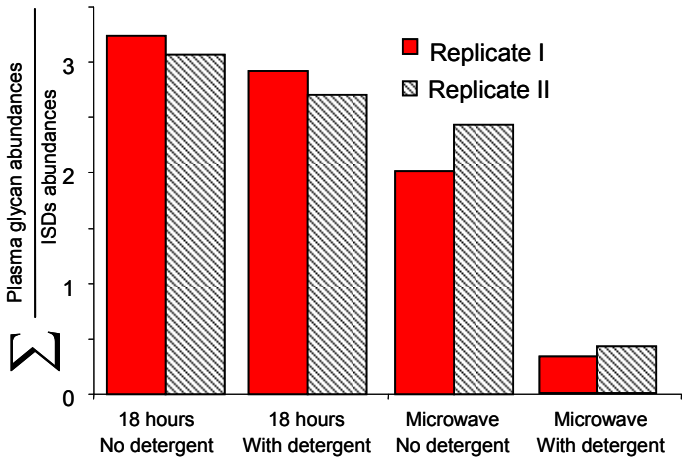

Figure 6.2 The ratio factor (glycan abundance) is plotted as a function of different experimental conditions. Two samples were carried through each experimental condition. The NP40 detergent did not have a significant impact on 18 hour incubations performed at 37°C while the detergent significantly suppressed glycan abundance using the microwave. Microwave conditions: 250 W, 25° C, 20 mins.

Figure 6.2 compares the absolute glycan abundance using the glycan ratio factor (y-axis) for four different experimental conditions. Two technical replicates were investigated for each set of conditions. Microwave-assisted cleavage with and without NP40 was compared to conventional 18 hour digestion with and without NP40. Surprisingly, there were minimal differences in the ratio factors

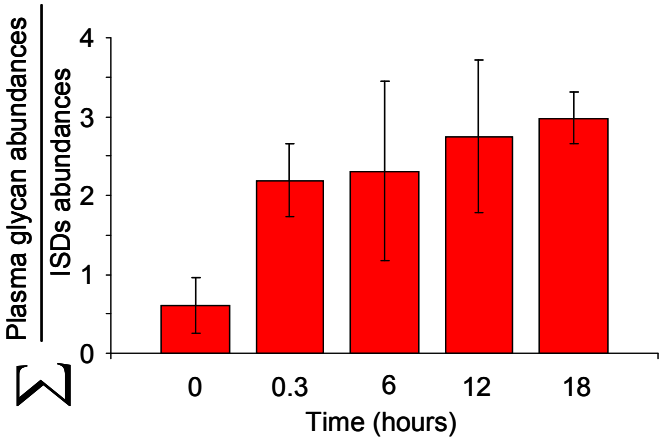

Figure 6.3 The 95% CI in the average ratio factor (n=3) is plotted as a function of 5 different incubation times at 37°C. Glycan abundance increased significantly after just 20 minutes of incubation and began to level off after 12-18 hours. It is important to note that some of the less abundant glycans were not always present at shorter incubation lengths (e.g., 20 mins and 6 hours). The 18 hour digestion was the most reproducible.

(glycan abundance) between the 18-hour digestion with and without the detergent. The microwave experiments without NP40 were comparable to the 18 hour digestion; however, they were completed in only 20 minutes at 25° C – a 50-fold reduction in digestion time. Interestingly, in the presence of detergent, glycan abundance was significantly lower (**Figure 6.2**).

Due to the capability to perform parallel processing under conventional enzymatic procedures as opposed to serial processing with the microwave procedure, it was clear that for a large sample set it would be more beneficial to optimize the 18 hour digestion protocol. To further increase throughput, the length of incubation and its effect on glycan abundance was investigated. **Figure 6.3** shows the ratio factor as a function of incubation time. Five different time periods were investigated: 1) T=0; 2) T=20 mins; 3) T=6 hours; 4) T=12 hours; 5) T=18 hours. For each period there were 3 technical replicates for a total of 15 samples. All samples were digested without the presence of NP40. As displayed in **Figure**

6.3, the ratio factor significantly increases with only 20 minutes of incubation at 37°C. As the length of incubation increases, glycan abundance also increases. The ratio factor begins to level off at 12 to 18 hours; however, the highest reproducibility was achieved by the 18-hour incubation, indicated by the small range in the confidence interval. Although comparable ratio factors were obtained with these shorter incubation times (T=20 mins and T=6 hours) some of the less abundant glycans in plasma were not always detected in these samples (data not shown).

The final step of development was to evaluate the reproducibility of the 18 hour non-microwave digestion procedure. The comparison of the average ratio in the triplicate injection of three technical replicates was used to determine the inter-sample variability of three glycans. Relatively large RSDs were observed by adding the internal standards just prior to LC/MS. As a result, the ISDs were introduced at the initial stages of sample processing and resulted in significantly higher reproducibility. **Figure 6.4** displays the precision of the method between adding

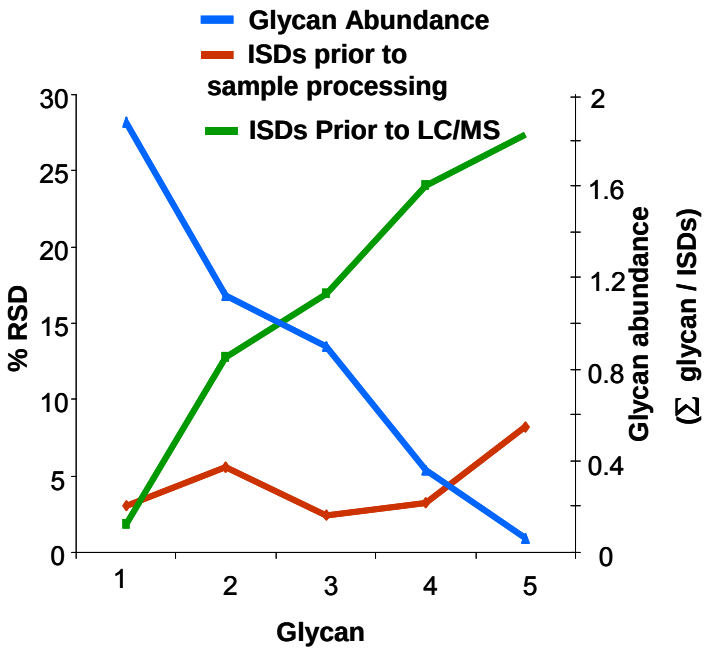

Figure 6.4 Compares the precision of the method between adding the ISDs before or after sample processing (prior to LC-MS) as a function of 5 different glycans with varying abundances.

Table 6.2: Glycan compositions identified using the described protocol. All compositions were in the aldehyde form.

	Theoretical [M+H]	Composition	95% CI MMA (ppm) n=5
1	911.3350	$Hex_3HexNAc_2$	0.75 ±0.52
2	1073.3878	$Hex_4HexNAc_2$	0.76 ±0.93
3	1114.4150	$Hex_3HexNAc_3$	0.88 ±0.53
4	1235.4410	$Hex_5HexNAc_2$	2.12 ±0.37
5	1260.4730	$Hex_3HexNAc_3Fuc_1$	0.90 ±0.42
6	1276.4670	$Hex_4HexNAc_3$	1.03 ±0.70
7	1317.4940	$Hex_3HexNAc_4$	1.31 ±0.32
8	1397.4940	$Hex_6HexNAc_2$	1.34 ±0.44
9	1405.5100	$Hex_3HexNAc_3NeuAc_1$	1.01 ±0.77
10	1438.5176	$Hex_5HexNAc_3$	0.49 ±0.48
11	1463.5520	$Hex_3HexNAc_4Fuc_1$	1.83 ±0.30
12	1479.5470	$Hex_4HexNAc_4$	0.95 ±0.21
13	1520.5732	$Hex_3HexNAc_5$	1.18 ±0.16
14	1600.5728	$Hex_6HexNAc_3$	1.77 ±0.46
15	1625.6050	$Hex_4HexNAc_4Fuc_1$	1.84 ±0.14
16	1641.5994	$Hex_5HexNAc_4$	1.49 ±0.32
17	1666.6310	$Hex_3HexNAc_5Fuc_1$	2.13 ±0.06
18	1682.6260	$Hex_4HexNAc_5$	1.43 ±0.23
19	1713.6205	$Hex_4HexNAc_3Fuc_1NeuAc_1$	1.19 ±0.30
20	1729.6154	$Hex_5HexNAc_3NeuAc_1$	0.81 ±0.61
21	1770.6520	$Hex_4HexNAc_4NeuAc_1$	1.38 ±0.32
22	1787.6573	$Hex_5HexNAc_4Fuc_1$	1.12 ±0.24
22	1828.6839	$Hex_4HexNAc_5Fuc_1$	1.68 ±0.14
23	1844.6788	$Hex_5HexNAc_5$	1.00 ±0.31
24	1891.6682	$Hex_6HexNAc_3NeuAc_1$	1.52 ±0.86
25	1916.6999	$Hex_4HexNAc_4Fuc_1NeuAc_1$	1.29 ±0.22
26	1932.6848	$Hex_5HexNAc_4NeuAc_1$	2.09 ±0.25
27	1973.7214	$Hex_4HexNAc_5NeuAc_1$	0.85 ±0.52
28	1990.7367	$Hex_5HexNAc_5Fuc_1$	0.58 ±0.49
29	2078.7527	$Hex_5HexNAc_4Fuc_1NeuAc_1$	1.81 ±0.12
30	2119.7793	$Hex_4HexNAc_5Fuc_1NeuAc_1$	1.13 ±0.83
31	2135.7742	$Hex_5HexNAc_5NeuAc_1$	1.31 ±0.46
32	2223.7902	$Hex_5HexNAc_4NeuAc_2$	1.20 ±0.49
33	2281.8321	$Hex_5HexNAc_5Fuc_1NeuAc_1$	1.23 ±0.31
34	2297.8270	$Hex_6HexNAc_5NeuAc_1$	0.56 ±0.58
35	2369.8481	$Hex_5HexNAc_4Fuc_1NeuAc_2$	1.32 ±0.52
36	2426.8696	$Hex_5HexNAc_5NeuAc_2$	0.74 ±0.91
37	2572.9275	$Hex_5HexNAc_5Fuc_1NeuAc_2$	1.60 ±0.62
38	2588.9224	$Hex_6HexNAc_5NeuAc_2$	0.83 ±0.97
39	2734.9803	$Hex_6HexNAc_5NeuAc_2Fuc_1$	1.21 ±1.02
40	2880.0178	$Hex_6HexNAc_5NeuAc_3$	1.07 ±0.68
41	3026.0757	$Hex_6HexNAc_5Fuc_1NeuAc_3$	1.14 ±0.38
42	3536.2454	$Hex_7HexNAc_6NeuAc_4$	1.31 ±1.09

the internal standards prior to any processing steps and adding them just prior to LC/MS as a function of 5 different glycans found in plasma. As the glycan abundance (displayed as the 2nd axis in **Figure 6.4**) decreases in plasma the precision of the method where the ISDs where added just prior to LC/MS significantly decreases (i.e., %RSD increases). For the method where the ISDs were added prior to any processing steps there is an inter-sample reproducibility of less than 10% (%RSD) across a 50 fold-dynamic range.

Glycans identified in plasma, using the described procedure, are shown in **Table 6.2**. The high *mass measurement accuracy* afforded by the FT-ICR mass spectrometer

provides a confident glycan composition as the upper limit of the 95% confidence interval in the average MMA was below 3 ppm. The absolute MMAs originating from 5 different runs were used to perform this calculation. It is important to note that several glycans containing sialic acid residues were also identified. These glycans are thought to mediate various critical physiological processes.[33] Changes in the amount, type, and bonding of sialic acids to neighboring molecules have also been reported in human cancers.[34-36] The ability to identify and determine differential expression of these species across a large sample set will prove critical for future biomarkers studies.

6.4 Conclusions

A fast and robust method for profiling *N*-linked glycans from glycoproteins in plasma is reported. A large experimental space was initially explored and is summarized. The final procedure is described in detail and requires no protease digestion, one solid phase extraction step, and no glycan derivatization. Internal standards were spiked into the samples and provided a point of reference to normalize plasma glycans across numerous experimental conditions. Incubation times, effects of NP40 detergent, and the use of microwave irradiation were investigated. Although microwave irradiation and lower incubation times could potentially be used to increase throughput, these processes yielded slightly lower glycan abundances as determined through the use of internal standards. Future studies will utilize the described optimized procedure for initial screening of glycan

profiles derived from plasma taken from benign gynecologic tumor controls and epithelial ovarian cancer patients in efforts to discover a diagnostic marker regardless of disease progression. Structures of glycans identified to be significantly different between EOC and control groups will then be determined from tandem MS spectra.

6.5 References

1. Apweiler, R., H. Hermjakob, and N. Sharon, On the frequency of protein glycosylation, as deduced from analysis of the SWISS-PROT database. *BBA-Gen. Subjects*, 1999. **1473**. 4-8.

2. Wu, H.C., et al., Comparative Studies on Carbohydrate-Containing Membrane Components of Normal and Virus-Transformed Mouse Fibroblasts .I. Glucosamine-Labeling Patterns in 3t3 Spontaneously Transformed 3t3 and Sv-40-Transformed 3t3 Cells. *Biochemistry*, 1969. **8**. 2509-&.

3. Rostenberg, I., J. Guizarvazquez, and R. Penaloza, Altered Carbohydrate Content of Alpha-1-Antitrypsin in Patients with Cancer. *J. Natl. Cancer Inst.*, 1978. **61**. 961-965.

4. Gehrke, C.W., et al., Quantitative Gas-Liquid-Chromatography of Neutral Sugars in Human-Serum Glycoproteins - Fucose, Mannose, and Galactose as Predictors in Ovarian and Small Cell Lung-Carcinoma. *J. Chromatogr.*, 1979. **162**. 507-528.

5. Casey, R.C., et al., Cell membrane glycosylation mediates the adhesion, migration, and invasion of ovarian carcinoma cells. *Clin. Exp. Metastasis*, 2003. **20**. 143-152.

6. Dennis, J.W., M. Granovsky, and C.E. Warren, Protein glycosylation in development and disease. *BioEssays*, 1999. **21**. 412-421.

7. Lau, K.S. and J.W. Dennis, N-Glycans in cancer progression. *Glycobiology*, 2008. **18**. 750-760.

8. Hollingsworth, M.A. and B.J. Swanson, Mucins in cancer: Protection and control of the cell surface. *Nat. Rev. Cancer*, 2004. **4**. 45-60.

9. Hakomori, S., Glycosylation defining cancer malignancy: New wine in an old bottle. *Proc. Natl. Acad. Sci. U. S. A.*, 2002. **99**. 10231-10233.

10. Gorelik, E., U. Galili, and A. Raz, On the role of cell surface carbohydrates and their binding proteins (lectins) in tumor metastasis. *Cancer Metast. Rev.*, 2001. **20**. 245-277.

11. Zhao, Y.Y., et al., Functional roles of N-glycans in cell signaling and cell adhesion in cancer. *Cancer Science*, 2008. **99**. 1304-1310.

12. Kirmiz, C., et al., A serum glycomics approach to breast cancer biomarkers. *Mol. Cell. Proteomics*, 2007. **6**. 43-55.

13. Kyselova, Z., et al., Breast cancer diagnosis and prognosis through quantitative measurements of serum glycan profiles. *Clin. Chem.*, 2008. **54**. 1166-1175.

14. An, H.J., et al., Profiling of glycans in serum for the discovery of potential biomarkers for ovarian cancer. *J. Proteome Res.*, 2006. **5**. 1626-1635.

15. Isailovic, D., et al., Profiling of human serum glycans associated with liver cancer and cirrhosis by IMS-MS. *J. Proteome Res.*, 2008. **7**. 1109-1117.

16. Kyselova, Z., et al., Alterations in the serum glycome due to metastatic prostate cancer. *J. Proteome Res.*, 2007. **6**. 1822-1832.

17. Schiffman, G., E.A. Kabat, and W. Thompson, Immunochemical Studies on Blood Groups 30 - Cleavage of a B + H Blood-Group Substances by Alkali. *Biochemistry*, 1964. **3**. 113-&.

18. Williams, T.I., D.A. Saggese, and D.C. Muddiman, Studying O-linked protein glycosylations in human plasma. *J. Proteome Res.*, 2008. **7**. 2562-2568.

19. Bereman, M.S., T.I. Williams, and D.C. Muddiman, Development of a nanoLC LTQ Orbitrap Mass Spectrometric Method for Profiling Glycans Derived from Plasma from Healthy, Benign Tumor Control, and Epithelial Ovarian Cancer Patients. *Anal. Chem.*, 2009. **81**. 1130-1136.

20. Ogata, S. and K.O. Lloyd, Mild Alkaline Borohydride Treatment of Glycoproteins - a Method for Liberating Both N-Linked and O-Linked Carbohydrate Chains*. Anal. Biochem.*, 1982. **119**. 351-359.

21. Guerardel, Y., et al., The nematode Caenorhabditis elegans synthesizes unusual O-linked glycans: identification of glucose-substituted mucin-type O-glycans and short chondroitin-like oligosaccharides*. Biochem. J.*, 2001. **357**. 167-182.

22. Morelle, W. and J.C. Michalski, Analysis of protein glycosylation by mass spectrometry*. Nature Protocols*, 2007. **2**. 1585-1602.

23. Lattova, E., et al., Mass spectrometric profiling of N-linked oligosaccharides and uncommon glycoform in mouse serum with head and neck tumor*. J. Am. Soc. Mass Spectrom.*, 2008. **19**. 671-685.

24. Atwood, J.A., et al., Quantitation by isobaric labeling: Applications to glycomics*. J. Proteome Res.*, 2008. **7**. 367-374.

25. Ruhaak, L.R., et al., Hydrophilic interaction chromatography-based high-throughput sample preparation method for N-glycan analysis from total human plasma glycoproteins*. Anal. Chem.*, 2008. **80**. 6119-6126.

26. Tarentino, A.L., C.M. Gomez, and T.H. Plummer, Deglycosylation of Asparagine-Linked Glycans by Peptide - N-Glycosidase-F*. Biochemistry*, 1985. **24**. 4665-4671.

27. Alpert, A.J., Hydrophilic-Interaction Chromatography for the Separation of Peptides, Nucleic-Acids and Other Polar Compounds*. J. Chromatogr.*, 1990. **499**. 177-196.

28. Andrews, G.L., et al., Coupling of a vented column with splitless nanoRPLC-ESI-MS for the improved separation and detection of brain natriuretic peptide-32 and its proteolytic peptides*. J. Chromatogr. B* 2009. **877**. 948-854.

29. Ceroni, A., et al., GlycoWorkbench: A tool for the computer-assisted annotation of mass spectra of Glycans*. J. Proteome Res.*, 2008. **7**. 1650-1659.

30. Williams, T.I., et al., Investigations with O-linked protein Glycosylations by Matrix-Assisted Laser Desorption/Ionization Fourier Transform Ion Cyclotron Resonance Mass Spectrometry*. J. Mass Spectrom.*, 2008. **43**. 1215-1223.

31. Sandoval, W.N., et al., Rapid removal of N-linked oligosaccharides using microwave assisted enzyme catalyzed deglycosylation*. International Journal of Mass Spectrometry*, 2007. **259**. 117-123.

32. Prater, B.D., et al., High-throughput immunoglobulin G N-glycan characterization using rapid resolution reverse-phase chromatography tandem mass spectrometry*. Anal. Biochem.*, 2009. **385**. 69-79.

33. Varki, A., Sialic acids in human health and disease*. Trends in Molecular Medicine*, 2008. **14**. 351-360.

34. Dallolio, F. and D. Trere, Expression of Alpha-2,6-Sialylated Sugar Chains in Normal and Neoplastic Colon Tissues - Detection by Digoxigenin-Conjugated Sambucus-Nigra Agglutinin*. European Journal of Histochemistry*, 1993. **37**. 257-265.

35. Dwek, M.V. and S.A. Brooks, Harnessing changes in cellular glycosylation in new cancer treatment strategies*. Current Cancer Drug Targets*, 2004. **4**. 425-442.

36. Martersteck, C.M., et al., Unique alpha 2, 8-polysialylated glycoproteins in breast cancer and leukemia cells*. Glycobiology*, 1996. **6**. 289-301.

CHAPTER 7

Increasing the Hydrophobicity and Electrospray Response of Glycans through Derivatization with Novel Hydrazides.

7.1 Introduction

Chemical derivatization has long been employed in the field of mass spectrometry for various purposes. Early on in the history of chemical tagging, investigators demonstrated the use of trimethylsilyl (TMS) derivatives for improved volatility and separation of alcohols by gas chromatography.[1, 2] TMS derivatization is now common practice for improved detection of analytes by GC-MS.

In the mid 1980's the development of electrospray ionization (ESI) expanded the need and purpose for chemical derivatization. With the discovery of hydrophobicity as the main driving force for electrospray resonse[3], investigators have developed tags to increase the hydrophobicity of various types of biological molecules.[4-7] In addition, reports have exploited the quantitative potential of mass spectrometry using labeled and unlabeled tags for comparative peptide analysis.[8-10]

The study of the function, structure and conformation of glycans attached or released from glycoproteins, commonly referred to as glycomics, is an emerging research area with mass spectrometry becoming a powerful and prominent tool for such investigations.[11] The analysis of mixtures is difficult as the complexity of glycans presents a significant challenge for complete characterization. Glycans are

often derivatized prior to mass spectral analysis via *permethylation*[12, 13] or *peracetylation*[13, 14] to increase ionization efficiency and provide stability of labile monomers under MALDI conditions. The main pitfall in these procedures is the significant wet chemistry steps involved which limits throughput and leads to sample loss and/or contamination. In addition, incomplete reaction efficiencies can disperse a single species into multiple *m/z* channels, thus reducing sensitivity and complicating data interpretation.

Another potential reactive site exists on glycans which contain a reducing terminus. This site is in equilibrium between its cyclic hemi-acetal and open-ring aldehyde forms. The most common derivatization technique presently employed is reductive amination utilizing widely available primary amines. These amines react with the aldehyde functional group and form an imine intermediate. Due to the instability of the Schiff base[15], the species is reduced *in situ* to the corresponding secondary amine. This procedure is common practice for glycan analysis by a variety of detection methods[16] and has recently been utilized to increase hydrophobicity[15, 17] and incorporate a stable isotope label for relative quantification.[17] This reductive amination procedure suffers from low throughput due to the need to purify the glycans utilizing a SPE step after reduction. An alternative to reductive amination for glycan derivatization is hydrazone formation between the aldehyde group and a hydrazide tag. This method offers a significant advantage due to essentially the absence of any cleanup after derivitazation.[18] Thus this chemistry is facile and carried out in both high yield and with minimal

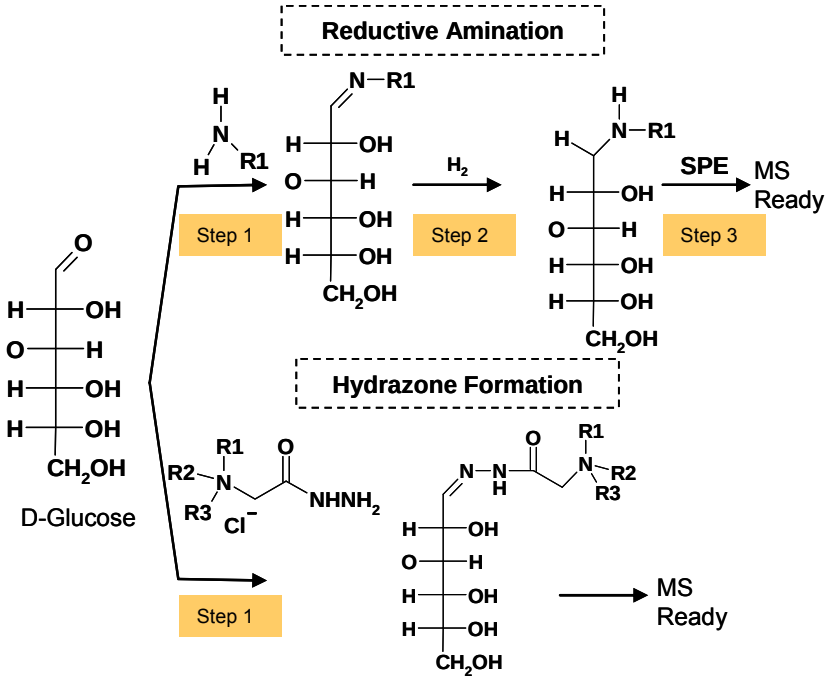

Figure 7.1 The different derivatization procedures for glycans. Hydrazone formation affords much higher throughput than reductive amination

processing steps which reduce sample loss; however, this method is less common, perhaps due to the lack of many commercially available hydrazides. **Figure 7.1** summarizes the different derivatization procedures.

In this work, two novel hydrazide reagents were synthesized, shown in **Figure 7.2**, both with a permanent charge and hydrophobic character. These reagents provide for as great as a 12-fold increase in electrospray response of a simple standard compared to the previously reported[18] and commercially available Girard's T reagent. A correlation is provided between non-polar surface area, retention time in HILIC, and ion abundance. Finally, ion abundances and tandem

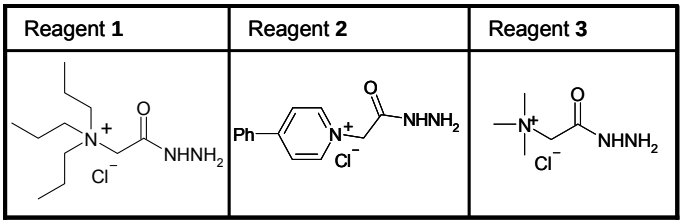

Figure 7.2 The different reagents investigated. Reagents **1** and **2** were synthesized in-house. Reagent **3** or Girard's T Reagent is commercially available.

MS spectra are compared from both native and derivatized N-linked glycans released from plasma glycoproteins.

7.2 Experimental

7.2.1 Materials

Maltoheptaose was obtained from Sigma Aldrich (St Louis, MO). Picofrits and Picotips were obtained from New Objective. HPLC grade acetonitrile and water were purchased from Burdick & Jackson (Muskegon, MI). Pooled human plasma was purchased from Innovative Research (Novi, MI). Graphitized solid phase extraction cartridges (Part Number 210101) were from Alltech (Deerfield, IL).

7.2.2 HILIC-FT-ICR Mass Spectrometry

HILIC nanoLC mass spectrometry was performed using an Eksigent nanoLC system coupled to a Thermo Fisher hybrid LTQ-FT-ICR mass spectrometer. Solvents A and B were 50 mM ammonium acetate (pH=4.5) and acetonitrile, respectively. A vented column configuration was used in these studies and is described elsewhere in detail.[19] 8 μL of sample were injected onto a 10 μL loop and flushed out of the loop onto a ~5 cm self packed

IntegraFrit (New Objective, Woburn, MA) trap at 2 μL/min (80% ACN). During the wash phase the nano-flow pumps were running over a 15 cm self-packed IntegraFrit "dummy" column to provide sufficient backpressure prior to the valve switching. After approximately 10 trap washes, the 10-port valve (VICI, Houston, TX) switched in-line with the gradient and data collection commenced. Glycans were eluted at 500 nL/min from a 75 μm I.D. PicoFrit capillary column with a 15 μm I.D. tip (New Objective, Woburn, MA) packed in-house (10 cm) with TSK-Gel Amide80 stationary phase (Tosoh Biosciences, San Francisco, CA). After 3 minutes, the gradient ramped to 60% solvent A over 37 minutes, held constant for 5 minutes and was then brought back to initial conditions (80% B) to re-equilibrate the column for an additional 10 minutes. The total run time was 60 minutes.

Mass spectrometric analyses were performed using a hybrid linear ion trap Fourier transform ion cyclotron resonance mass spectrometer (Thermo Fischer Scientific, San Jose, CA) equipped with a 7 Tesla superconducting magnet. The instrument was calibrated by following the manufacturer's standard procedure. Electrospray ionization was achieved by applying a potential of 2 kV to a liquid junction pre-column. The capillary and tube lens voltage were set to 42 V and 120 V, respectively. The capillary temperature was 225° C. Full scans were performed in the ICR cell at a resolving power of $100{,}000_{FWHM}$ @ *m/z* 400, AGC of 1×10^6, and a maximum injection time (IT) of 1 second. Five MS/MS scans were performed in the ion trap per full scan at a normalized collisional energy of 26. For MS/MS

spectra the AGC was set to 1×10^4 with a maximum IT of 400 ms. A dynamic exclusion of 120 s was used to avoid repeated interrogation of abundant peaks. The integrated areas under the EIC were determined by Xcalibur software version 2.0.5 and used to evaluate the electrospray response of different species.

7.2.3 Experimental Design

Four 100 μL aliquots were taken from a stock standard solution of maltoheptaose and pipetted in 4 eppendorf tubes. Three aliquots were individually derivatized with the two newly synthesized reagents (1 and 2) and Girard's T Reagent (3), while one was left underivatized (native species) and served as a control. Hydrazone formation was completed as previously discussed by Harvey et al.,[18] with approximately a 20-fold excess of reagent. The samples were diluted and then combined in equal volumes for an equimolar mixture and subsequently analyzed by HILIC nanoLC-MS. Calculations for determining the nonpolar surface area (i.e. hydrophobicity) of each tag were estimated based on bond lengths and Van der Waals radii of each atom.[20]

The procedure for cleavage and purification of *N*-linked glycans from plasma was performed as previously reported.[21] For derivatization of *N*-linked glycans derived from plasma glycoproteins, a 65-fold excess of reagent to internal standard was utilized. Five μL of the glycan mixture was utilized after lyophilization and reconstitution of the solid phase extraction eluents.

7.3 Results and Discussion

Figure 7.3 displays an extracted ion chromatogram of the different maltoheptaose species from the nano HILIC-MS analysis of an equal molar mixture. In addition, the derivatives formed as a result of various tags are shown. The tripropyl derivatized species afforded approximately a 5-fold and 12-fold increase in electrospray response compared to the native species and the species derivatized with the Girard's T Reagent, respectively. In addition, this species was determined both theoretically and experimentally to be the most hydrophobic, as it was calculated to have the largest non-polar surface area and was the least retained by HILIC. (**Table 7.1**). Although the Girard's T reagent did impart additional non-polar surface area to the analyte, it was experimentally discovered to be the most hydrophilic (most retained) and yielded the lowest ion abundance. We hypothesize that the limited amount of hydrophobic moieties (3 methyl groups) was not sufficient to overcome the hydrophilicity imparted by the permanent charge. However, this decrease in ion

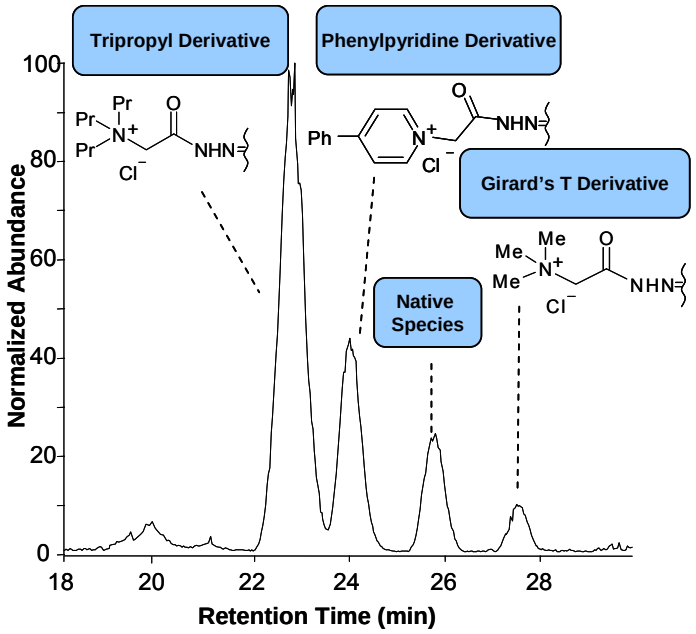

Figure 7.3 The relative responses for the analysis of an equal molar mixture of the native and various maltoheptaose derivatives.

abundance is contradictory to previous results in which the Girard's T derivatized maltoheptaose was reported for both an increase in ESI and MALDI-MS analysis when compared to the native species.[18] Data summarizing the non-polar surface area (i.e., degree of hydrophobicity) and response ratios of the different species are summarized in **Table 7.1**.

Table 7.1 Summary of the maltoheptaose experiment

Species	Tripropyl	Phpyridine	Native	Girard's T
Mass Added (Da)	198.2	210.1	-	114.1
Non-Polar SA of Tag (Å²)	213.3	131.1	-	99.6
Retention Time (min)	22.5	23.5	25.3	26.8
Ratio to Native	4.6	1.8	1.0	0.4
Ratio to T-Girard	12.0	4.6	2.6	1.0

This preliminary work indicated the potential of these tags to increase glycan electrospray response; however, the ultimate goal is the application of these reagents to glycan biomarker discovery where samples are much more complex. Potential markers for disease are most likely at relatively low abundances and any increase in electrospray response (i.e., lower limit of detection) afforded by a fast and high yielding derivatization procedure would be of considerable importance. Since Reagent 1 afforded the greatest ion abundance from the model experiments, we chose to investigate the utility of this reagent for derivatization of *N*-linked glycans derived from plasma glycoproteins.

Figure 7.4 displays an extracted ion chromatogram of a monosialylated glycan (native) overlaid with its tripropyl derivatized counterpart. As shown, approximately a 4.5-fold increase in electrospray response was observed for the derivatized species when compared to native. Similar to the model system, we

observed a decrease in retention time which indicated an increase in hydrophobicity for the derivatized glycan.

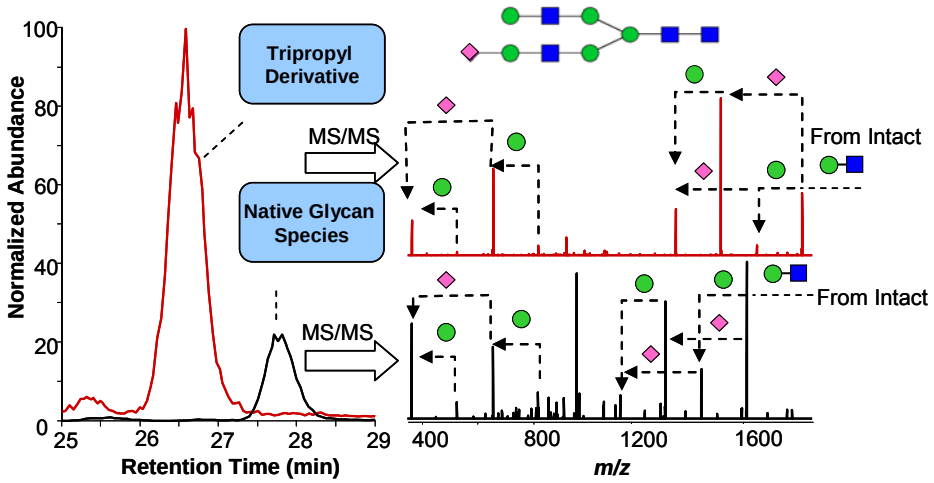

Figure 7.4 Compares the ESI response and fragmentation patterns of an *N*-linked glycan between native and derivatized species. The tag did not fragment or otherwise hinder tandem MS experiments.

It is possible that increasing the number of vibrational modes and/or imparting a permanent charge on the molecule, as others have previously theorized[17], would negatively effect glycan fragmentation. Therefore, it was necessary to evaluate the effect of derivatization on glycan fragmentation via *collision induced dissociation* (CID). The inset in **Figure 7.4** compares the fragmentation spectra of the derivatized species to that of the native species. A high similarity exists between both fragmentation spectra. The signal-to-noise ratio of the tandem MS spectrum resulting from the derivatized species is approximately 10-fold greater compared to the native glycan. The majority of fragment peaks greater than m/z 1000 contain the reducing end of this particular glycan (y-type)

which explains the offset of approximately 198 Daltons, the added mass of the tag, between the derivatized and native species. Species less than 1000 Daltons often correspond to b-type ions or internal fragments and do not contain the reducing terminus; thus, these peaks have the same *m/z* for both the derivatized and native species.

7.4 Conclusion

In this work two new hydrazide reagents were synthesized. Both reagents afford greater ESI response of glycans as compared to the commercially available and previously reported Girard's T Reagent. It is clear that increasing the hydrophobicity of glycans significantly increases the electrospray response. Future work will explore the synthesis of a stable isotope labeled version of a hydrophobic tag which will allow for both increased sensitivity and relative quantification of *N*-linked glycans released from plasma glycoproteins.

7.5 References

1. Sharkey, A.G., R.A. Friedel, and S.H. Langer, Mass Spectra of Trimethylsilyl Derivatives. *Anal. Chem.*, 1957. **29**. 770-776.

2. Sweeley, C.C., et al., Gas-Liquid Chromatography of Trimethylsilyl Derivatives of Sugars and Related Substances. *J. Am. Chem. Soc.*, 1963. **85**. 2497-&.

3. Fenn, J.B., Ion Formation from Charged Droplets - Roles of Geometry, Energy, and Time. *J. Am. Soc. Mass Spectrom.*, 1993. **4**. 524-535.

4. Null, A.P., A.I. Nepomuceno, and D.C. Muddiman, Implications of hydrophobicity and free energy of solvation for characterization of nucleic acids by electrospray ionization mass spectrometry. *Anal. Chem.*, 2003. **75**. 1331-1339.

5. Frahm, J.L., et al., Achieving augmented limits of detection for peptides with hydrophobic alkyl tags. *Anal. Chem.*, 2007. **79**. 3989-3995.

6. Mirzaei, H. and F. Regnier, Enhancing electrospray ionization efficiency of peptides by derivatization. *Anal. Chem.*, 2006. **78**. 4175-4183.

7. Williams, D.K., et al., Synthesis, characterization, and application of iodoacetamide derivatives utilized for the ALiPHAT strategy. *J. Am. Chem. Soc.*, 2008. **130**. 2122-+.

8. Gygi, S.P., et al., Quantitative analysis of complex protein mixtures using isotope-coded affinity tags. *Nature Biotechnology*, 1999. **17**. 994-999.

9. Hall, M.P. and L.V. Schneider, Isotope-differentiated binding energy shift tags (IDBEST (TM)) for improved targeted biomarker discovery and validation. *Expert Review of Proteomics*, 2004. **1**. 421-431.

10. Ross, P.L., et al., Multiplexed protein quantitation in Saccharomyces cerevisiae using amine-reactive isobaric tagging reagents. *Mol. Cell. Proteomics*, 2004. **3**. 1154-1169.

11. Zaia, J., Mass Spectrometry and the Emerging Field of Glycomics. *Chemistry & Biology*, 2008. **15**. 881-892.

12. Ciucanu, I. and F. Kerek, A Simple and Rapid Method for the Permethylation of Carbohydrates. *Carbohydr. Res.*, 1984. **131**. 209-217.

13. Dell, A., Preparation and Desorption Mass-Spectrometry of Permethyl and Peracetyl Derivatives of Oligosaccharides. *Methods Enzymol.*, 1990. **193**. 647-660.

14. Bourne, E.J., et al., Studies on Trifluoroacetic Acid .1. Trifluoroacetic Anhydride as a Promoter of Ester Formation between Hydroxy-Compounds and Carboxylic Acids. *J. Chem. Soc.*, 19492976-2979.

15. Harvey, D.J., Electrospray mass spectrometry and fragmentation of N-linked carbohydrates derivatized at the reducing terminus. *J. Am. Soc. Mass Spectrom.*, 2000. **11**. 900-915.

16. Lamari, F.N., R. Kuhn, and N.K. Karamanos, Derivatization of carbohydrates for chromatographic, electrophoretic and mass spectrometric structure analysis. *Journal of Chromatography B-Analytical Technologies in the Biomedical and Life Sciences*, 2003. **793**. 15-36.

17. Bowman, M.J. and J. Zaia, Tags for the stable isotopic labeling of carbohydrates and quantitative analysis by mass spectrometry. *Anal. Chem.*, 2007. **79**. 5777-5784.

18. Naven, T.J.P. and D.J. Harvey, Cationic derivatization of oligosaccharides with Girard's T reagent for improved performance in matrix-assisted laser desorption/ionization and electrospray mass spectrometry. *Rapid Commun. Mass Spectrom.*, 1996. **10**. 829-834.

19. Andrews, G.L., et al., Coupling of a vented column with splitless nanoRPLC-ESI-MS for the improved separation and detection of brain natriuretic peptide-32 and its proteolytic peptides*. J. Chromatogr. B* 2009. **877**. 948-854.

20. Williams, D.K., et al., Evaluation of the ALIPHAT Method for PC-IDMS and Correlation of Limits-of-Detection with Non-Polar Surface Area*. J. Am. Soc. Mass Spectrom.*, 2009 submitted.

21. Bereman, M.S., et al., Development of a Robust and High Throughput Method for Profiling N-Linked Glycans Derived from Plasma Glycoproteins by NanoLC−FTICR Mass Spectrometry*. J. Proteome Res.*, 2009Published online.

CHAPTER 8

Glycan Biomarker Discovery for Epithelial Ovarian Cancer

8.1 Introduction

Global glycan profiling in complex biological samples (e.g., plasma) is emerging as a potential avenue for biomarker discovery in cancer.[1-5] *Glycosylation*, occurring on half of all proteins,[6] is a critical and prevalent post translational modification. Changes in protein glycosylation as a result of cancer were first identified several decades ago.[7, 8] Recent research continues to emphasize the major role of this post translational modification in cancer development.[9-12]

CA-125, a heavily glycosylated protein,[13] is the only FDA approved test for the detection of ovarian cancer. The major problem with this blood test is it lacks the *sensitivity* and *specificity* to be used in the general population to screen individuals for the disease.[14] As a result the blood test is only administered to women who are deemed in a high risk category for the disease. There remains a great need for a highly sensitive and specific marker regardless of disease progression.

In this study, the glycan profile of 48 plasma samples derived from women who have been diagnosed with epithelial ovarian cancer are compared to 48 control plasma samples derived from women who were diagnosed with a benign gynecologic tumor. These control samples are age-, menopause-, and draw-matched to each EOC sample. In addition, 8 plasma samples were integrated into

the study and were derived from women who were deemed healthy. *N*-linked glycans were cleaved off all plasma glycoproteins, separated, purified and analyzed by nanoLC FTICR mass spectrometry.[15] The abundances were compared by normalizing the plasma glycan abundances to internal standards that were spiked in prior to any sample processing.

Data interpretation and comparisons were performed utilizing *receiver operator characteristic* (ROC) statistics. ROC curves have become the gold standard in evaluating the accuracy of a diagnostic test and consist simply of a plot of the *sensitivity* of a test as a function of the false positive rate (1-specificity). The *sensitivity* of a test can be qualitatively described as how well the test identifies people who have the disease. *Specificity* describes the ability of a diagnostic test to identify people without the disease. Sensitivity and specificity are described in **Equations 8.1** and **8.2**, respectively. The accuracy of a diagnostic test can be evaluated by integrating the area under the ROC curve. An ideal diagnostic test would have a sensitivity of 100%, specificity of 100%, and an area under the curve (AUC) of 1.0. A test offering no diagnostic value would have an AUC of 0.5.

$$Sensitivity = \frac{True\ Positives}{True\ Positives + False\ Negatives} \qquad \textbf{(8.1)}$$

$$Specificity = \frac{True\ Negatives}{True\ Negatives + False\ Positives} \qquad \textbf{(8.2)}$$

8.2 Experimental

8.2.1 Materials

Peptide-N-Glycosidase F (2.5 mU/μL) was purchased from Prozyme (San Leandro, CA). β-mercaptoethanol, sodium dodecyl sulfate, formic acid, trifluoroacetic acid (TFA), ammonium acetate, lacto-*N*-difucohexaose I (LND), lacto-*N*-fucopentose (LNF), maltoheptoase, pronase E (6 U/mL) were purchased from Sigma Aldrich (St Louis, MO). HPLC grade acetonitrile and water were obtained from Burdick & Jackson (Muskegon, MI). Pooled human plasma was purchased from Innovative Research (Novi, MI). Graphitized solid phase extraction cartridges (Part Number 210101) were from Alltech (Deerfield, IL).

8.2.2 Sample Preparation

The method for cleavage, purification and analysis of *N*-linked glycans derived from plasma glycoproteins was performed as previously reported.[15] Briefly, 40 μL of a 10 μM internal standard glycan mixture was added to 50 μL of plasma and the resulting mixture was lyophilized to dryness. The plasma proteins and internal standards were reconstituted in 50 mM Tris-HCl buffer (pH=7.5) and then heated with SDS and B-mercaptoethanol for 5 minutes at ~95°C. After cooling to room temperature (20 minutes), 5 μL of PNGase F (12.5 mU) were added to the mixture and heated for 18 hours @ 37°C. The enzymatic activity was quenched by the addition of 500 μL of 0.1% TFA and then purified by SPE using graphitized extraction cartridges. The four elutions were lyophilized to dryness and

reconstituted in 10 μL of water and combined. All samples were stored at -20°C prior to analysis. Five μL of sample were mixed with 100 μL of ACN:H_2O and 4 μL of the resulting mixture were injected on column.

8.2.3 Nano LC-MS

Liquid chromatography was performed using an Eksigent nanoLC-2D system (Dublin, CA) operating under hydrophilic interaction chromatography (HILIC) conditions.[16] Solvents A and B were 50 mM ammonium acetate (pH=4.5) and acetonitrile, respectively. A vented column configuration was used in these studies and is described elsewhere.[17] Four μL of sample were injected onto a 10 μL loop and flushed out of the loop onto a ~5 cm self packed IntegraFrit (New Objective, Woburn, MA) trap at 2 μL/min (80% ACN). During the wash phase the nano-flow pumps were running over a 15 cm self-packed IntegraFrit "dummy" column to provide sufficient backpressure prior to the valve switching. After approximately 10 trap washes, the 10-port valve (VICI, Houston, TX) switched in-line with the gradient and data collection commenced. Glycans were eluted at 500 nL/min from a 75 μm I.D. PicoFrit capillary column with a 15 μm I.D. tip (New Objective, Woburn, MA) packed in-house (10 cm) with TSK-Gel Amide80 stationary phase (Tosoh Biosciences, San Francisco, CA).

Mass spectrometric analyses were performed using a hybrid linear ion trap Fourier transform ion cyclotron resonance mass spectrometer (Thermo Fischer

Scientific, San Jose, CA) equipped with a 7 Tesla superconducting magnet. The instrument was calibrated by following the manufacturer's standard procedure. Electrospray ionization was achieved by applying a potential of 2 kV to a liquid junction pre-column. The capillary and tube lens voltage were set to 42 V and 120 V, respectively. The capillary temperature was 225° C. Full scans were performed in the ICR cell at a resolving power of $100{,}000_{FWHM}$ @ *m/z* 400, AGC of 1×10^6, and a maximum *injection time* (IT) of 1 second. Five MS/MS scans were performed in the ion trap per full scan at a normalized collisional energy of 22. For MS/MS spectra the AGC was set to 1×10^4 with a maximum IT of 400 ms. A dynamic exclusion of 120 s was used to avoid repeated interrogation of abundant peaks.

8.2.4 Data Analysis

Glycans were identified by using the OSCAL software provided by the Lebrilla laboratory (Personal Communication) and Glycoworkbench.[18] Xcalibur software version 2.0.5 was used for data analysis and peak integration. The area under the extracted ion chromatogram of each plasma glycan was divided by the area under the curve of the internal standard. This simple calculation normalized the abundance of plasma glycans and effectively accounted for differences in the sample preparation process (e.g. SPE step) and/or LC-MS analysis process (e.g., amount of material loaded). This number was utilized to compare glycan abundances across the sample set. ROC analysis was performed using JMP 7.0 (SAS Inc, Cary, NC). Box plots were constructed utilizing *Analyze-It* which is an add-in for Microsoft Excel. Glycan structures were determined by manual

interpretation of tandem MS spectra and by utilizing a search algorithm, SIMGlycan 2 version 2.5.5, from Premier Biosoft International. Tandem MS spectra in conjunction with accurate masses were searched against all *N*-linked glycans found on plasma glycoproteins in the database.

8.2.5 Sample Procurement and Experimental Design

The sample set investigated in these studies consisted of 104 samples: 48 plasma samples taken from women diagnosed with EOC; 48 control samples that were age-, menopause- and draw-matched to each EOC sample; and 8 plasma samples that were derived from completely healthy women. The controls in this study were derived from women who were diagnosed with benign gynecologic tumors. The 104 samples were divided into 8 cycles for sample processing and analysis. **Figure 8.1** displays the distribution of the different stages of EOC throughout the 8 cycles. It is important to note that the majority of samples in the study were derived from women who were diagnosed

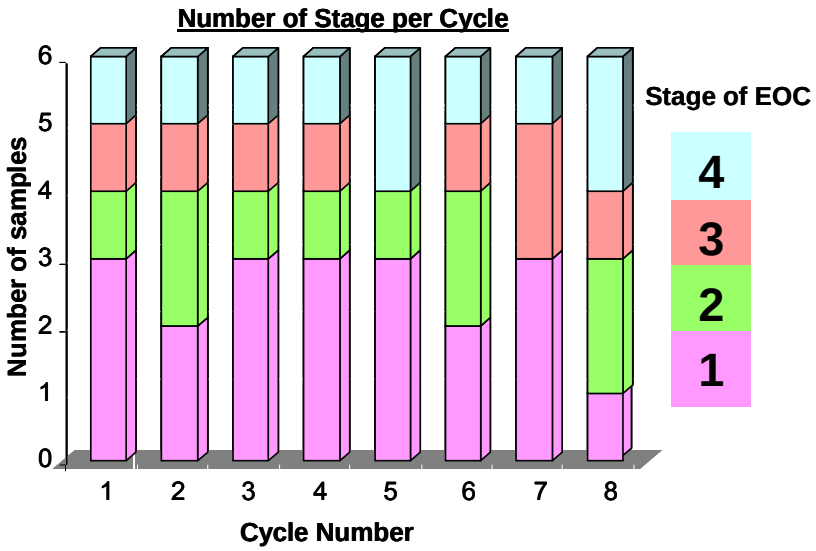

Figure 8.1 The number of samples per stage in each cycle. Samples were divided into 8 cycles for sample processing and mass spectral analysis.

with early stage EOC. In each cycle there was 6 EOC samples (**Figure 8.1**), 6 matched controls, 1 healthy sample and 1 pooled plasma sample which served as a control throughout each cycle (14 total samples/cycle).

8.3 Results and Discussion

Approximately 50 glycan species have been identified by accurate mass measurements and tandem MS/MS experiments. The data presented are a small sample of the overall data set where the abundances of three different glycans have been compared between EOC, control, and healthy samples. The three different glycan structures are shown in **Figure 8.2**. Glycan 1 was chosen based on previous work that demonstrated its potential to differentiate healthy from control and diseased samples[19] (Chapter 5). Glycans 2 and 3 were chosen based on literature reports that emphasize the importance of sialic acid containing glycans in cancer.[9, 10, 20] The structures were determined from manual interpretation of tandem MS/MS spectra and by using SIMGlycan 2 version 2.5.5 from Premier Biosoft International.

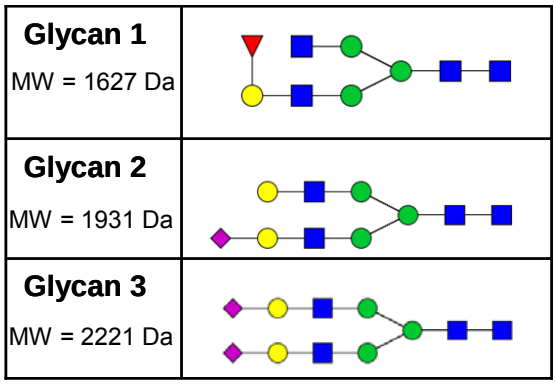

Figure 8.2 Displays the structures of the three different glycans used for statistical analyses. N-acetylglucosamine (blue circle); mannose (green circle); galactose (yellow circle); fucose (red triangle); sialic acid (pink diamond). From now structures will be referred to by number.

Figure 8.3 displays three box plots of the retention time reproducibility of the three glycan species across one of the cycles. A very high RT reproducibility was obtained for the three species as the 95% confidence interval in the average

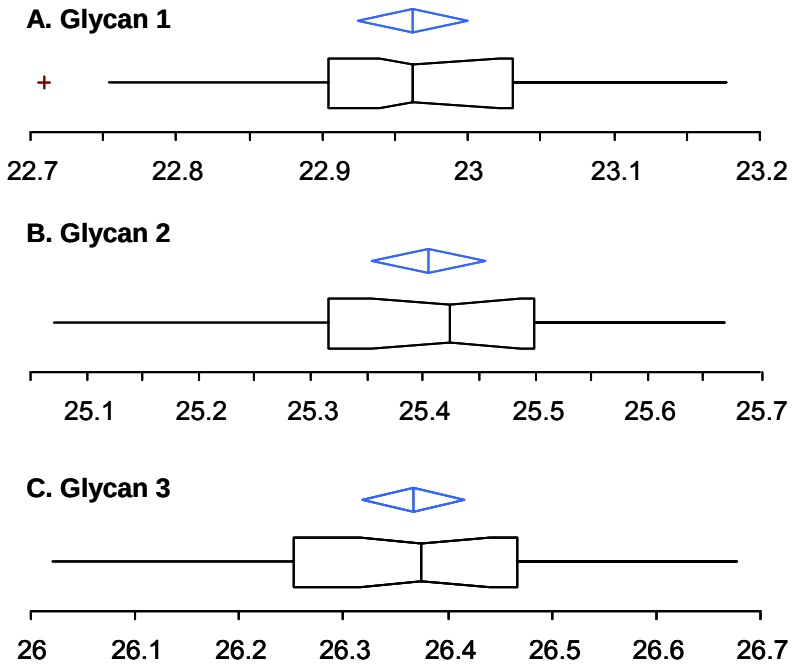

Figure 8.3 Displays box plots of the retention time reproducibility of each glycan throughout one of the cycles. The 95% confidence intervals in the average RT for these three glycans were ±3.03 seconds. See text for further interpretation of box plots.

retention time for each glycan was less than ± 3.03 seconds. The diamond represents the mean and the 95% confidence interval of the mean. The median of the data is represented by the line crossing the box while the notches in the box show the 95% confidence interval of the median. The box also displays the upper and lower quartiles. The solid lines connect the nearest data points within 1.5 interquartile ranges (IQRs) of the lower and upper quartiles. The crosses (+)

display the near outliers (between 1.5 and 3.0 IQRs away). Data were collected over 3.5 days and 39 points were used to construct each plot.

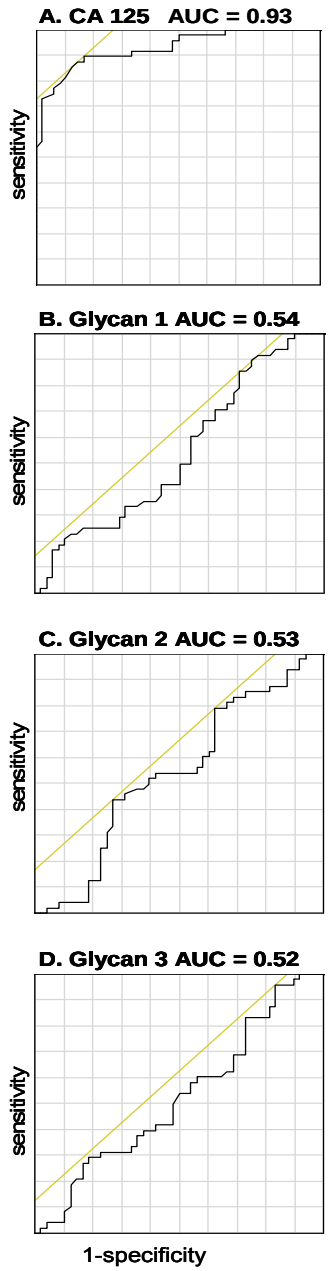

Figure 8.4 ROC curves comparing the diagnostic value of the three different glycans with the gold standard in EOC detection, CA 125, in distinguishing EOC samples from control.

Figure 8.4 shows the ROC analysis of the three glycan markers and the gold standard in EOC detection, CA 125. The three glycan markers chosen for these statistical analyses showed little if any diagnostic value (areas under the curve less than 0.6), when utilized to distinguish control vs. EOC samples. CA 125 demonstrated good diagnostic value with an AUC of 0.93. Using a cutoff value of 35 U/mL[21], CA 125 was able to provide a sensitivity of 88% and a specificity of 77%. Although these values are considerably higher than the ones provided by the glycan markers (**Figure 8.4**), the values are still not high enough for an adequate population screening test. An ideal screening method for EOC would have both high specificity (>99%) and high sensitivity (>99%) to yield a positive predictive value of at least 10%.[22]

Although the glycan markers did not

perform nearly as well as CA-125 in distinguishing disease vs. benign control, the markers did offer a moderately accurate test when using them to distinguish between healthy and EOC samples as shown in **Figure 8.5**. Utilizing both glycans 1 and 2, an area under the curve of 0.73 was achieved corresponding to a sensitivity and specificity of 88% and 62% respectively.

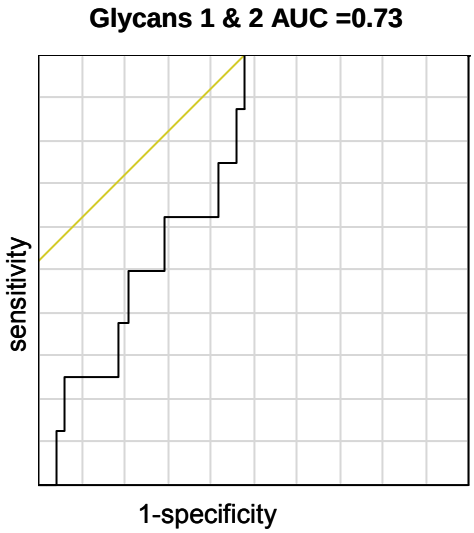

Figure 8.5 ROC analysis using glycans 1 and 2 between healthy and EOC samples.

8.4 Conclusions

We have examined the efficacy of distinguishing EOC, control, and healthy samples utilizing different glycan markers. The three markers that were chosen demonstrated poor diagnostic value when distinguishing EOC from control samples. Moderately accurate values were obtained when utilizing two of the markers to distinguish between healthy and EOC samples. CA-125 outperformed all three of the markers and gave the highest sensitivity and specificity. Further data interpretation is warranted taking into account all of the glycan markers that have been identified in plasma (~50 species). In addition, future work will look at the ability of these markers to distinguish between early and late stage EOC as well as control versus early and late stage EOC.

8.5 References

1. An, H.J., et al., Profiling of glycans in serum for the discovery of potential biomarkers for ovarian cancer. *J. Proteome Res.*, 2006. **5**. 1626-1635.

2. Kirmiz, C., et al., A serum glycomics approach to breast cancer biomarkers. *Molecular & Cellular Proteomics*, 2007. **6**. 43-55.

3. Kyselova, Z., et al., Alterations in the serum glycome due to metastatic prostate cancer. *J. Proteome Res.*, 2007. **6**. 1822-1832.

4. Kyselova, Z., et al., Breast cancer diagnosis and prognosis through quantitative measurements of serum glycan profiles. *Clinical Chemistry*, 2008. **54**. 1166-1175.

5. Isailovic, D., et al., Profiling of human serum glycans associated with liver cancer and cirrhosis by IMS-MS. *J. Proteome Res.*, 2008. **7**. 1109-1117.

6. Apweiler, R., H. Hermjakob, and N. Sharon, On the frequency of protein glycosylation, as deduced from analysis of the SWISS-PROT database. *Biochimica Et Biophysica Acta-General Subjects*, 1999. **1473**. 4-8.

7. Wu, H.C., et al., Comparative Studies on Carbohydrate-Containing Membrane Components of Normal and Virus-Transformed Mouse Fibroblasts .I. Glucosamine-Labeling Patterns in 3t3 Spontaneously Transformed 3t3 and Sv-40-Transformed 3t3 Cells. *Biochemistry*, 1969. **8**. 2509-&.

8. Gehrke, C.W., et al., Quantitative Gas-Liquid-Chromatography of Neutral Sugars in Human-Serum Glycoproteins - Fucose, Mannose, and Galactose as Predictors in Ovarian and Small Cell Lung-Carcinoma. *J. Chromatogr.*, 1979. **162**. 507-528.

9. Kim, Y.J. and A. Varki, Perspectives on the significance of altered glycosylation of glycoproteins in cancer. *Glycoconjugate Journal*, 1997. **14**. 569-576.

10. Varki, A., Sialic acids in human health and disease. *Trends in Molecular Medicine*, 2008. **14**. 351-360.

11. Varki, A., Biological Roles of Oligosaccharides - All of the Theories Are Correct. *Glycobiology*, 1993. **3**. 97-130.

12. Hollingsworth, M.A. and B.J. Swanson, Mucins in cancer: Protection and control of the cell surface. *Nature Reviews Cancer*, 2004. **4**. 45-60.

13. Wong, N.K., et al., Characterization of the oligosaccharides associated with the human ovarian tumor marker CA125. *J. Biol. Chem.*, 2003. **278**. 28619-28634.

14. Mills, G.B., R.C. Bast, and S. Srivastava, Future for ovarian cancer screening: Novel markers from emerging technologies of transcriptional profiling and proteomics. *Journal of the National Cancer Institute*, 2001. **93**. 1437-1439.

15. Bereman, M.S., et al., Development of a Robust and High Throughput Method for Profiling N-Linked Glycans Derived from Plasma Glycoproteins by NanoLC−FTICR Mass Spectrometry. *J. Proteome Res.*, 2009Published online.

16. Alpert, A.J., Hydrophilic-Interaction Chromatography for the Separation of Peptides, Nucleic-Acids and Other Polar Compounds. *J. Chromatogr.*, 1990. **499**. 177-196.

17. Andrews, G.L., et al., Coupling of a Vented Column with Splitless NanoRPLC-ESI-MS for Improved Separation and Detection of Brain Natriuretic Peptide-32 and its Proteolytic Peptides. *Journal of Chromatography B*, 2009. **In Press**.

18. Ceroni, A., et al., GlycoWorkbench: A tool for the computer-assisted annotation of mass spectra of Glycans. *J. Proteome Res.*, 2008. **7**. 1650-1659.

19. Bereman, M.S., T.I. Williams, and D.C. Muddiman, Development of a nanoLC LTQ Orbitrap Mass Spectrometric Method for Profiling Glycans Derived from Plasma from Healthy, Benign Tumor Control, and Epithelial Ovarian Cancer Patients. *Anal. Chem.*, 2009. **81**. 1130-1136.

20. Peracaula, R., et al., Altered glycosylation pattern allows the distinction between prostate-specific antigen (PSA) from normal and tumor origins. *Glycobiology*, 2003. **13**. 457-470.

21. Institute, N.C., www.cancer.org. *accessed August 18, 2009*.

22. Pearson, V.A.H., Screening for Ovarian-Cancer - a Review. *Public Health*, 1994. **108**. 367-382.

Appendix Glossary

Air Amplifier – An aerodynamic device employed to increase the transmission of analytes from atmospheric pressure into the mass analyzer during ESI.

Air ejector – A device that enables the transfer of remotely generated ions by DESI to the mass spectrometer up to three feet away.

Atmospheric-pressure sampling analysis probe (ASAP) – an ambient ionization technique which uses heated nitrogen gas to desorb volatiles off a surface and then ionization occurs through an electrical discharge.

Biomarker – an identifiable trait used either to identify the presence of disease or monitor disease progression

Breast Cancer susceptibility gene 1 (BRCA 1) – A gene known to increase a woman's risk for breast cancer and ovarian cancer when it is found in the mutated form.

Breast Cancer susceptibility gene 2 (BRCA 2) – A gene known to increase a woman's risk for breast cancer and ovarian cancer when it is found in the mutated form.

Collision induced dissociation (CID) – A dissociation technique used in mass spectrometry to determine structural information.

Cyclotron frequency – The number of "orbits" an ion makes per second in the ICR cell. Cyclotron frequency is directly proportional to the amount of charge and the strength of the magnetic field and indirectly proportional to the mass.

Desorption electrospray ionization – Introduced in 2004 DESI was one of the first ambient direct analysis methods. Similar spectra are observed between ESI and DESI of proteins.

Direct analysis in real time (DART) – an ambient ionization technique which utilizes metastable atoms as the primary method to desorb and ionize analyte.

Droplet-pickup – A possible DESI mechanism for peptides and proteins in which droplets hit the surface and remove soluble analyte and offspring droplets undergo ESI-like mechanisms for the generation of multiply charged species.

Electrospray-assisted laser desorption electrospray ionization (ELDI) – an ambient technique which utilizes high energy laser pulses to desorb neutrals from the surface and then charged droplets for subsequent ionization.

Electrospray Ionization (ESI) – An ionization technique with the capability of producing gas phase ions up to 100 kDa. Multiple charging of proteins is characteristic of this technique which is advantageous for numerous reasons.

Electrosonic spray ionization (ESSI) – A technique developed by Cooks utilizing high speed nitrogen gas to aid in desolvation.

Fused Droplet Electrospray Ionization – An ionization method that uses the fusion of droplets to increase the salt tolerance of ESI leading to higher throughput.

Glycosylation – An extremely important post translation modification (PTM). It has been estimated that over 50% of all proteins are glycosylated. Majority of glycans are linked to an asparagine residue (*N*-linked) or to a serine or threonine residue (*O*-linked).

GRAVY scores – are the grand average hydropathy score for amino acids in a sequence. Positive values indicate hydrophobic proteins while negative values indicate hydrophilic ones.

Hydrophilic interaction liquid chromatography – The use of a polar stationary phase with MS compatible solvents (i.e. Reverse phase solvents).

Hysterectomy – removal of the uterus.

Incidence or Incidence rate – Used to describe how common a disease is in the general population. Expressed as the number of new cases in a specified time period (usually 1 year).

Infrared laser desorption electrospray ionization – Similar to ELDI and MALDESI however, uses an infrared laser for desorption.

Injection time (IT) – The amount of time allowed for an ion trap to collect ions and reach a specified ion population. If this limit is not reached in the maximum time set (user) then the mass analyzer will stop collection and start the analysis.

Infrared-multiphoton dissociation (IRMPD) – a dissociation technique that uses low energy photons to slowly heat molecules in FT-ICR mass spectrometry. This

technique is performed inside the ICR cell and requires tedious laser alignments for optimal results.

Lactation – Process of breast feeding young.

Laser ablation electrospray ionization – Similar to MALDESI and ELDI; however, an IR laser is used for laser desorption.

Limits-of-detection (LOD) – the lowest concentration or amount of material that can produce an appreciable signal, usually defined as signal-to-noise ratio of 3:1.

Lock Mass – a method to achieve high MMA in the orbitrap via internal calibration.

Lorentz Force – a force that a charge particle experiences when placed in a uniform magnetic field which is both perpendicular to the magnetic field and the velocity of the particle.

Mass measurement accuracy (MMA) – A metric which determines the degree of accuracy between an experimental mass and theoretical mass of a molecule. Less than 3 ppm MMA is routine in FT-ICR-MS measurements.

Matrix-assisted laser desorption ionization (MALDI) – Another ionization technique capable of producing gas phase ions from large biomolecules. Analytes are usually mixed with an UV-absorbing matrix, spotted onto a metal plate, and are desorbed using a UV laser. Singly charge ions are the dominate charge state observed in this technique.

Matrix-assisted laser desorption electrospray ionization (MALDESI) – similar to ELDI, however a matrix is required for optimal results.

Multiple charging – Characteristic of ESI of proteins, the ability of an ion to have several like charges.

Offspring droplets – droplets that are emitted from the parent droplet due to coulombic explosions.

Parent droplet – the primary droplet formed at the onset of ESI.

Parity – the number of times a woman has given birth.

Pathogenesis – the step by step development of a particular disease.

Peak capacity – Maximum number of resolvable peaks possible.

Peracetylation – Similar to permethylation but with an acetyl group.

Permethylation – A derivatization procedure often used for glycans in which a methyl group replaces all hydroxyl Hydrogens and Hydrogens attached to Nitrogen.

Prognostic – Markers that are used to monitor the development of a disease. Often used to monitor a patient's response to treatment.

Phase coherence – A result of the excitation event in FT-ICR-MS, ions of the same *m/z* must travel in tight ion packets in order to induce appreciable signal and achieve optimal resolving power.

Plasma – Free moving form of charge particles including ions, electrons and metastable atoms.

Precursor ion – an ion that is isolated prior to dissociation is called the "precursor ion"

Rayleigh limit – The point at which the forces due to charge repulsion become greater than the forces due to surface tension. At this point the "parent droplet" breaks up into several daughter droplets.

Resolving Power – Usually defined at full width half maximum (FWHM), high resolving power is critical for MS analysis of complex samples (serum).

Risk factors – Any variable that increases the probability or "risk" of developing a particular disease (e.g., smoking increases a person's risk for lung cancer).

Sensitivity – Describes how well a diagnostic test identifies people with the disease.

Space-charge effects – Detrimental to achieving high MMA, space charge occurs due to the Coloumbic repulsions of like charges in the ICR cell.

Specificity – Describes how well a diagnostic test identifies people without the disease.

Sustained off-resonance irradiation (SORI) – a type of *collision induced dissociation* performed inside the ICR cell. Ions are excited off-resonance and collide with the collision gas producing fragment ions.

Taylor cone – A term referring to the charge accumulation at the end of an ESI capillary. This “cone” forms prior to the onset of the electrospray process.

Transvaginal ultrasonography – a procedure used to image a woman’s reproductive organs.